Lidija Milković

Beneficial effects of lipid peroxidation in the bone cell growth on bioactive glass - New perspectives in tissue engineering and regenerative medicine

PhD THESIS

Osijek, 2014.

BASIC DOCUMENTATION CARD

Josip Juraj Strossmayer University of Osijek   **PhD thesis**
University of Dubrovnik
Ruđer Bošković Institute
University Postgraduate Interdisciplinary Doctoral Study of
Molecular biosciences

Scientific Area: Interdisciplinary Area of Science
Scientific Fields: Biology and Basic Medical Sciences

Beneficial effects of lipid peroxidation in the bone cell growth on bioactive glass - New

perspectives in tissue engineering and regenerative medicine

Lidija Milković

Thesis performed at: Laboratory for Oxidative Stress of the Ruđer Bošković Institute

Supervisor/s: Prof Neven Žarković, PhD, MD, Senior Scientist

Short abstract:
This research has revealed the role of lipid peroxidation, as well as its product 4-hydroxynonenal in the process of stimulating osteogenesis assisted by using bioactive glass. Since the bioactive glass has found its important application in bone tissue engineering, new discoveries will open new possibilities for creating improved bioactive glass on which is based the focus of today's regenerative medicine.

Number of pages: 101
Number of figures: 27
Number of tables: 4
Number of references: 121
Original in: English
Key words: bone fracture healing, lipid peroxidation, 4-hydroxynonenal, bioactive glass, cooper, enhanced osteogenesis

Date of the thesis defence: 22.07.2014.

Reviewers:
1. **Prof Jerko Barbić, PhD, MD**, Full professor
2. **Prof Neven Žarković, PhD, MD**, Senior scientist (supervisor)
3. **Prof Vera Cesar, PhD**, Full professor
4. **Ana Čipak Gašparović, PhD**, Research associate (substitute)

Thesis deposited in: National and University Library in Zagreb, Ul. Hrvatske bratske zajednice 4, Zagreb; City and University Library of Osijek, Europska avenija 24, Osijek; Josip Juraj Strossmayer University of Osijek, Trg sv. Trojstva 3, Osijek

TEMELJNA DOKUMENTACIJSKA KARTICA

Sveučilište Josipa Jurja Strossmayera u Osijeku　　　　　**Doktorska disertacija**
Sveučilište u Dubrovniku
Institut Ruđer Bošković
Sveučilišni poslijediplomski interdisciplinarni
doktorski studij Molekularne bioznanosti

Znanstveno područje: Interdisciplinarno područje znanosti
Znanstvena polja: Biologija i Temeljene medicinske znanosti

Pozitivni učinci lipidne peroksidacije u rastu stanica kosti na bioaktivnom staklu - nove mogućnosti tkivnog inženjerstva i regenerativne medicine

Lidija Milković

Rad je izrađen u: Laboratoriju za oksidacijski stres Instituta Ruđer Bošković

Mentor/i: Prof. dr.sc. Neven Žarković, Znanstveni savjetnik, trajno zvanje

Kratki sažetak doktorskog rada:
Istraživanje je ukazalo na ulogu lipidne peroksidacije, kao i njezinog produkta 4-hidroksinonenala u procesu poticanja osteogeneze potpomognute korištenjem bioaktivnih stakala. Obzirom da su bioaktivna stakla našla svoju značajnu primjenu u inženjerstvu tkiva kosti, nove spoznaje će otvoriti i nove mogućnosti kreiranja poboljšanih bioaktivnih stakala na čemu se i temelji naglasak današnje regenerativne medicine.

Broj stranica: 101
Broj slika: 27
Broj tablica: 4
Broj literaturnih navoda: 121
Jezik izvornika: Engleski jezik
Ključne riječi: cijeljenje fraktura kosti, lipidna peroksidacija, 4-hidroksinonenal, bioaktivno staklo, bakar, potaknuta osteogeneza

Datum obrane: 22.07.2014.

Stručno povjerenstvo za obranu:
1. **Prof. dr. sc. Jerko Barbić**, redoviti profesor
2. **Prof dr. sc. Neven Žarković**, znanstveni savjetnik, trajno zvanje (mentor)
3. **Prof. dr. sc. Vera Cesar**, redovita profesorica
4. **Dr. sc. Ana Čipak Gašparović**, znanstvena suradnica (zamjena)

Rad je pohranjen u: Nacionalnoj i sveučilišnoj knjižnici Zagreb, Ul. Hrvatske bratske zajednice 4, Zagreb; Gradskoj i sveučilišnoj knjižnici Osijek, Europska avenija 24, Osijek; Sveučilištu Josipa Jurja Strossmayera u Osijeku, Trg sv. Trojstva 3, Osijek

Dedication/Acknowledgement

Nothing is impossible when your loved ones believe in you!

This is for all of us!

I would like to thank my mentor Prof N. Žarković for giving me the opportunity to pursue my dreams and for his kind support

I am very grateful to Prof R. Wildburger for her kind support and our good collaboration

I am thankful for starting collaborating with Prof Boccaccini, Rainer and Alex. I appreciate all your kind support and our fruitful collaboration.

I am also so happy that I had an opportunity to start working with Marija Balić, PhD and Nadia Dandachi, PhD. Thank you both for all that you have done for me. I will cherish it always.

Many thanks to all of my colleagues (current or past) from the Laboratory for Oxidative Stress: Marina, Ana, Morana, Luka, Suzana, Nena, both Teas and Iva. I learned from you, I smiled with you and I am so privileged to work with you. Thank you for making my work so wonderful!

To all my friends...thank you for being there for me, cheering me and not questioning, even just for a second, that I would not succeed.

To my mother and my brother...There are not enough words to express my appreciation. Thank you for believing in me.

To my husband and our best friend Miki...thank you for being you! Your unconditional love was my strength.

Table of contents

1. INTRODUCTION

1.1. Bone

Human skeleton of an adult is composed of 206 bones and its main functions are providing a strong, supportive structure for soft tissues and muscles, allowing body movement, protection of many vital organs and it serves as a production site of blood cells as well as a storage for certain minerals like calcium. Therefore, a great variety of bones that build our body can be classified according to their shape, position, size and structure.

All bones, when looked in transverse section, are formed of two main types of osseous tissue: cancellous and cortical bone.

Cortical bone, also known as compact bone, presents an outer layer of a bone which seems very dense and compact but in reality it is highly porous and composed of closely packed cylindrical parts called osteons or Haversian systems. The osteon consists of a central canal called the Haversian canal, which is surrounded by a number of lamellae, bone matrix in a form of concentric rings. The Haversian canals contain blood vessels that are parallel with the long axis of the bone. These blood vessels interconnect, by way of perforating canals, called Valksmann's canals, with vessels on the surface of the bone. Between the lamellae, there are spaces, called lacunae which are occupied by the bone cells, osteocytes. Moreover, these lacunæ are connected with each other and with the central Haversian canal by a number of small, hairlike channels, canaliculi. Their main role of the canaliculi is to provide passageways through the hard matrix (Fig. 1).
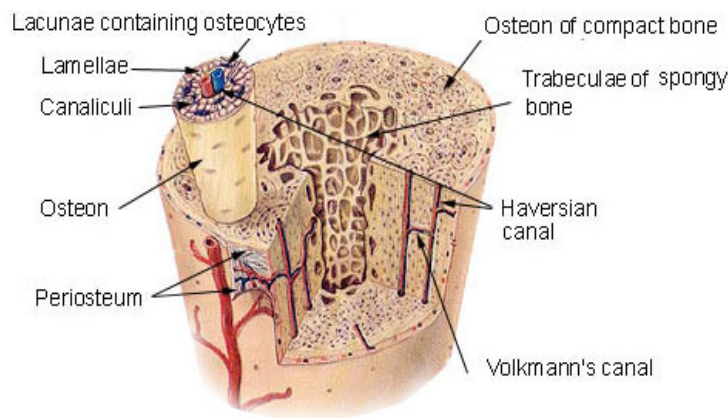
Fig. 1. Cortical bone and cancellous bone

(Source of illustration: http://training.seer.cancer.gov/anatomy/skeletal/tissue.html)

Thus every part of the Haversian system is supplied with nutrient fluids derived from the vessels in the Haversian canal and distributed through the canaliculi and lacunæ [1,2].

On the other hand, cancellous bone, also known as spongy or trabecular bone, has a lighter and less dense structure than compact bone. Cancellous bone consists of plates (trabeculae) and bars of bone adjacent to small, irregular cavities which contain red bone marrow. Since the cancellous bone does not contain the Haversian canal, its canaliculi are connected to the adjacent cavities in order to receive their blood supply. Although it may appear that the organisation of the trabeculae is poor and rather haphazardous, in reality they are organized very precisely along the lines of stress in order to provide maximum strength similar to braces that are used to support a building [2].

Furthermore, based on the pattern of collagen forming the osteoid (unmineralized, organic portion of the bone matrix), bone can be classified into two types: woven bone and lamellar bone [3].

Woven bone is characterized by a loosely organization of collagen fibres with no normal lamellar pattern like observed in cancellous and cortical bone and therefore is weaker than lamellar bone [3,4]. It is produced by osteoblasts in cases of need for a rapid bone production which occurs in all foetal bones and in fracture healing. Thus formed newly bone is further replaced by more resilient lamellar bone in a process of bone remodelling [3].

Lamellar bone is characterized by a regular parallel alignment of collagen into layers (lamellae). As a result of the alternating orientations of collagen fibrils, lamellar bone has a significant mechanical strength [3,5].

Virtually all the bone in the healthy mature adult is lamellar bone.

1.1.1. Bone composition

Bone is composed of 50 to 70% mineral, 20 to 40% organic matrix, 5 to 10% water, and <3% lipids [6]. Bone itself can be divided into the basic areas of matrix, cells and bioactive factors. Bone matrix is composed of organic and inorganic part. Organic part of the matrix are bone proteins of which 85 to 90% are collagenous proteins and mostly type I collagen [7]. Noncollagenous proteins compose 10 to 15% of total bone protein. They are generally divided into several categories, including proteoglycans, glycosylated proteins, glycosylated proteins with potential cell-attachment activities, and γ-carboxylated (gla) proteins. The most abundant

noncollagenous matrix bone proteins are osteonectin, osteocalcin, osteopontin, bone sialoprotein, and alkaline phosphatase, as well as fibronectin, decorin and bioglycan [8]. The remaining noncollagenous proteins of bone matrix include bone morphogenetic proteins, growth factors, and a variety of other molecules that may affect bone cell activity. Since many of the bone proteins seem to have multiple functions, including regulation of bone mineral deposition and turnover and regulation of bone cell activity, the roles of each of them are still not well defined [6].

Osteonectin is the most prevalent noncollagenous protein, accounting for approximately 2% of total protein in developing bone. It is considered as a bone-specific nucleator of mineralization because of its strong affinity for both collagen and mineral. *In vitro* studies indicate that osteonectin can bind collagen and regulate angiogenesis, metalloproteinase expression, cell proliferation, and cell-matrix interactions. Moreover, osteonectin-null mice develop osteopenia with defects in the function of both osteoblasts and osteoclasts [9].

Osteocalcin "synthesized by osteoblasts was initially thought to function as a promoter or initiator of calcium deposition at the nidus between the ends of collagen fibrils and therefore regarded as a marker of bone formation" [6]. Recent results suggest that osteocalcin inhibits bone formation because of a high bone mass phenotype observed in the osteocalcin knockout mice. Aside its osteoblast synthesis, osteocalcin is also derived from matrix release by osteoclast activity, because of which currently it is rather regarded as a marker of bone turnover than a specific marker of bone formation [6].

Osteopontin is abundant bone matrix protein functioning as an inhibitor of mineralization and/or as a mediator of cell-matrix and matrix-matrix/mineral adhesion (cohesion) during the formation, turnover, and repair of normal and pathological mineralized tissues [10].

Alkaline phosphatase is the main glycosylated protein present in bone where it is bound to osteoblast cell surfaces via a phosphoinositol linkage but it can also be found free within mineralized matrix. [11]. Although the mechanism of its action is not completely understood, alkaline phosphatase remains an excellent indicator of bone differentiation and mineralization.

The mineral content of bone is mostly hydroxyapatite $[Ca_{10}(PO_4)_6 (OH)_2]$, with small amounts of carbonate, magnesium, and acid phosphate, with missing hydroxyl groups that are normally present. Hydroxyapatite crystals in bone are very small, when compared to geologic hydroxyapatite crystals, measuring only approximately 200 Å in their largest dimension. These

small, poorly crystalline, carbonate-substituted crystals are more soluble than geologic hydroxyapatite crystals, thereby allowing them to support mineral metabolism [6]. Matrix maturation is associated with expression of alkaline phosphatase and several noncollagenous proteins, including osteocalcin, osteopontin, and bone sialoprotein. It is thought that these calcium- and phosphate-binding proteins help regulate ordered deposition of mineral by regulating the amount and size of hydroxyapatite crystals formed [6].

1.1.2. Bone cells

Bone cells are essential for the process of bone renewal that is occurring in human body during the lifetime. Particularly interesting cells present in bone include osteoblasts that synthesize and mineralize bone matrix, osteocytes responsible for maintenance of the matrix, and, osteoclasts required for bone resorption (Fig. 2).

Osteoblasts are mononucleated "bone-forming" cells found near the surface of bones. They are derived from multipotent mesenchymal stem cells. Osteoblasts are responsible for making osteoid, which consists mainly of collagen. The osteoblasts secrete other matrix proteins including alkaline phosphatase to create sites for calcium and phosphate deposition, which allows the growth of bone mineral crystals and thus mineralisation of the osteoid. They are also important in the regulation of osteoclastogenesis through secretion of receptor activator of nuclear factor κ B ligand (RANKL) and osteoprotegerin (OPG) [12]. Moreover, osteoblasts communicate with osteocytes to receive mechantransduction signals through gap junctional connexions [12].
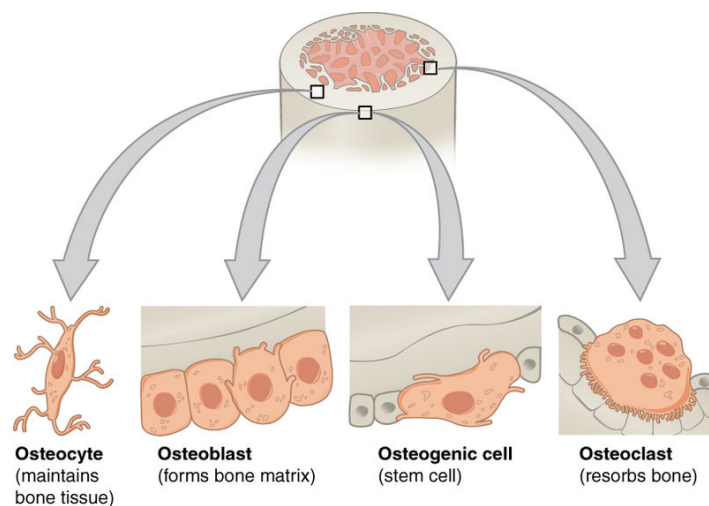

Fig 2. Bone cells

(Source of illustration: Anatomy & Physiology, http://cnx.org/content/col11496/1.6/)

Osteocytes represent terminally differentiated osteoblasts that are embedded into the secreted bone matrix and therefore are found in lacunae between the lamellae in bone. Their main role is homeostasis – maintaining the correct oxygen and mineral levels in the bone, achieved by their inner communication through connexin-mediated gap junctions in fillipodial extensions within the canalicular network. Osteocytes do not contain alkaline phosphatase, but produce osteopontins, among other bone matrix proteins [12].

Osteoclasts are large multinucleated cells with a unique ability to resorb bone. They bind to bone matrix via integrin receptors in their membrane linking to bone matrix peptides such as osteopontin, bone sialoprotein, and others. Upon binding, osteoclasts polarize and develop ruffled border with acidified vesicles. The sealing zone surrounds and isolates the acidified resorption compartment from the surrounding bone surface. Osteoclasts secrete acid phosphatase, which unfixes the calcium in mineralised bone to break it down [13].

1.1.3. Bone remodelling and bone fracture healing

Bone remodelling occurs during the lifetime to maintain calcium homeostasis and to repair micro-fractures that are result of mechanical stress. A highly complex interplay between osteoblasts, osteocytes and osteoclasts is controlling this bone resorption and rebuilding process via OPG/RANKL/RANK system. Abnormalities in this system lead to imbalance in bone formation/resorption and to increased or decreased bone strength [14].

As a dynamic and highly vascularised tissue, bone has a unique internal repair capacity to heal and remodel without scarring [15]. Skeletal development and fracture repair includes the coordination of multiple events such as migration, differentiation, and activation of multiple cell types and tissues [16]. The molecular events that govern fracture healing are a complex network of signals signifying tissue damage, cell death, cell recruitment, cell proliferation, cell differentiation, and tissue formation [17]. The stages of fracture healing reiterate the sequential stages of embryonic endochondral bone formation. Histological observations distinguish two basic types of bone healing. Primary healing is rare and refers to a direct attempt of the cells in cortical bone to re-establish the disrupted continuity. It requires absolute contact of the fragments and almost complete stability and minimisation of the inter-fragmentary strains [18]. Secondary bone healing occurs in the vast majority of bony injuries. This type of bone healing involves both intramembranous and endochondral ossification and leads to callus formation. Likewise, committed osteoprogenitor cells of the periosteum and undifferentiated multipotent mesenchymal stem cells (MSCs) are activated. Callus is a physiological reaction to inter-

fragmentary movement and requires the existence of residual cell vitality and adequate blood flow [18]. Certain biologic prerequisites have been identified in this cascade of events. Many local and systemic regulatory factors, cytokines and hormones, as well as extracellular osteoconductive matrix are seen to interact with several cell types. A vibrant cell population is a mandatory first element for an unimpeded bone repair process. Multipotent mesenchymal cells are recruited at the fracture injury site or transferred to it with the blood circulation.

Different set of phases can be observed during the fracture healing, such as hematoma formation, inflammation, angiogenesis, cartilage/callus formation, and bone remodelling (Fig. 3). Therefore, the healing process can be divided into three separate but overlapping stages: 1) the early inflammatory stage; 2) the repair stage; and 3) the late remodelling stage [19].

In the inflammatory stage, hematoma develops within the fracture during first few hours and days. The fracture hematoma has been proven to be a source of signalling molecules: interleukins (IL-1, IL-6), tumour necrosis factor-a (TNF-a), fibroblast growth factor (FGF), insulin-like growth factor (IGF), platelet-derived growth factor (PDGF), vascular endothelial growth factor (VEGF), and the transforming growth factor β (TGFβ) superfamily members) that may induce a cascade of cellular events that initiate healing [18].
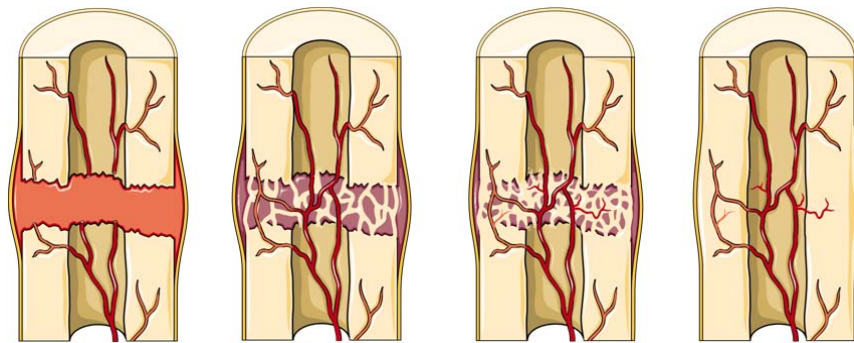
Figure 3. Stages in fracture repair. Picture obtained by the Servier Medical Art

Since bone cells at the ends of the fracture are dead, this necrotic material elicits acute inflammatory response observed as infiltration of inflammatory cells such as polymorphonuclear leukocytes and macrophages. Cytokines and pro-inflammatory factors released by these cells start healing cascade by attraction of undifferentiated mesenchymal cells and fibroblasts and support vascular ingrowth. This results in the formation of granulation tissue [19]. In addition, undifferentiated mesenchymal cells differentiate into chondrocytes and osteoblasts.

In the reparative stage, fibroblasts and chondrocytes, which secrete collagen and proteoglycans, create fibrocartilaginous callus, known as soft callus that replaces the dead bone and provide mechanical support. Eventually, the soft callus is ossified resulting in a woven bone hard callus, which occurs via a combination of intramembranous and endochondral ossification. In the final stage of repair, the woven bone is slowly replaced by lamellar bone through the remodelling stage in which the healing bone is restored to its original shape, structure, and mechanical strength [19].

At the molecular level, different sets of molecules interact with both local cells and circulating cells to coordinate the healing cascade: effectors of inflammation (IL-1, IL-6, COX-2), mitogens (transforming growth factor beta (TGFβ), insulin-like growth factor (IGF), fibroblast growth factor (FGF) and platelet derived growth factor (PDGF)), morphogens (bone morphogenetic proteins (BMPs)), and angiogenic factors (vascular endothelial growth factor (VEGF) and angiopoietins) [16].

1.2. Bone grafts

Bone fractures, especially of long bones or large joints, represent difficult medical disorder and are often not followed by successful recovery in particular in elderly patients, in patients that suffer from multifragmentary bone fractures or in polytraumatized patients. In a large number of cases the resulting skeletal deficiencies require surgical intervention and repair.

Currently there are three different grafts in usage for reconstructive surgery: autogenic grafts, allogenic grafts and bone substitutes.

Autologous bone graft, that is, bone taken from another part of the patient's own body, has been the gold standard of bone replacement for many years because it provides osteogenic cells as well as essential osteoinductive factors needed for bone healing and regeneration [20]. It is commonly taken in the form of trabecular bone from the patient's iliac crest, but cortical bone can be used as well. However, and although it presents relatively good percentages of success, the spectrum of cases in which it can be used is restricted, mainly due to the limited amount of the autograft that can be obtained and due to donor site morbidity [20].

Allograft, bone taken from somebody else's body, could be an alternative. However, the rate of graft incorporation is lower than with the autograft. Allograft bone also introduces the possibilities of immune rejection and of pathogen transmission from donor to host, and although infrequent, infections could occur in the recipient's body after the transplantation [20].

Although autologous bone grafts are considered as a golden standard there are also some limitations present in their usage like donor site morbidity and limited donor bone supply. On the other hand allografts can exhibit further negative effects like rejection phenomena and risk of viral infection. Therefore, attempts of the regenerative medicine today is to find/create a bone substitute that will enhance normal bone healing/remodelling, will be easily accessible and applicable without unwanted side-effects, that will be able to form a normal bone structure or by integration into the bone or by its resorbtion and replacement with a newly formed bone. As a consequence, biomaterials that posses mentioned properties have found their place in the field of tissue engineering and regenerative medicine.

1.3. Biomaterials – bioactive glasses

The drawbacks of autografts and allografts led to a production of a wide range of bioactive materials currently present in the market. Some of the most interesting are representatives of calcium phosphate ceramics (Ca-P), bioactive glasses (BG) and bioactive glass-ceramics.

Bioactive material is by definition "one that elicits a specific biological response at the interface of the material that results in the formation of a bond between the tissues and the material" [21]. These materials generate a carbonated hydroxyapatite layer that is equivalent chemically and structurally to the biological mineral of bone, what is known to be the determining step for the biointegration [22]. Furthermore, it was found that bioactive glasses with composition of less than 55% SiO_2 exhibit not only osteoconductivity (able to support abundant bone formation), but are also responsible for osteoproduction by stimulating proliferation and differentiation of osteprogenitor cells [23].

The major bone-bioactive material known to date is 45S5 BG [21]. This material is highly bioactive and it is both osteoinductive (able to induce bone formation) and osteoconductive. The mechanisms of bioactivity and bone bonding of 45S5 BG have been widely studied, and described [24]. Based on those studies, the bonding of 45S5 BG to bone has been attributed to the formation of a carbonate-substituted hydroxyapatite-like (HCA) layer on the glass surface in contact with the body fluid. Because this HCA layer is similar to the mineral constituent of bone, it bonds firmly with living bone and tissue. While some details of the chemical and structural changes are not clear, the HCA layer is generally believed to form as a result of a sequence of reactions on the surface of the BG implant, as described by Hench [24]:

Stage 1: Rapid ion exchange reactions between the glass network modifiers (Na^+ and Ca^{2+}) with H^+ (or H_3O^+) ions from the solution, leads to hydrolysis of the silica groups and the creation of silanol (Si−OH) groups on the glass surface: e.g.

$$Si−O−Na^+ + H^+ \rightarrow Si−OH + Na^+(aq)$$
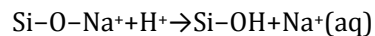
The pH of the solution increases due to the consumption of H^+ ions.

Stage 2: The increase in pH (or OH^- concentration) leads to attack of the SiO_2 glass network, and the dissolution of silica, in the form of silicic acid, $Si(OH)_4$, into the solution, and the continued formation of Si−OH groups on the glass surface:

$$Si−O−Si + H_2O \rightarrow Si−OH + OH−Si$$
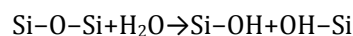
While the solubility of silica is low, the products of 45S5 BG and glass–ceramic dissolution in aqueous solutions have shown an increase in Si concentration [24] indicating that dissolution of silica is an important mechanism. However, other mechanisms could also contribute to the increase in Si concentration.

Stage 3: Condensation and polymerization of an amorphous SiO_2-rich layer (typically 1–2 μm thick) on the surface of the glass depleted in Na^+ and Ca^{2+}.

Stage 4: Further dissolution of the glass, coupled with migration of Ca^{2+} and $(PO_4)^{3-}$ ions from the glass through the SiO_2-rich layer and from the solution, leading to the formation of an amorphous calcium phosphate (ACP) layer on the surface of the SiO_2-rich layer.

Stage 5: The glass continues to dissolve, as the ACP layer incorporates $(OH)^-$ and $(CO_3)^{2-}$ from the solution and crystallizes as an HCA layer.

Figure 4. Reaction stages of bioactive glasses in contact with human tissue/fluid [25]

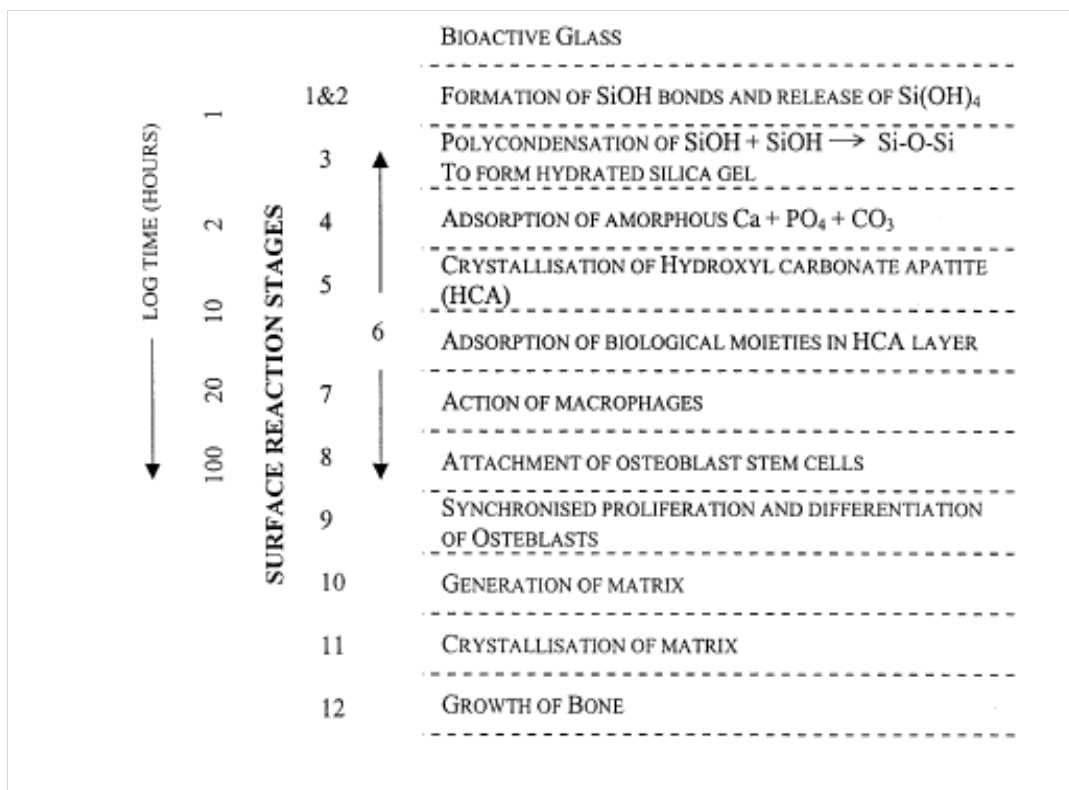With the initial formation of an HCA layer, the biological mechanisms of bonding to bone are believed to involve adsorption of growth factors, followed by attachment, proliferation and differentiation of osteoprogenitor cells [24]. Osteoblasts, which are bone-forming cells, create

extracellular matrix, mainly of collagen, which mineralizes to form a nanocrystalline mineral and collagen on the surface of the glass implant while the degradation and conversion of the glass continues over time [24].

BG type 45S5 remains the gold standard for bioactive glass but, as a scaffold material, it has several limitations. One limitation is the difficulty of processing 45S5 BG into porous 3-D scaffolds. Porous bioactive glass scaffolds are commonly prepared by heating (sintering) glass particles, already formed into the desired 3-D geometry, to bond the particles into a strong glass phase containing an interpenetrating network of pores. Because of the limited ability of 45S5 BG to sinter by viscous flow above its glass transition temperature (Tg), and the narrow window between Tg and the onset of crystallization, severe difficulties are encountered in sintering the particles into a dense network. Consequently the scaffold often has low strength [26]. Commonly, the glass devitrifies during sintering to form a predominantly combeite crystalline phase ($Na_2O-2CaO-3SiO_2$). While devitrification does not inhibit the ability of 45S5 BG to form an HA-like surface layer, it has the effect of reducing the rate of conversion to HA [27]. Another limitation of 45S5 BG is its slow degradation rate and conversion to an HA-like material [28], which makes it difficult to match the degradation rate of the scaffold with the rate of new tissue formation. The conversion of the scaffold to an HA-like material is often incomplete, so therefore a portion of unconverted glass containing SiO_2 could remain in the scaffold, raising uncertainty about the long-term effects of SiO_2 *in vivo*.

A complication with the use of 45S5 BG and other BGs and other biodegradable materials is that the local biological microenvironment can be influenced significantly by their degradation. Increases in the concentration of ions, such as Na^+ and Ca^{2+}, and changes in the pH occur as a result of the degradation, particularly in the early stages when the degradation rate is fast [24]. The biological effects of these changes are difficult to predict from *in vitro* experiments. Furthermore, the biological roles of these soluble species, their toxicity and their removal are often not clearly understood.

Moreover, it has been shown that the ionic dissolution products of 45S5 BG may enhance new bone formation (osteogenesis) through direct control over genes that regulate cell induction and proliferation [29]. Recent report demonstrates that the dissolution products of 45S5 BG create an extracellular environment that is capable of supporting osteoblast phenotype expression and extracellular matrix deposition and mineralization *in vitro* in human foetal osteoblasts [30]. There are also indications from previous reports of *in vivo* studies [31] that bioactive glass (45S5 BG) enhances vascularization of tissue engineering constructs.

Another silicate-based bioactive glass that we examined in our research is 13-93 BG with a slightly modified 45S5 composition (higher SiO_2 content and additional network modifiers, such as K_2O and MgO). Products of 13–93 BG have been approved for *in vivo* use in Europe.

Because 13–93 BG has better processing characteristics by viscous flow sintering (larger window between Tg and the onset of crystallization), the glass phase in porous 3-D scaffolds can be sintered to high density without crystallization. However, 13–93 BG degrades (and converts to an HA-like material) more slowly than 45S5 BG [24].

The 13-93 BG supports the *in vitro* growth and differentiation of MC3T3-E1 preosteoblastic cells [32] and quantitative measurement of DNA showed no significant difference in cell proliferation between dense disks of 45S5 and 13–93 BGs [33].

1.4. Oxidative Stress

The mechanisms and pathways involved in oxidative stress are conserved in mammalian cells. Oxidative stress results from an imbalance between pro-oxidants (free radicals) and anti-oxidants in the favour of the former [34]. Free radicals can be defined as molecules or molecular fragments containing one or more unpaired electrons. The presence of unpaired electrons usually confers a considerable degree of reactivity upon a free radical. Radicals that are derived from oxygen represent the most important class of such species generated in living systems [35].

Reactive oxygen species (ROS) comprise both free radical and non-free radical oxygen intermediates of which the most common are hydrogen peroxide (H_2O_2), superoxide anion ($O_2\bullet^-$) and hydroxyl radical ($\bullet OH$). Additionally, ROS can be produced from a variety of both endogenous and exogenous sources. Endogenously ROS are generated as by-products of normal cellular metabolism from mitochondrial electron transport chain, nicotinamide adenine dinucleotide phosphate (NADPH) oxidase (NOX), xanthine oxidase (XO), peroxisomes and cytochrome P450 [36,37]. Exogenous sources of ROS include ultraviolet light, ionizing radiation, environmental agents, pharmaceuticals, and industrial chemical. ROS, as highly reactive molecules, may cause damage to the cellular macromolecules like DNA, proteins and lipids, leading to changes in chromosome instability, genetic mutation, and/or modulation of cell growth [37–39]. To avoid the damage, cells have evolved endogenous antioxidant defence mechanisms including non-enzymatic antioxidants such as glutathione, thioredoxin, ascorbic acid, uric acid, alpha-lipoic acid, coenzyme Q, ferritin, bilirubin, metallothionein, l-carnitine, melatonin and also enzymatic ones such as catalase (CAT), superoxide dismutase (SOD), glutathione signalling (GPX) and peroxiredoxins (PRXs) [40].

Superoxide anion, arising either through metabolic processes or following oxygen "activation" by physical irradiation, is considered the "primary" ROS, and can further interact with other molecules to generate "secondary" ROS, either directly or prevalently through enzyme- or metal-catalyzed processes [41]. It is a produced both enzymatically by NADPH oxidase and xanthine oxidase, and non-enzymatically, when a single electron is directly transferred to O_2 in electron transport chain within mitochondria. Superoxide anion does not react directly with polypeptides, sugars, or nucleic acids, and its ability to peroxidise lipids is controversial [42]. The superoxide anion can be easily converted by superoxide dismutases into H_2O_2.

H_2O_2 is produced in mitochondria or by NOX enzymes upon their activation with various growth factors and cytokines [43]. It is relatively stable, membrane permeable and can diffuse within the cell making H_2O_2 considerably important ROS in redox signalling. If it is not eliminated by the cell's antioxidant system (CAT, GPX and thioredoxin signalling), in the presence of metal ions (iron, copper, chromium, vanadium and cobalt), H_2O_2 can be further transformed to the most reactive of ROS, hydroxyl radical *via* Fenton reaction [44,45].

The current knowledge is recognizing the Janus-like roles of ROS and antioxidant system in regulation of cellular processes, meaning that fluctuations in their levels could lead to diverse effects. Alterations in ROS levels can modulate biologic activity through aberrant stimulation/suppression of certain signalling pathways and through direct modifications of biomolecules, especially proteins [46]. ROS, once perceived as the main actors in cell's damage, are now recognized as important signalling molecules. To illuminate their role in redox signalling, it should be mentioned that ROS are oxidants by nature and hence could influence the redox status by inducing either a positive response (cell proliferation) or a negative cell response (growth arrest or cell death), depending on their concentration.

Therefore, redox balance is playing a critical role in maintaining the biologic processes since the redox system relies mostly on direct oxidative modifications of the redox-sensitive signalling proteins which reflect in the regulation of their expression, posttranslational modifications and stabilities [46,47].

For that reason, to act as effective biological messengers, ROS have to bring about a reversible change in the activity of a protein, which generally involves modification of a thiol group on a cysteine residue that mediates redox signalling [48,49]. For example, when H_2O_2 acts as a redox signal it oxidizes the thiol group on the target protein to a disulphide group, thereby changing the function of the protein. Once the level of H_2O_2 has returned to basal levels the alteration is reversed and the activity of the protein reverts to its initial level [49,50].

Moreover, ROS, acting as signalling molecules, can induce cellular proliferation by affecting several biochemical pathways from epidermal growth factor receptor (EGFR) to mTOR (mammalian target of rapamycin) which involve key signalling proteins, such as nuclear factor erythroid 2-related factor 2 (Nrf2), kelch-like protein 19 (Keap1), Ras, Raf, mitogen activated protein kinases (MAPK) such as ERK1/2, MEK, p38α, c-Jun N-terminal kinase (JNK), c-myc, p53 and protein kinase C (PKC) [40,51,52]. Among them, Nrf2 is considered to be the master regulator of the antioxidant response, but others are also important.

Additionally, ROS has been implicated in regulation of the cytosolic calcium concentration (which itself regulates the above-mentioned biological activities), regulation of protein phosphorylation, and activation of certain transcription factors such as NF-κB and the AP-1 family factors [35,44].

Disruption in redox homeostasis leads to an overall increase of intracellular ROS level. Thus generated excessive ROS constantly attack proteins, DNA and lipids, which could lead to severe and irreversible oxidative damage. Depending on the target and the form of oxidative damage, protein oxidation can be reversible or irreversible with certain side chains (lysine, arginine, histidine, proline and threonine) more susceptible to oxidation [46,53]. Processes involved include intramolecular or intermolecular protein cross-linkage, glutathionylation, nitrosylation, disulfide bond–mediated protein cross linkage or secondary oxidative modifications such as adduct formation between oxidized proteins and lipid peroxides or glycation products. These products can generate aggregation of bulky protein complexes, which may inactivate both 26S and 20S proteasome, leading to accumulation of damaged proteins and cell death [54].

Although DNA may seem less susceptible to oxidative modifications, because of its double helix structure together with the protective shield from histone and other coating proteins, oxidative nuclear DNA damage is detectable under various conditions. Albeit more than 20 base lesions have been identified, the most studied is 8-oxo-2'deoxyguanosine (8-OH-dG). The consequence of oxidative base lesions persisting in DNA is mutation which is one of the crucial steps in carcinogenesis [55].
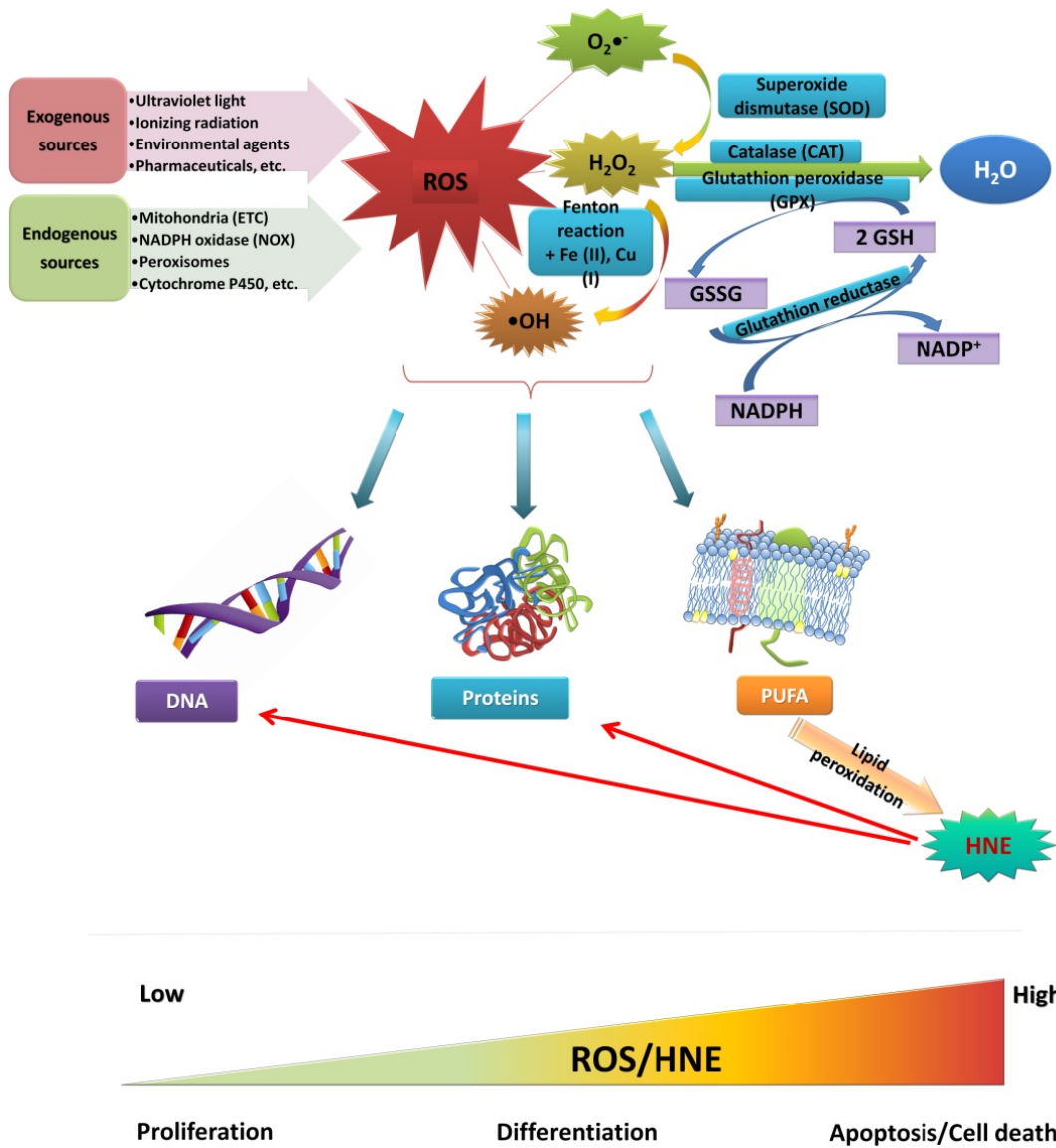
Figure 5. Molecular mechanism of reactive oxygen species (ROS) formation, involvement of
antioxidative defense and impact of ROS on cellular macromolecules
ETC=electron transport chain

1.4. Lipid peroxidation and 4-hydroxynonenal

The vast majority consider lipids to be the most susceptible macromolecules to oxidative modification and, among them, polyunsaturated fatty acids (PUFAs) in particular. The process initiated by the oxidation of PUFAs, known as lipid peroxidation, is an autocatalytic process that results in a formation of highly reactive aldehydes (Fig. 6) which are more stable than ROS, has longer half-life, can diffuse from their site of origin and thus affect targets distant from the initial free radical attack. Increased lipid peroxidation has been implied with varying extents as causative cofactor of various common age-associated diseases (type 2 diabetes mellitus, atherosclerosis), some forms of neurodegenerative disorders and some types of cancer (liver, kidney, brain, skin) [56,57]. On the other hand, today it is well-known that lipid peroxidation plays important role in cell physiology, influencing the signal transduction pathways [58].
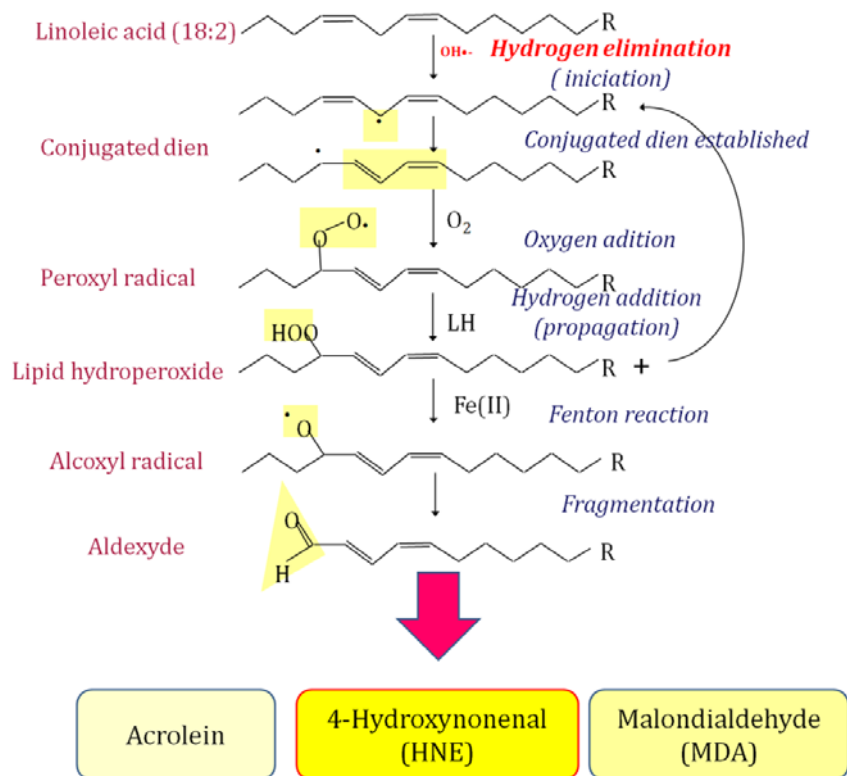
Figure 6. Mechanism of lipid peroxidation

One of the main products generated during lipid peroxidation, and the most intensively studied one, is the α,β-unsaturated aldehyde 4-hydroxynonenal (HNE) which is derived from ω-6 PUFAs such as arachidonic acid and linoleic acid [59,60]. HNE has a dichotomous role depending on its concentration. Whereas if present in excess, HNE express a variety of cytotoxic effects such as the inhibition of DNA, RNA and protein synthesis, cell cycle arrest, mitochondrial dysfunction, and thus plays an important role in pathology of various diseases [61]. On the other hand, at a low (physiological) level, HNE can induce proliferation, differentiation and apoptosis affecting genome function and interacting with other growth regulating factors, in particular cytokines [59,62–67]. Intracellular HNE reacts rapidly with thiol groups of GSH and cysteine and with lysine and histidine residues of proteins leading to significant functional alterations affecting signalling pathways [65,68,69].

The role of HNE in signalling processes is intriguing because, as already mentioned, of its double-edged effects which are concentration dependent. For this reason, the regulation of intracellular concentrations of HNE might be crucial for the nature of cell cycle signalling. It was found that HNE can induce cell growth, accompanied by the activation of MAPKs (ERK, JNK and p38) and induction of c-fos, c-jun gene expression, and AP-1 DNA binding activity [70]. Studies have also shown that HNE induces various enzymes including phospholipase C, adenylate cyclase, caspase 3, protein kinase C and other kinases involved in signal transduction cascades, strongly comprising a role of HNE in signalling cascades [71]. It is also able to influence cellular functions by regulating the genes encoding for other molecules such as heat-shock protein genes [72], c-myc[73], c-fos [74] , c-jun [75], c-myb [76], cyclins[73], p53 gene family[77], procollagen type I [78], and TGF-β1 [79]. Moreover, HNE is found to be a physiological constituent of many human and animal tissues [80] however its physiological role has yet to be clarified, but it is likely that HNE could have an important role in the regulation of cellular growth [66,71,81].

Relatively high steady state concentrations of HNE in cell membranes indicated the primary site of its origin, from where it can diffuse acting as a second messenger of free radicals. Unlike free radicals or the other ROS, HNE has the unique feature to remain stable for some time and binds to macromolecules with high reactivity, especially to proteins, causing alteration of their tertiary structure and their function. These alterations are mainly conducted through formation of covalent bond with cysteine, lysine and histidine amino acid residues [65,67]. HNE mostly reacts with SH groups of proteins and peptides generating HNE-protein conjugates that can be detected by the use of monoclonal antibodies. On the other hand, such reaction with glutathione (GSH) represents its most important detoxification mechanism [62].

Once formed, HNE is rapidly degraded by three major reactions: reduction to 1,4-dihydroxy-2-nonene by alcohol dehydrogenases, oxidation to 4-hydroxy-2-nonenoic acid by aldehyde dehydrogenase, or formation of the glutathione-conjugate (GS-HNE) catalyzed by glutathione-S-transferase (GST). Thus formed GS-HNE conjugate can easily be exported from cells in an ATP-dependent manner or, which is more often, by RLIP76, a GTPase-activating protein [82,83] and as such is a major factor in the mechanisms of drug resistance [83].

In addition, detoxification mechanisms of HNE are important to define the amount of cellular protein modified by HNE. GSH is the most important intracellular antioxidant that protects cells from HNE. Consequently, after administration of HNE, the amount of HNE-proteins adducts can be deduced by intracellular level of GSH. This level is crucial for cellular sensitivity to HNE toxicity [62]. Although GSH could act alone, detoxification reaction is accelerated by GSH metabolizing enzymes such as glutathione S-transferases (GSTs). Noteworthy, Ramana et al. [84] reported that conjugates of GSH with HNE activate PKC and stimulate NF-κB and AP-1-dependent gene transcription leading to an increase in cell growth. In conclusion, the unique pathways and the primary molecular targets of intracellular signal transduction mediated by HNE are still unknown. However, it seems that a unique receptor is not necessary for HNE to achieve growth regulating effect. On the other hand, complexity of possible interactions with signal-transduction pathways increased enormously (Fig. 7).
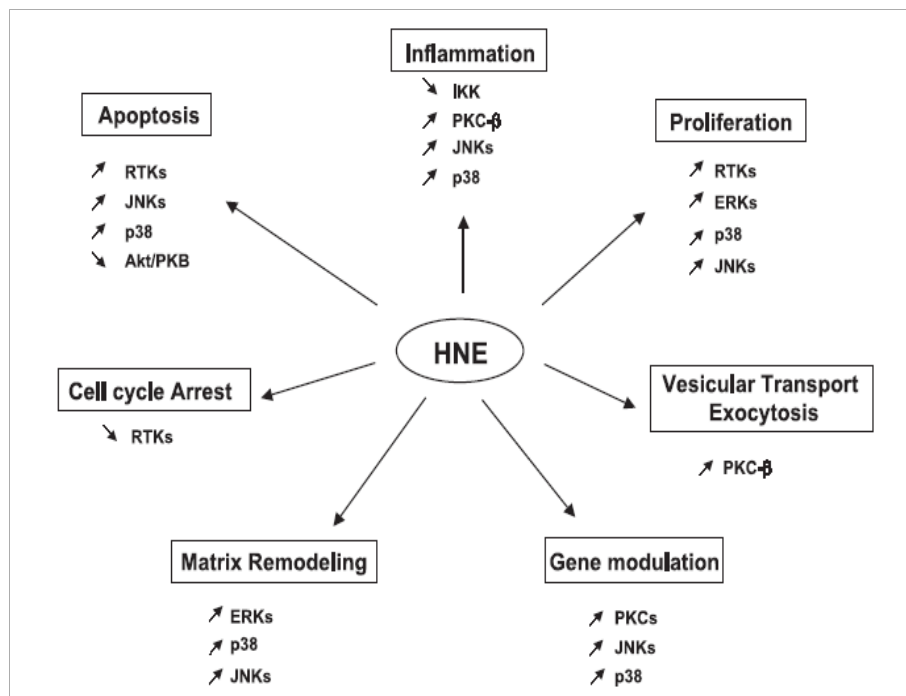

Figure 7. Potential signalling by HNE in patophysiology. Figure taken from [85]

1.5. Hypothesis and Aims

Our previous research have revealed connection of stress response with the phenomenon of enhanced osteogenesis in patients with traumatic brain injury that exert very short period of bone healing followed by heterotopic ossification or hypertrophic callus formation. This stress response involves hormonal imbalance associated with the change of growth factor activities, in particular bFGF [86] and IGF-1 [87] together with oxidative stress and lipid peroxidation [88]. Thus, lipid peroxidation was defined as important parameter of systemic response in patients with traumatic brain injuries and with bone fractures.

Lipid peroxidation occurs when ROS, generated during oxidative stress damage lipids mostly present in plasma, mitochondrial, and endoplasmic reticulum membranes. Recent results have shown that the end product of lipid peroxidation HNE, acts as a growth regulating factor interfering with the activity of cytokines and thus may affect the growth of cultured human bone cells [71,89]. HNE is known as a major bioactive marker of lipid peroxidation [67] that acts as a second messenger of free radicals and a signalling molecule interfering with the activities of various signal kinases, such as protein kinase C (PKC) and mitogen-activated protein kinases (MAPKs), to regulate cellular processes from proliferation to differentiation and apoptosis [85]. Because of its involvements, HNE is considered as particularly interesting biomolecule that might therefore play important role regulating regeneration of damaged tissue such as bone.

Therefore, the main hypothesis of this work is that lipid peroxidation and more precisely HNE may be involved in the process of bone regeneration supported by the BGs, and as such could potentially be interesting in the tissue engineering and designing of the new BGs. Reasons for this lies in fact that ionic dissolution products of BGs stimulate certain growth factors that could give rise to endogenous ROS levels. Thus generated ROS, possibly, could not be neutralised by antioxidative system of the cell, especially during the initial phase, before the boosting of antioxidative capacity, and therefore this excess of ROS can attack macromolecules, among which are lipids. Consequently, lipid peroxidation is initiated leading to generation of HNE. Since BGs support growth of bone cells, the levels of HNE should be in physiological range, not detrimental for the cell. Moreover, both HNE and growth factors were found to regulate the cell growth with the involvement of MAPK pathway (Fig. 8).
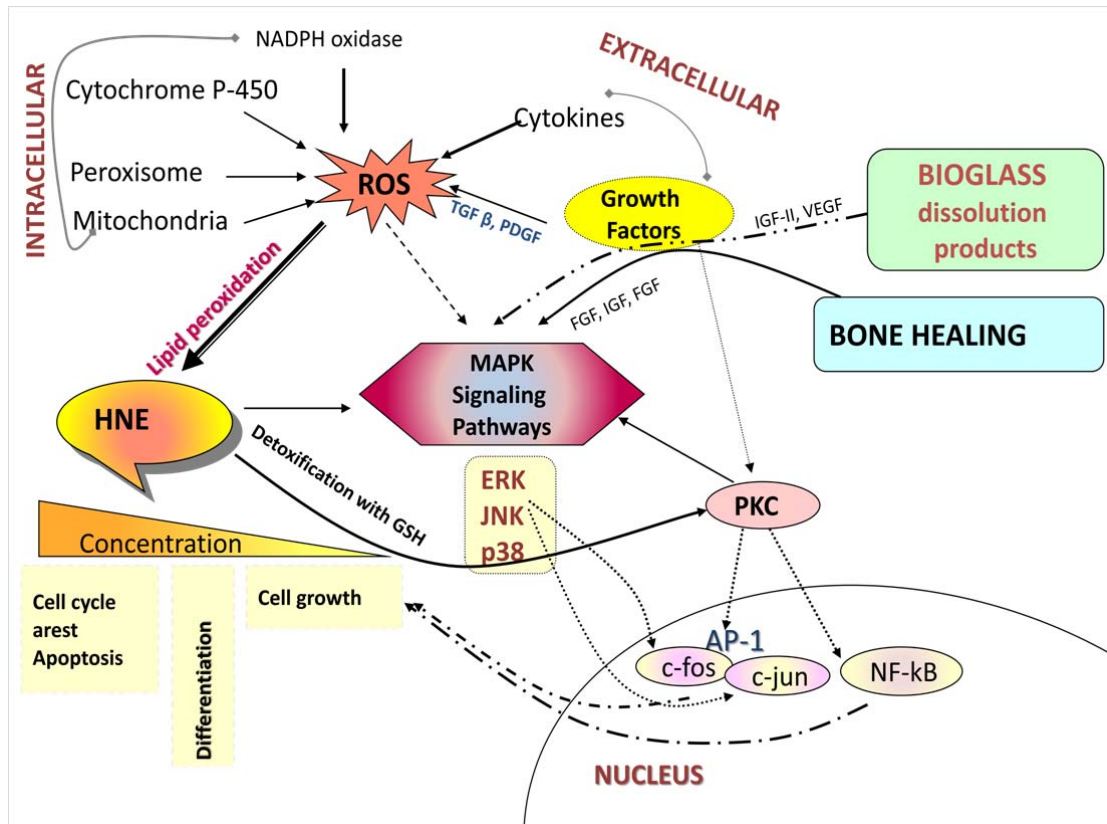
Figure 8. Possible involvement of lipid peroxidation in cell growth on the BGs

Previous research of our laboratory has elucidated HNE's role in differentiation, apoptosis and cell proliferation [89] in human osteoblast-like cells as well as its ability to increase cell growth in physiological concentration [71]. To test the hypothesis, first aim is to find whether there is a presence of HNE-protein adducts while in contact with BGs types 45S5 and 13-93 during bone growth *in vitro*.

Subsequently, if lipid peroxidation has its function in the growth of bone cells on BGs, the mechanisms involved should be revealed as well as if manipulation of lipid peroxidation, in this case, coating with HNE could more benefit the growth of bone cells on BGs. Especially implication of MAP kinase pathway will be investigated.

Furthermore, after revealing a role of lipid peroxidation in cell growth on BGs, the next step is to prepare new, more functional and potentially better BGs. It is well known that certain trace elements can improve properties of BGs. Cooper could be an interesting trace element, as it is known both as an essential cofactor of several enzymes and for its proangiogenic and

antimicrobial properties that stimulate osteogenic differentiation [90]. Copper ions are also well-known inducers of oxidative stress and consequently of lipid peroxidation [91]. Therefore, designing a novel Cu-doped BG coupled with a lipid peroxidation osteoinducing readout could provide new directions in the field of bone tissue engineering.

This work will for the first time investigate the effects of a Cu-containing BG, i.e. 45S5 Bioglass® on the growth of a human osteoblast-like cell line (i.e., HOS) and the correlation of lipid peroxidation (i.e., cellular production of HNE), with cell growth.

2. MATERIALS AND METHODS

2. MATERIALS AND METHODS

2.1. Bioactive glasses

2.1.1. Bioactive glasses 45S5 and 13-93

Commercially available bioactive glasses (BGs), types 45S5 (GL-0160 Bioactive Glass) and 13-93 (GL-0811 Bioactive Glass), were purchased as 10 cm long bars (MoSci Corporation, HyPoint North Rolla, Missouri, USA). Composition of both bioactive glasses is shown in Table 1. For experiments, these bars were cut into discs with following dimensions: 10 mm in diameter × 2 mm. Prior to use in cell culture experiments, BG pellets were sterilized by dry sterilization at 200°C for 3 hours. Sterilized discs were put in 24-well plate (TPP, Trasadingen, Switzerland) and proceeded for surface coating treatments.

Table 1. Composition of bioactive glasses 45S5 and 13-93

Typical compositions (wt%)	SiO_2	Na_2O	K_2O	CaO	P_2O_5	MgO
45S5	45	24.5	-	24.5	6	-
13-93	53	6	12	20	4	5

2.1.2. Surface coating treatments

Surfaces of BGs (MoSci Corporation), types 45S5 and 13-93 were coated with 0,5 mg/ml bovine serum albumin (Sigma Aldrich Chemie GmbH, Steinheim, Germany), 2.5 µM 4-hydroxynonenal (HNE) and with HNE-BSA adducts obtained by mixing HNE and BSA, the same concentrations as for the separate treatments. Necessary dissolutions were made with ddH_2O.

HNE was prepared from (E)-4-hydroxynonenal-dimethylacetal (HNE-DA, Alexis Biochemicals) in n-hexane. Before use, HNE-DA was activated according to the manufacturer's protocol. Briefly, HNE-DA was evaporated by nitrogen blow and 1mM HCl was added to

hydrolyze HNE for 1h. HNE concentration was determined by spectrophotometer measuring the spectra from 200 to 350 nm and calculated value upon the absorption maximum at 223nm. HNE concentration was calculated according to the formulae c(mol/l)= A×d/13750, where is c the concentration of HNE in mol/l; A-measured absorbance; d-sample dilution; 13750-molar extinction coefficient of HNE in water.

2.1.3. Evaluation of the coating efficiency - Immunochemical analysis of HNE adsorption to the glass surface

To evaluate whether the coating of the BG surfaces were efficient, normal glass (8-chamber glass slide; Thermo Scientific Nunc Lab-Tek system) was treated with different concentrations of HNE (0; 2.5; 10; 200 µM) either given alone or in combination with BSA.

Higher concentrations, than used in the coating treatments, were used to be certain that at least some results will be obtained.

Normal glass was used to be able to evaluate obtained results properly because BGs tend to form crystals when embedded in culture medium. The surface coating was made in the same manner like for BG samples and afterwards, complete medium was added to the chambers (without the cells). After 3 days, media was replaces and slide was washed twice in Phosphate buffered saline (PBS) and fixed in 10% buffered formalin.

Immunostaining for the HNE-modified proteins was carried with monoclonal antibodies obtained from culture medium of the clone "HNE 1g4", produced by a fusion of Sp2-Ag8 myeloma cells with B-cells of a BALB-c mouse immunized with HNE modified keyhole limpet hemocyanine. The antibody is specific for the HNE-histidine epitope in HNE-protein (peptide) conjugates and gives only 5 % cross reactivity with HNE-lysine and 4% with HNE-cysteine [92]. Immunostaining was performed as described before [93] using LSAB kit (DAKO, Glostrup, Denmark). Briefly, a glass slide was incubated with anti-HNE monoclonal antibodies (dilution 1:10) over night in humid chambers at room temperature, washed three times for 5 minutes with phosphate-buffered saline (PBS) and then incubated with biotinylated secondary antibody during 30 min. After washing with tris-buffered-saline (TBS), three times for 5 minutes, samples were incubated with streptavidin peroxidase during 30 min. Finally, the reaction was visualized by a DAB (3,3-diaminobenzidine tetrahydrochloride in organic solvent; DAKO, Denmark) giving a brown colour that indicated the presence of HNE. Qualitative evaluation of differences in DAB

intensity was done by inverted microscopy (Krüss Optotronic, Germany) and quantitative evaluation was done with ImageJ software.

2.1.4. Preparation of bioactive glass samples

Cu-containing melt derived BG (type 45S5) was produced by mixing analytical-grades of silicon oxide (SiO_2, Merck, Darmstadt, Germany), sodium carbonate (Na_2CO_3, Merck, Darmstadt, Germany), calcium carbonate ($CaCO_3$, Merck, Darmstadt, Germany), tricalcium phosphate ($Ca_3(PO_4)_2$, Sigma-Aldrich, Germany) and copper carbonate (($Cu_3(OH)_2(CO_3)_2$, Sigma-Aldrich, Germany). Table 2 shows the glass compositions used in this study. The raw materials were homogenized in a planetary mill and melted in a platinum crucible at 1450 °C for 45 min. The glass was fritted, pre-milled in a jaw crusher and milled in a planetary mill to the final particles size of ~5 μm. The powder was pressed to pellets (diameter 10 mm, height 2 mm) and sintered at 1050 °C for 140 min. The heating rate was 2 K/min.

Table 2. Nominal 45S5 Bioglass® derived glass compositions with different copper contents.

Glass	Composition in % (w/w)				
	SiO_2	Na_2O	P_2O_5	CaO	CuO
45S5-Ref	45	24.5	6	24.5	-
45S5-0.1Cu	45	24.5	6	24.4	**0.1**
45S5-1Cu	45	24.5	6	23.5	**1**
45S5-2.5Cu	45	24.5	6	22	**2.5**

Prior to use in cell culture experiments, BGs were sterilized by dry sterilization at 200°C for 3 hours.

2.2. Cell culture

In vitro cell culture studies were performed using the human osteosarcoma cell line (HOS, CRL 1543) as a cellular model of human osteoblastic functions. Cells were obtained from American Type Culture Collection (ATCC) and cultured in a Dulbecco's modified Eagle's medium (DMEM; Sigma-Aldrich, St Louis, USA), supplemented with 10 % (v/v) foetal calf serum (FCS; Sigma-Aldrich, Steinheim, Germany), 1 % (v/v) penicillin and streptomycin solution and incubated at 37°C in a humidified atmosphere (5% CO_2 in 95% air), with the medium change every other day. The semi-confluent cultures were detached from BG substrates with a 0.25 % (w/v) trypsin-EDTA solution for 5 minutes. Viable cells (upon Trypan Blue exclusion) were counted in a Bürker-Türk hemocytometer and used for experiments.

In every experiment cells were cultivated in the same manner with a small distinction depending whether the BGs types 45S5 and 13-93 from MoSci Company were used or newly prepared BG type 45S5 with a cooper (Cu). Since BGs from MoSci Company did not fit into the 48-well plates, these BG samples were cultivated in 24-well plates (TPP, Trasadingen, Switzerland) as follows: 2×10^4 cells in 100 µl of medium was seeded on the upper side of BG samples and left for 4-5 hours to allow cell attachment to the BG surface prior to addition of the rest of the media, 400 µl, to cover the BG samples (Fig. 9).
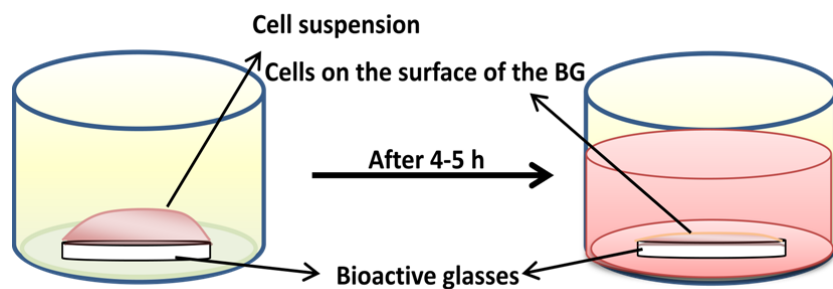
Figure 9. Protocol for cell cultivation on the BG samples, types 45S5 and 13-93 (MoSci

Company)

On the other hand, newly prepared BG samples type 45S5 with Cu were placed in 48-well plates (1 BG sample/well) (Nunc/Thermo Fisher Scientific, Roskilde, Denmark) followed by cell seeding at a density of 2×10^4 cells/well in 400 µl of the culture medium (Fig. 10).
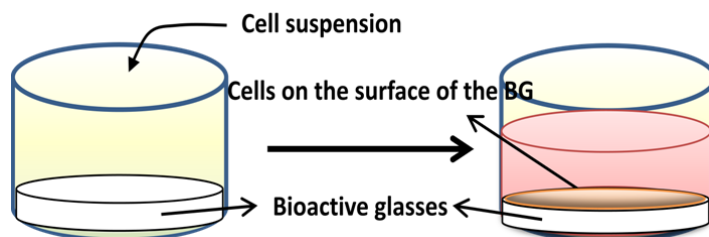
Figure 10. Protocol for cell cultivation on the BG samples, type 45S5 with cooper

2.3. Immunocytochemistry

Transparent BG samples, types 45S5 and 13-93, at day 3 of cell culturing were used for immunocytochemistry. Cells were seeded as described in previous section. Cell cultures developed on the standard histological glass served as controls.

Immunostaining for the HNE-modified proteins was carried on formalin-fixed cell samples as described in the Section 2.1.3. Qualitative evaluation of differences in DAB intensity was done by inverted microscopy (Krüss Optotronic, Germany).

The same protocol was repeated for transparent BG samples, types 45S5 and 13-93, with or without surface coatings performed at days 3, 7 and 14.

2.4. Cell proliferation

Cell proliferation on the BGs types 45S5 and 13-93 from MoSci Company was analyzed with Trypan Blue exclusion method. The method is based on the fact that viable cells have intact membranes and as such they are able to exclude trypan blue dye, while dead cell are not able to do so and as such they are blue. Cells were seeded as described in Section 3.2. and cultivated for 3, 7 and 14 days with the media changed every second day.

At specified time points cells were trypsinized with a 0.25 % (w/v) trypsin-EDTA solution for 5 minutes and based on a colour appearance, counted as live or dead in a Bürker-Türk hemocytometer.

2.5. Cell viability

Cell viability was measured at 3 different time points: days 3, 7 and 14, with the MTT assay (EZ4U; Biomedica, Vienna, Austria) according to manufacturer's instruction [94]. Briefly, the method is based on the ability of living cells to reduce slightly coloured or uncoloured tetrazolium salts into intensely coloured formazan derivatives. After addition of the dye solution, the cells were incubated at 37°C for 4 h. The optical density was measured at 450 and 620 nm as a reference, to correct the values for nonspecific background.

2.6. Cell growth and apoptosis for the BGs types 45S5 and 13-93

Cell growth on the BGs types 45S5 and 13-93 was monitored by the invert microscope (Krüss Optotronic, Germany). Detection of apoptosis, micronucleus formation and necrosis was performed at day 3 by the DAPI staining.

2.6.1. DAPI staining

For DAPI staining cells grown on BG samples were fixed in 4% formaldehyde (w/v in PBS), permeabilized for 2 minutes in ice cold methanol and stained with 1 µg/ml DAPI (4',6-diamidino-2-phenylindole; Sigma, St. Louis, USA) for 30 minutes. Before each step, samples were washed twice in PBS, respectively. The intercalation of DAPI was visualized with a fluorescence microscope (DM6000 CFS, Leica, Wetzlar, Germany) and for each sample at least 500 cells from 3 different representative areas was counted and classified as normal, apoptotic, mitotic, necrotic or with micronucleus.

2.7. Cell growth and material characterization for the BG type 45S5 with Cu

Cells were cultured and grown on the bioactive glass surfaces, as described in the section 3.2. The growth was monitored with DAPI staining and scanning electron microscopy (SEM) analysis. DAPI staining was performed at day 14 and SEM analysis was carried out at day 7, respectively. Material composition was determined by energy dispersive X-ray (EDX) analysis.

2.7.1. DAPI staining

The procedure for the DAPI staining was as described in the section 2.6.1. Images were obtained with a fluorescence microscope (DM6000 CFS, Leica, Wetzlar, Germany).

2.7.2. SEM and EDX analysis

For SEM analysis, the cell culture medium was removed and the BG samples were washed with PBS, fixed with a solution containing 3 % (v/v) glutaraldehyde (Sigma, Taufkirchen, Germany) and 3 % (v/v) paraformaldehyde (Sigma, Taufkirchen, Germany) in 0.2 M sodium cacodylate buffer (pH 7.4) and finally rinsed three times with PBS. All samples were dehydrated in a graded ethanol series (30, 50, 75, 90, 95 and 99.8 % (v/v)). Samples were maintained at 99.8 % (v/v) ethanol and critical-point dried. Prior to SEM examination the samples were sputtered with gold and analyzed on an ESEM (Quanta 200, FEI, Netherlands) equipped with secondary electron and backscattered electron detectors. The operating voltage was 20 kV. Energy dispersive X-ray (EDX) analysis was performed to determine materials composition in areas of interest.

2.8. Analyses of ROS production

Cells were cultivated on the BG samples in quadruplicates for 72 hours. Analyses of ROS production were performed with addition of a nonfluorescent probe for intracellular ROS detection 2',7'-dichlorofluorescin diacetate (DCFH-DA, Fluka), final concentration 10 µM, to cell medium on the day 3. This cell-permeable dye remains nonfluorescent inside the cell until the acetate groups are removed by intracellular esterases and oxidized by intracellular ROS to the

fluorescent compound 2',7'-dichlorofluorescein (DCF) which can be detected as a measure of intracellular ROS. Fluorescence intensity was observed with a microscope (Zeiss Axiovert 25).

For quantification of intracellular ROS, samples prepared on the same way as previously described, were trypsinized and resuspended in 500 µl of Hanks' Balanced Salt Solution (HBSS). Technical duplicates of 200 µl were plated into white 96-well plates (Nunc, Roskilde, Denmark) and the fluorescence intensity was measured with a Cary Eclipse fluorescence spectrophotometer (Varian, USA) with excitation at 500 nm and emission at 529 nm. The arbitrary units were based directly on fluorescence intensity.

2.9. Dot-blot analysis

On days: 3, 7 and 14, cells were scraped from the BG surface in PBS and collected. Cell lysates were prepared by a freeze/thaw cycle. Prior to the immunoblot analysis, protein content in each sample was measured by the Bradford method [95]. A dot-blot analysis was performed, in cell lysates with adjusted protein content to 100 µg/ml, as previously described[96]. Briefly, 100 µl of each sample was loaded on a nitrocellulose membrane (Bio-Rad Laboratories, Hercules, CA, USA) and washed twice with PBS before blocking of the membrane in 2% (w/v) nonfat dry milk (Bio-Rad Laboratories, Hercules, CA, USA) in PBS for 1 hour at room temperature (RT). The membrane was then incubated overnight with mouse monoclonal antibody directed against HNE-histidine epitope. Next day, after blocking of endogenous peroxidases, the membrane was incubated with a secondary antibody (EnVision; Dako North America, Carpinteria, USA) for 1 hour/RT and immune complexes were visualized using 3,3'-diaminobenzidine (DAB; Dako North America, Carpinteria, USA) and scanned for quantification of signals. Signals were analyzed in ImageJ, a Java-based image processing program.

The results were recalculated from the standard curve prepared with HNE-BSA standards (0; 0.5; 1; 2.5; 5; 10; 20) and expressed as nmol of HNE-protein adducts/mg of proteins.

2.10. Cell differentiation – Alkaline phosphatase staining

At two time points, days 3 and 14, cells grown on BG samples (MoSci) were stained for alkaline phosphatase (ALP) by NBT/BCIP assay (Roche, Switzerland). This assay is based on a chromogenic reaction initiated by the cleavage of the phosphate group of BCIP by alkaline phosphatase present in the cells. Cell cultures were washed three times with tris-buffered saline

(TBS), pH 7.0 and fixed with 4% buffered paraformaldehyde for 30 minutes at 4°C. Staining was performed by adding 200 μl/well of stain and incubated at 37°C for 60 minutes. Images of purple precipitates were taken and analysed with ImageJ software.

For quantification, insoluble purple precipitates were solubilised with 200 μl of SDS 10% HCl and incubated for 18 h. The optical density measurement was done at 595 nm.

2.11.   Detection and quantification of mineralization with Alizarin Red

At day 14 the extent of matrix mineralization on the cell/BG samples (n = 3) was semi-quantified using Alizarin red staining, which binds to the Ca^{2+} of calcium deposition. Briefly, the BG samples were washed twice with PBS and fixed with 10% neutral buffered formalin for 30 min at room temperature. The samples were washed with distilled water (dH_2O) and incubated with 2% (w/v) Alizarin red S (Sigma-Aldrich) in dH_2O, pH 4.1, for 1 hour at room temperature. After which, unincorporated dye was washed away using several rinses of dH_2O. Images were taken on light microscope (Zeiss Axiovert 25).

 To quantify mineralization, Alizarin red–stained cells were solubilised in 0.5 N HCL and 5% SDS for 30 min and detected at 405 nm using a LabSystems Multiscan MS microplate reader. Quantification will be done according to the standard curve prepared by the modification of the Osteogenesis assay kit (Millipore) protocol. Briefly, standard curve will be prepared with different concentration of Alizarin Red stain (0 - 2mM) diluted in 0.5 N HCL and 5% SDS.

2.12.   RNA isolation and reverse transcription

Total RNA was extracted from cells grown on BGs samples, types 45S5 and 13-93, with or without surface coating on days 3 and 14. To ensure enough sample, on day 3 octaplicates were pulled together and for day 14 triplicates were pulled together. RNA was extracted using TRIzol Reagent (Invitrogen, Carlsbad, CA, USA) according to the manufacture's recommendation with minor modifications.. Briefly, homogenized samples were incubated for 15 minutes at room temperature and treated with 0.2 ml 1-Bromo-3-chloropropane (Sigma, St. Louis, MO, US) per ml TRIzol reagent. Aqueous phase was collected in new tube and proceeded to the RNA isolation with an RNeasy Mini kit (Qiagen, Hilden, Germany) while the organic phase was saved for protein isolation. On the aqueous phase 0.5 ml 70% ethanol per ml of TRIzol reagent was added

and transferred to an RNeasy spin column placed in a 2 ml collection tube and centrifuged for 15 s at ≥8000 x g. Spin column was reused for successive aliquots. Then the column was washed with RW1 buffer and RPE buffer, and RNA was eluated in 30 µl of RNase-free water.

RNA was quantified and assessed for purity by Nanodrop (ThermoScientific, Waltham, MA, USA). One microgram of total RNA was reverse transcribed using the QuantiTect Reverse Transcription Kit (Qiagen, Hilden, Germany) according to the manufacturer's instructions. The final volume of the reaction was 20 µl.

2.13.   Primer

Primers sequences were designed based on literature references and purchased from Eurofins MWG Operon (Ebersberg, Germany). Glyceraldehyde-3-phosphate dehydrogenase (GAPDH) was used as an „house-keeping" gene. PCR products showed a single melting peak in the melting analysis and a single band on an agarose gel (2.5% agarose in 1-fold TBE running buffer). Sequence specificity was verified by sequence analysis (3730 DNA Analyzer; Applied Biosystems, Foster City, CA, US). Sequences of primers are summarized in Table 3.

Table 3. Sequences of primers used for Real Time-PCR

Primer	RefSeq	Sequence	Amplicon	Ref.
Alkaline phosphatase	J04948	Forward-CCTACACGGTCCTCCTATAC	110	[97]
		Reverse-TGACTGCTGCCGATACTC		
Collagen type I	NM000088	Forward-GTGATGCTGGTCCTGTTGGT	123	[98]
		Reverse- CACCATCGTGAGCCTTCTCT		
Osteocalcin	NM199173	Forward- AGCGAGGTAGTGAAGAGAC	142	[97]
		Reverse- GAAAGCCGATGTGGTCAG		
Osteoprotegerin	NM002546	Forward- GCAGCGGCACATTGGACATG	135	[97]
		Reverse- AGGATCTGGTCACTGGGTTTGC		
Osteopontin	NM000582	Forward- GCGAGGAGTTGAATGGTG	140	[99]
		Reverse- CTTGTGGCTGTGGGTTTC		
Osteonectin	J03040	Forward- TCTTCCCTGTACACTGGCAGTTC	73	[97]
		Reverse- AGCTCGGTGTGGGAGAGGTA		
Glyceraldehyde-3-phosphate dehydrogenase	BT006893	Forward- CCACTCCTCCACCTTTGAC	102	[100]
		Reverse- ACCCTGTTGCTGTAGCC		

2.14.   Real time PCR

Real time PCR amplification and melting analysis were performed using a LightCycler 480 System (Roche Diagnostics GmbH, Mannheim, Germany). For the reaction, 20 ng cDNA was added to a reaction mix containing LightCycler 480 SYBR Green I Master (Roche Diagnostics GmbH, Mannheim, Germany) and 25 µM of each primer giving a final reaction volume of 20 µl. The PCR reaction mixture was subjected to an initial denaturation at 95°C for 10 minutes, followed by 45 cycles of denaturation at 95°C for 10 seconds, annealing at 60°C at 20 seconds and elongation at 72°C for 15 seconds. Melting analysis started with an initial denaturation at 95°C for 5 seconds followed by an increase in temperature from 65°C to 90°C with 10 acquisitions per degree. All qRT-PCR reactions were conducted in duplicate and the quantification cycle values were averaged. Gene expression was calculated by the comparative Ct method. GAPDH was used as reference gene.

2.15.   Protein isolation

Organic phase left during RNA isolation with TRIzol reagent was used for protein isolation according to the manufacturer's instructions. Protein concentration in each sample was measured according to Bradford method [95].

2.16.   Western blot analyses

Samples, containing the same amount of protein, were prepared with Laemmli buffer, heated at 95°C for 10 min and subjected to SDS-polyacrylamide gel electrophoresis (SDS-PAGE, 10%). After electrophoresis the separated proteins were transferred onto nitrocellulose membrane and probed for MAPKs using specific antibodies, according to the manufacturer's protocol.

The primary antibodies, all obtained from Cell Signalling (Austria) include the following: three rabbit antibodies from the MAPK family antibody sampler kit (catalogue no. 9926S), anti-p44/42 MAPK (ERK1/2; clone 137 F5), anti-SAPK/JNK (clone 56G8), or anti-p38 MAPK; three rabbit antibodies from the Phospho MAPK family antibody sampler kit (catalogue no. 9910S), anti-phospho-p38 MAPK (Thr180/Tyr182; clone D2F9), anti-phospho-p44/42 MAPK (ERK1/2; Thr202/Tyr294; clone D13.14.4E), or anti-phospho-SAPK/JNK (Thr183/Tyr185; clone 81E11); rabbit anti. A secondary antibody against rabbit IgG, conjugated with horseradish peroxidase

(HRP; Cell Signalling) was used in all cases, and signal was detected using enzyme-linked chemiluminescence with ECL Reagent (Calbiochem). Visualization of bound secondary antibody was done by Uvitec (Cambridge, UK).

The chemiluminescent signal was quantified from densitometric readings of digital images using ImageJ software.

2.17.   Statistical analysis

All assays were performed in at least triplicates and repeated in, at least, two independent experiments. Values were expressed as means ± SD. Unless otherwise stated, comparisons between groups were assessed by a two-tailed Student's t-test considering values of $p < 0.05$ as significant.

3. RESULTS

For more convenience and better fluency of obtained results, this Section is separated into two parts:

3.1. Results obtained with the commercially available BGs, types 45S5 and 13-93 and

3.2. Results obtained with the BG, type 45S5, with cooper, received from our colleagues from the Institute of Biomaterials, at the Department of Materials Science and Engineering, University of Erlangen-Nuremberg, Germany.

3.1. Results obtained with the bioactive glasses, types 45S5 and 13-93 (MoSci)

3.1.1. Immunochemical analysis of HNE adsorption to the glass surface

To evaluate whether the coating of the BG surfaces were efficient normal glass slide was treated with different concentrations of HNE (0; 2.5; 10; 200 µM) either given alone or in combination with BSA. Results have shown that even 2.5 µM HNE can be detected by monoclonal antibody used for immunocytochemistry. What is more important, there is no difference if the coating was done with just HNE in comparison to the one done with HNE-BSA, nevertheless that monoclonal antibody recognizes HNE bounded to the histidine residues of proteins. Therefore it can be concluded that coating treatment is successful and obtained results are due to the effect of HNE (Fig 10).
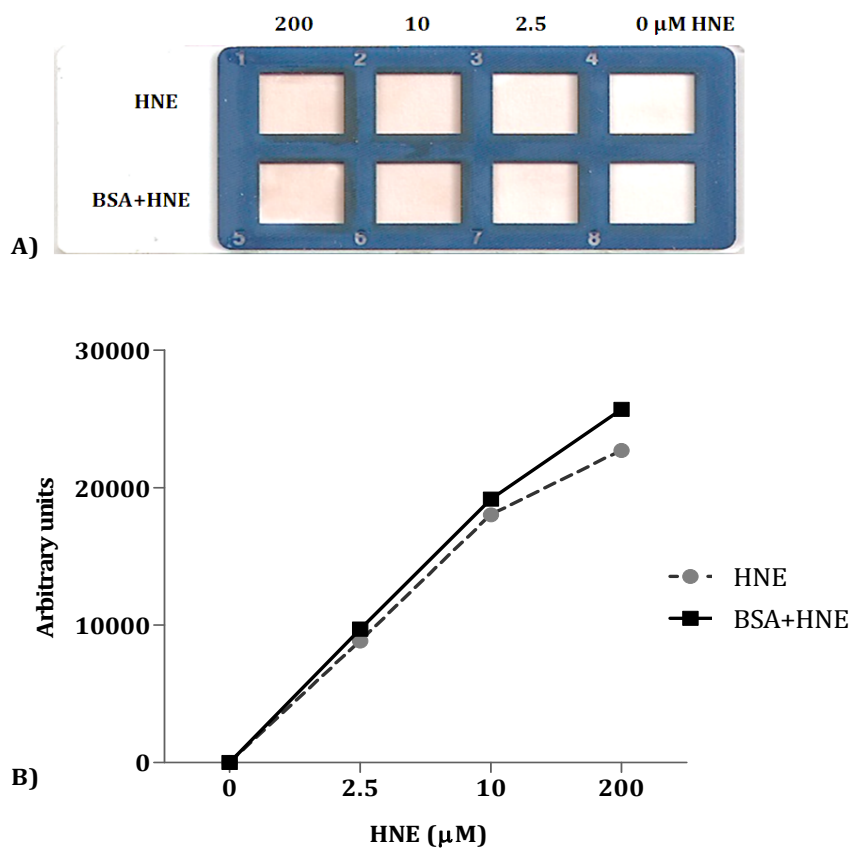

Figure 10. Efficiency of a coating treatment

    A) Picture of a glass slide after immunochemical detection with anti-HNE monoclonal antibody

    B) Semiquantification of the obtained results with ImageJ

3.1.2. Immunochemical analysis of cells grown on BGs

Immunochemical analysis revealed that during incubation of human osteoblast-like cells *in vitro* on BGs types 45S5 and 13-93, HNE is generated in the cells. Contrary, HNE-protein adducts were not observed in cells that were grown on the normal histological glass (Figure 11.).
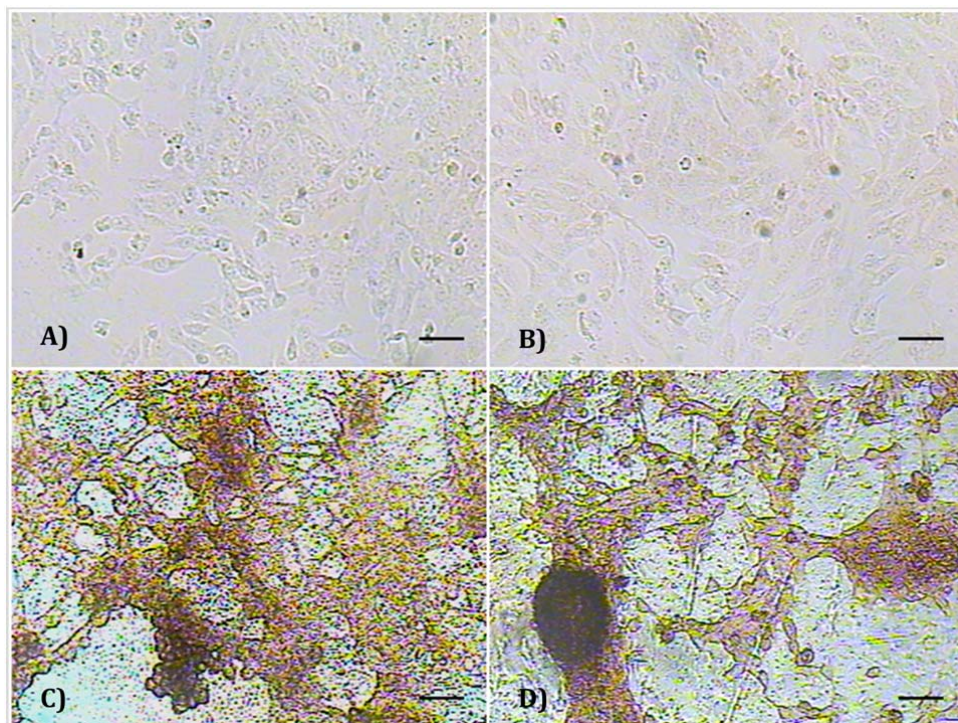
Figure 11. Immunochemical detection of the HNE-histidine adducts done by specific monoclonal antibodies after three days cultivation of HOS cells on standard histological glass or on BGs. Scale bar: 50 μm.

(A) HOS cell cultured on normal standard histology glass - negative control (without addition of primary antibody while proceeding immunostaining) - no brown coloured immunostaining can be observed;

(B) HOS cell cultured on normal standard histology glass - no brown coloured immunostaining can be observed either;

(C) HOS cell cultured on BG type 45S5 - intense brown colour can be observed showing abundant presence of HNE-protein adducts within the cells

(D) HOS cell cultured on BG type 13-93 with intense brown colour can be observed showing abundant presence of HNE-protein adducts within the cells

Cells grown on standard histological glass were growing as typical monolayer cultures and did not produce endogenous HNE-protein adducts, while those grown on BG were growing overlapping in a tissue-like form producing abundant HNE. Quadruplicates of cultures were prepared for type of glass, while representative images are presented on the Figure 11.

The immunocytochemical analysis was repeated for the BG samples coated with BSA, HNE and BSA-HNE and are given in Figure 12.
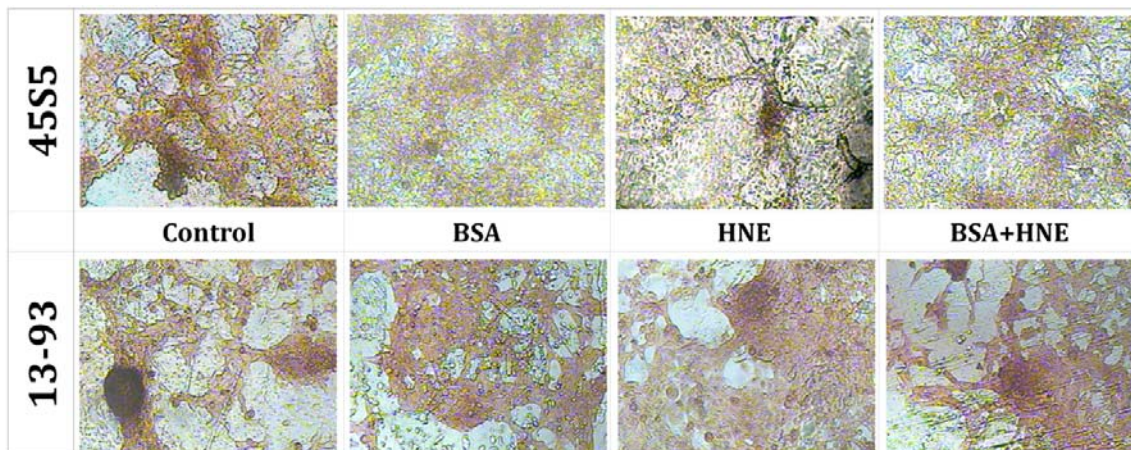

Figure 12. Immunochemical detection of the HNE-histidine adducts after 3 days in cell culture

Immunochemical detection of HNE present in cells has revealed very interesting results. HNE was also detected in cells that were grown on control and BSA coated BG samples implicating its possible role in osteogenesis.

3.1.3. Analyses of ROS production

To further reveal if the HOS cells grown on BGs undergo physiological oxidative stress manifested by ROS and HNE production, presence of endogenous ROS production during cell growth on the BGs was determined by specific fluorescence method (DCF, Figure 13).
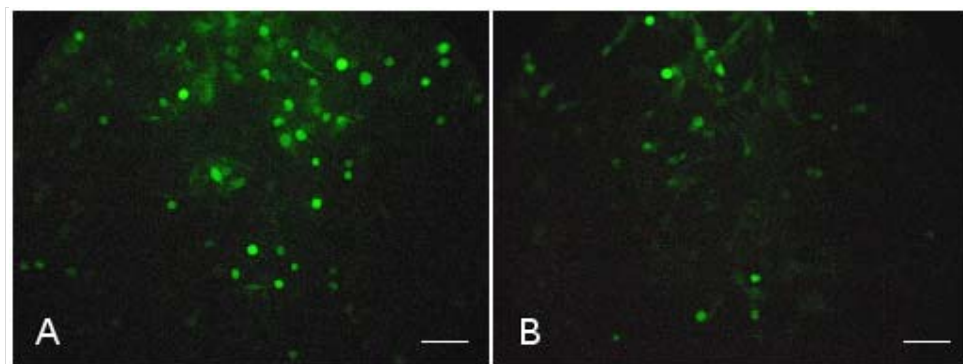

Figure 13. Detection of intracellular reactive oxygen species produced by HOS cells cultured for 3 days on BGs.

Reactive oxygen species (ROS) were visualized by fluorescence using 2',7' dichlorofluorescein (DCF). Scale bar: 100 μm.

A) HOS cells cultured for 3 days on BG type 45S5 – several cells show strong positivity of the endogenous ROS production, in particular if growing in the upper layer of the tissue-like culture

B) HOS cells cultured for 3 days on BG type 13-93 – as in case of 45S5 type BG, several cells show strong positivity of the endogenous ROS production, in particular if growing in the upper layer of the tissue-like culture

Quadruplicates of cultures were prepared for each BG, while representative images are presented on the Figure 13.

To quantify ROS levels, analysis of ROS production was carried out in cell lysates grown on differently coated surfaces. Results have shown that in all samples there is a significant increase of endogenous ROS production in comparison to the control (cells grown on polystyrene plastic in 48-well plates) with the $p < 0.001$, with exception for the sample 13-93 ($p < 0.005$).

Moreover, when samples were compared with its own control, BGs 45S5 and 13-93, significant increase in endogenous ROS was observed in samples that were coated with BSA for both BGs (45S5 B $p < 0.05$; 13-93 B $p < 0.001$) while coating with BSA+HNE increased ROS levels significantly just for 13-93 BG.
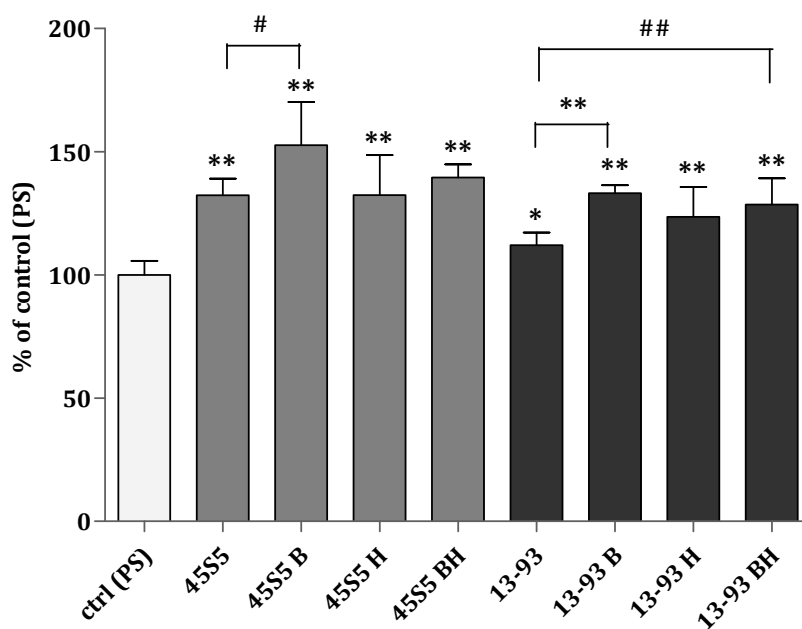
Figure 14. Analysis of ROS production measured with a Cary Eclipse fluorescence

Spectrophotometer

Marks: H – HNE; B – BSA; BH- BSA+HNE

# $p<0.05$; ## $p<0.01$; * $p< 0.005$; ** $p<0.001$

Results support immunocytochemical detection of HNE-protein adducts, since ROS should be primarily formed to initiate a process of lipid peroxidation and thus generation of HNE.

3.1.4. Cell proliferation

Results of cell proliferation are given in Figure 15. Stimulatory effect of the HNE treatment could be seen in all time points for BG type 45S5, with the significance $p < 0.05$ on day 7. BG type 13-93 is showing the same effect with the exception of day 3.
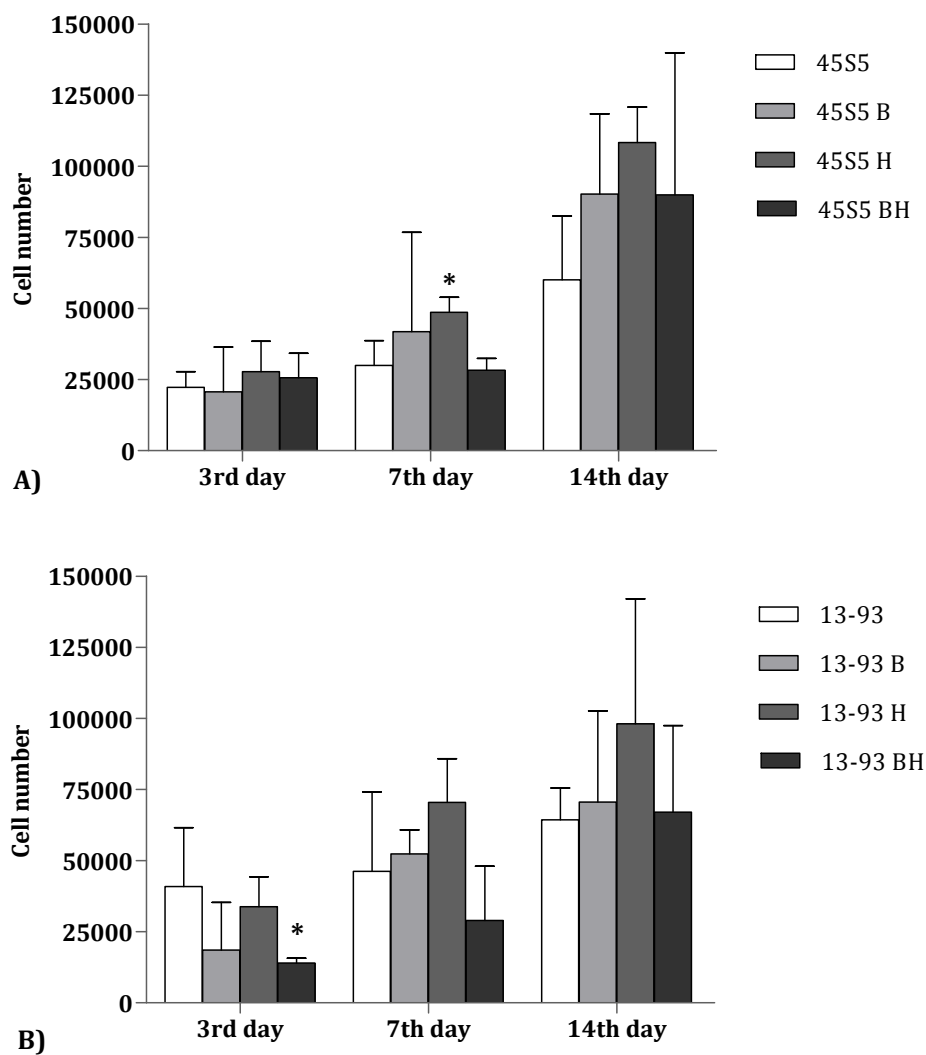
Figure 15. Proliferation of human osteoblast-like cells grown on the surface of the BGs A) type 45S5 and B) 13-93.

Marks: H – HNE; B – BSA; BH- BSA+HNE

$* p < 0.05$

While on the BG type 45S5 other coating treatments (BSA or BSA+HNE) excert mildly stimulatory effect, in the case of BG type 13-93, coating with the BSA-HNE tends to show a negative effect which is the most pronounced on day 3 ($p<0.01$). This negative effect is decreasing with the culture period and on day 14, there is approximately the same number of cells like on the control sample (without coating).

3.1.5. Cell viability

Cell viability was measured at 3 time points, days 3, 7 and 14. Stimulatory effect was seen for all coating treatments for BG 45S5 in comparison to the control but with slight differences regarding the time points.
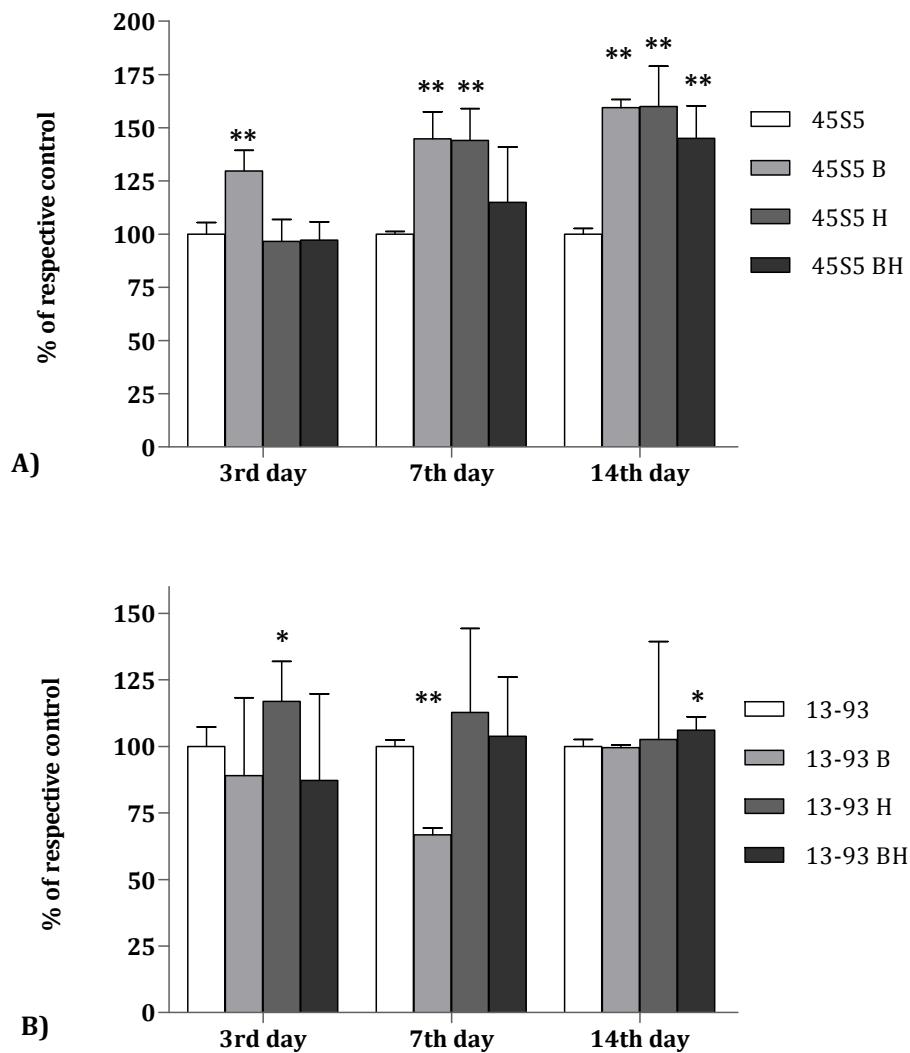
Figure 16. Cell viability of BG samples: A) 45S5 and B) 13-93

Marks: H – HNE; B – BSA; BH- BSA+HNE

* p< 0.01; ** p<0.001

Sample 45S5-B significantly increased cell viability in all time points (p<0.001). Samples 45S5-H and 45S5-BH did not increase viability in the first days of the cell culture, but later on. In case of 45S5-H, viability was significantly increased on days 7 and 14 (p<0.001) while sample 45S5-BH showed enhanced viability just after 14 days in cell culture (p<0.001).

On the other hand, BG 13-93 did not express such stimulatory effect but rather just a mild one, which was significantly increased in samples 13-93-H and 13-93-BH (p<0.01) on days 3 and 14, respectively. In sample 13-93-B, on day 7, significant decrease in cell viability was observed (p<0.001).

3.1.6. Cell growth and apoptosis

Genotoxycity analyses have shown that treatments are not harmful for cells (compared to control BGs that are currently used in reconstructive medicine) and no significant difference between BGs was observed (Fig 17).
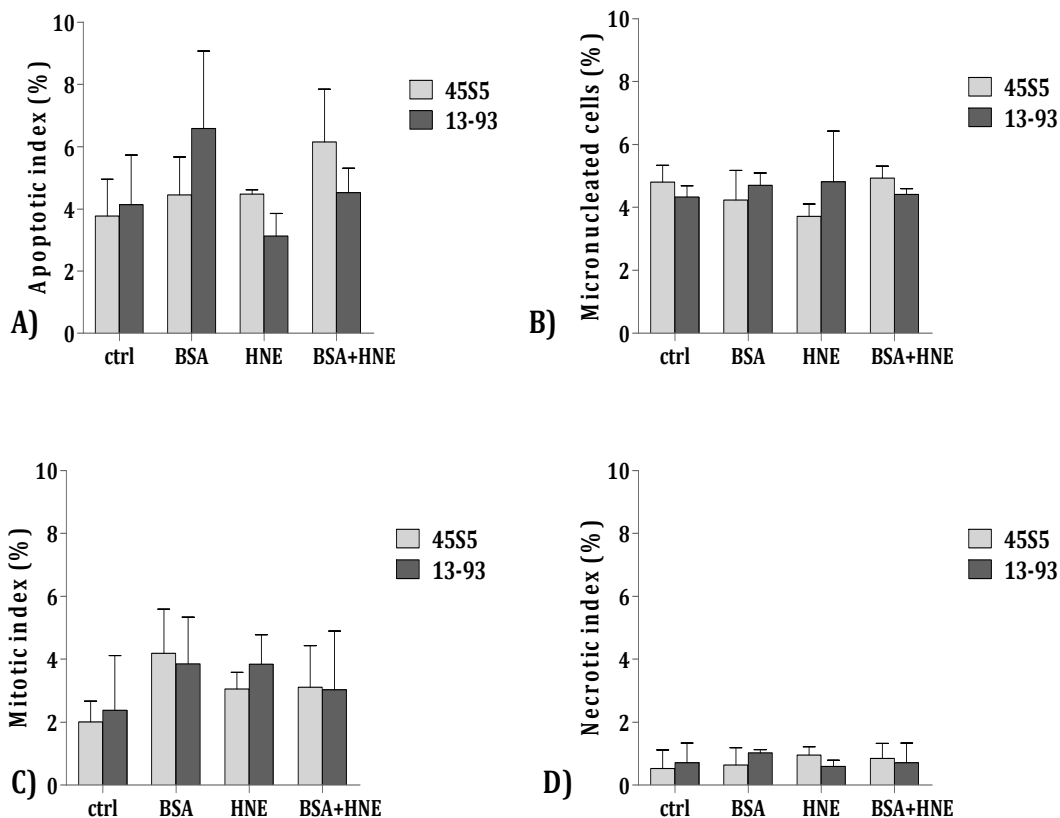
Figure 17. Analyses of: A) apoptotic, B) micronucleated, C) mitotic and D) necrotic cell index after 3rd day of human osteoblast-like cells growth on BGs types 45S5 and 13-93

3.1.7. Dot-blot analysis

Results for BG type 45S5 have shown a gradual increase in concentration of HNE-protein adducts for all surface coatings and for all time points, with the exception for the sample 45S5-BH in which a decrease can be seen on day 14 (Fig. 18 A).

From statistical point of view, if compared with the references sample, 45S5, for the specific time point, then a significant increase can be seen: on day 3 in all samples (45S5-B ($p<0.05$); 45S5-H and 45S5-BH ($p<0.001$)); on day 7 just in 45S5-BH ($p<0.05$); and on day 14 in samples, 45S5-B and 45S5-H ($p<0.05$). When all BG samples type 45S5 were compared with the initial concentration obtained for the reference sample (45S5 on day 3), with the exception of the sample 45S5 on day 7, all other samples are showing significant increase in the concentration of HNE-protein adducts with $p<0.05$, or $p<0.005$ for samples: 45S5-B and 45S5-H (on day 7) and 45S5-B (on day 14); and even $p<0.001$ for 45S5-BH (on day 3) and 45S5 (on day 14).
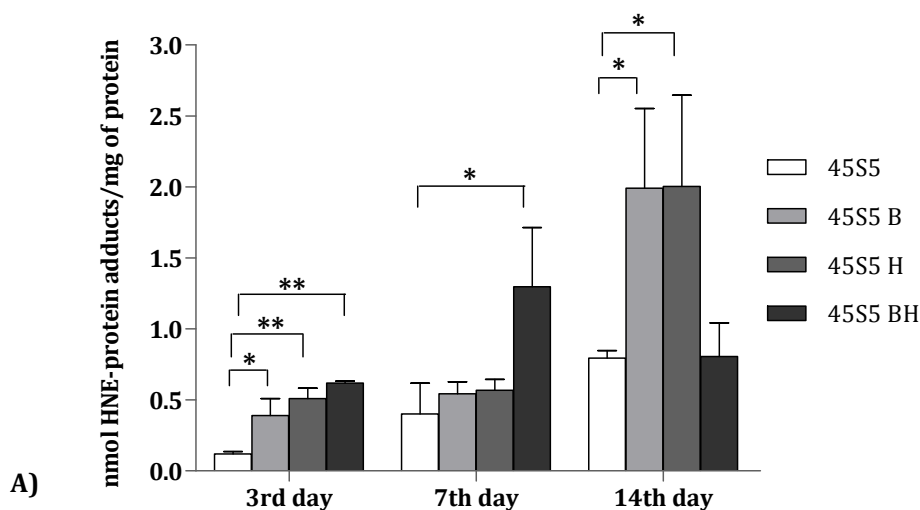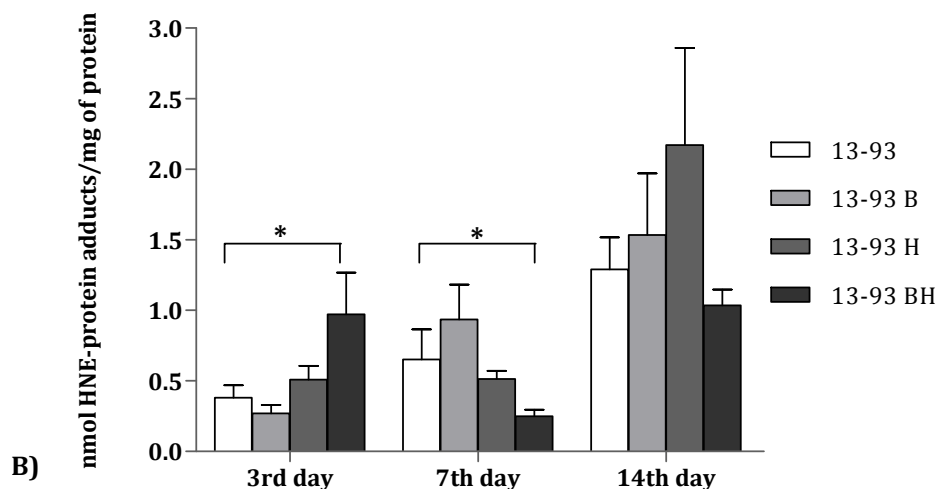
Figure 18. Dot-blot analysis of the cell lysates grown on the BG samples: A) 45S5 and B) 13-93

       Marks: H – HNE; B – BSA; BH- BSA+HNE

       * p< 0.05; ** p<0.001

As seen for BG type 45S5, results obtained with the type 13-93, are showing the same trend, gradual increase of HNE-protein adduct in all samples and again with the exception for the sample treated with BSA+HNE (Fig. 18 B).

Statistically, when compared with the references sample, 13-93, for the specific time point, significant increase in HNE-protein adduct can be seen in 13-93-BH on day 3 (p<0.05) while, on the other hand, significant decrease was observed in 13-93-BH on day 7 (p<0.05). When all BG samples type 13-93 were compared with the initial concentration obtained for the reference sample (13-93 on day 3), increase in concentration of HNE-protein adducts was seen in: 13-93-BH (day 3) and 13-93-B (day 7) with p<0.05; 13-93 (day 14) with p<0.005; as well as in 13-93-B and 13-93-H (day 14) with p<0.001. In contrast, sample 13-93-BH on day 14 has shown a significant decrease with p<0.001.

When both types of BGs were compared one to another, the same time point and the same treatment, there were few differences observed, like in reference samples (45S5 and 13-93) on day 3, with higher levels measured in 13-93 (p<0.01). Another example is coating treatment with BSA+HNE on day 7, which showed higher levels of HNE-protein adducts in BG type 45S5. The last difference was observed in reference samples again on day 14, with higher levels seen in BG 13-93.

3.1.8. Cell differentiation – Alkaline phosphatase staining

Obtained results were observed under the light microscope as well as semiquantitatively (Fig. 19).

Staining for ALP, which is a marker of osteoblast differentiation, has revealed some similarities and differences depending on the type of the BG used.

Both types of BGs have shown increase in ALP on day 14 if compared to the same sample on day 3, which was statistically significant for samples: 45S5 ($p < 0.05$), 45S5 H ($p < 0.001$), 13-93 H ($p < 0.01$), 13-93 BH ($p < 0.001$) (Fig. 19 B).

While there were no differences between the surface coating treatments and control sample for BG type 45S5 on day 3, in case of BG type 13-93 a significant decrease in ALP was observed in coatings with HNE ($p < 0.01$) and BSA+HNE ($p < 0.001$) (Fig. 19 B).

On the other hand, significant increase of ALP was observed in the sample of the BG type 45S5 coated with HNE ($p < 0.005$) while for the BG type 13-93 there is a tendency of ALP increase in samples coated with HNE and BSA+HNE (Fig. 19 B).

A)
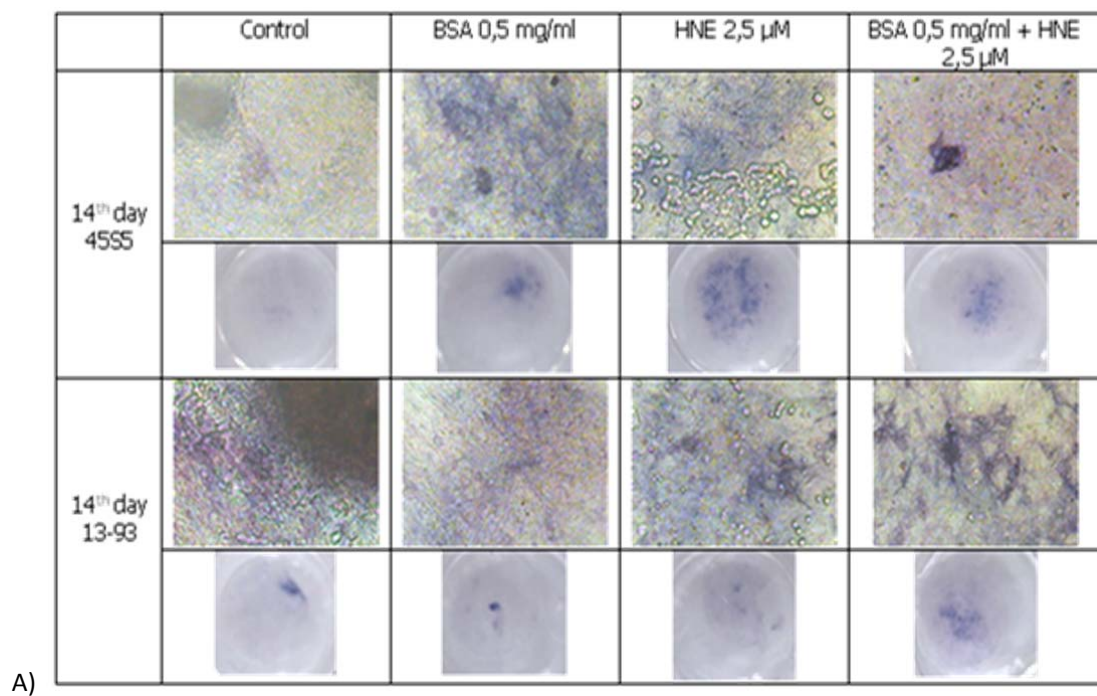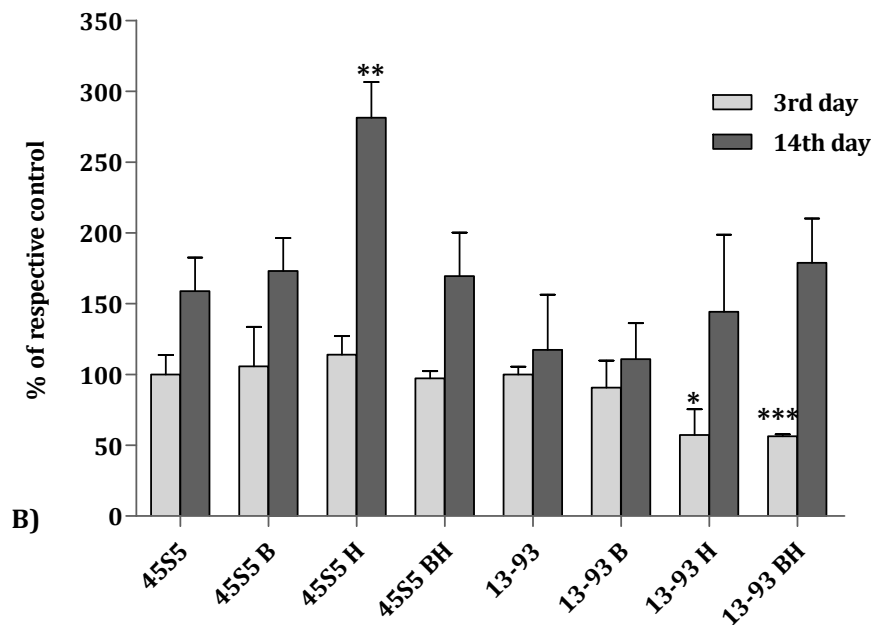
Figure 19. Observation of cell differentiation detected with alkaline phosphatase staining:

A) under a light microscope (magnification 200x; pictures in upper row for each bioactive glass) and on the surface of bioactive glass discs (below row for each bioactive glass);

B) quantification of observed differentiation with VersaDoc

* p< 0.01; ** p<0.005; *** p<0.001

3.1.9. Cell mineralization – Alizarin Red staining

Results of mineralization of cells grown on the BG samples are given in Fig 20.

On BG samples type 13-93, spherical cell structures are the most intensively stained but also some smaller nodal formations can be seen in all samples. BG samples type 45S5 have shown more evenly distributed staining with some nodal formation, especially observed in reference sample (Fig. 20 A).

A)

Standard curve

$y = 0.213x + 0.0451$
$R^2 = 0.9995$

B)
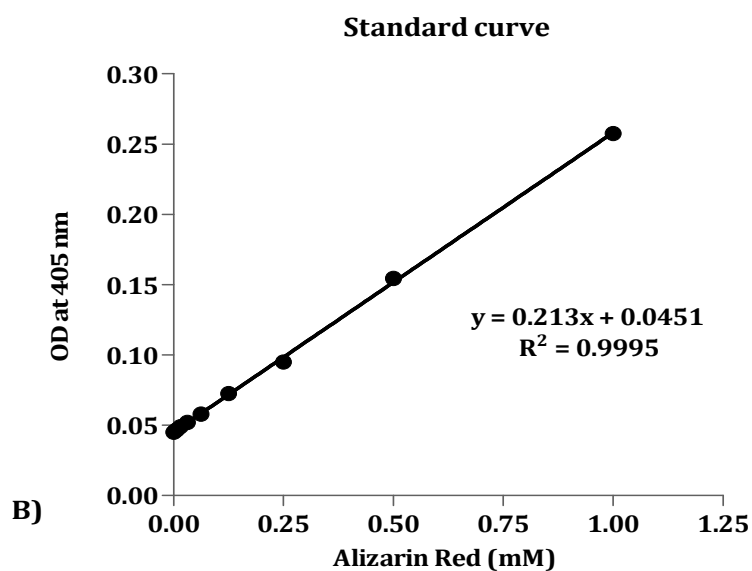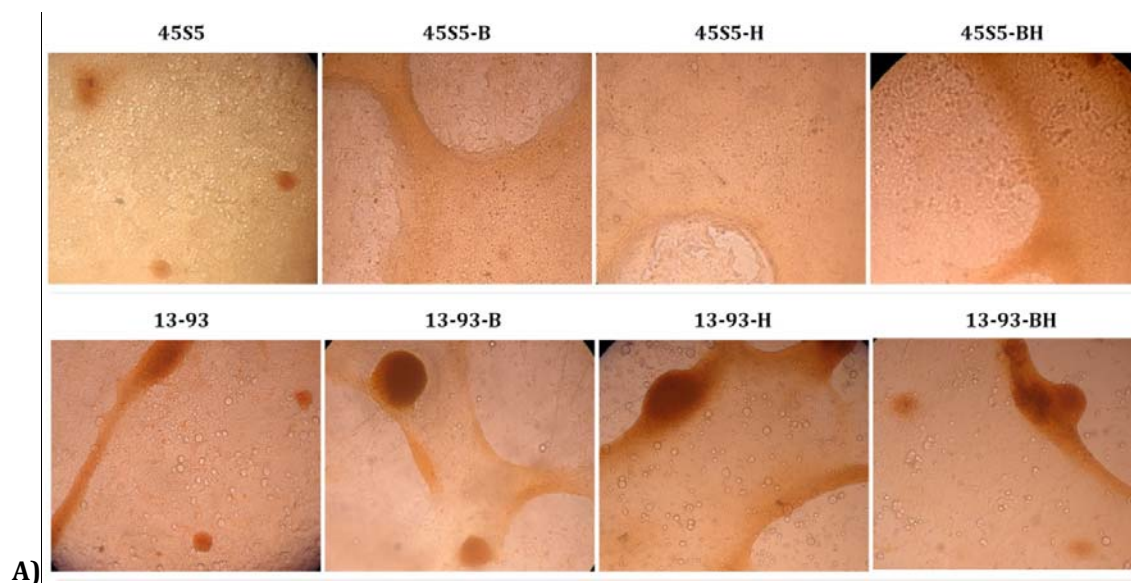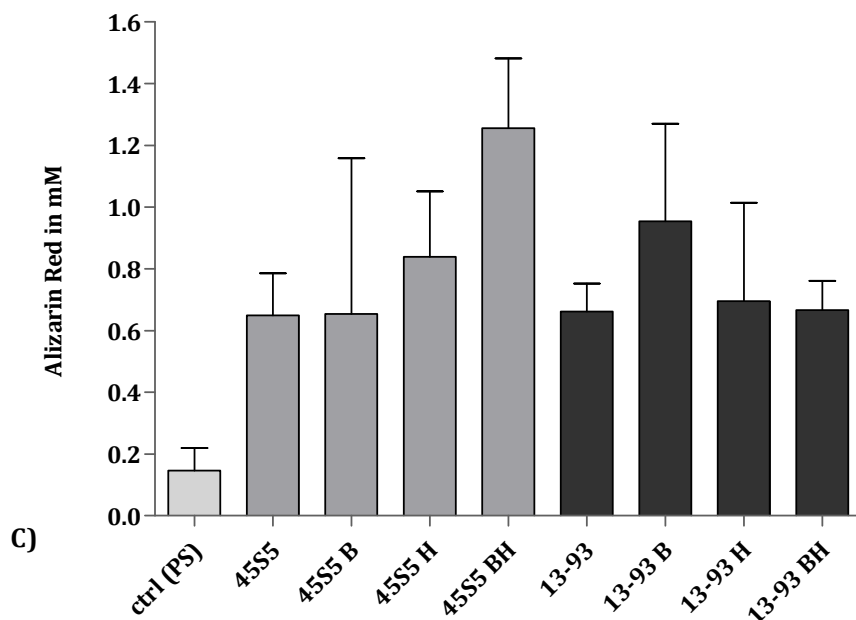
Figure 20. Detection of cell mineralization on the day 14 of cell culture – staining with Alizarin
Red

A) Observed under light microscope

B) Standard curve prepared with different concentrations of Alizarin Red diluted in 0.5 N
HCl and 5% SDS

C) Concentration of Alizarin Red in mM, recalculated from the standard curve

In all BG samples there is a significant increase in mineralisation of extracellular matrix observed in comparison to the control sample, cells grown in 48-well plate on polystyrene plastic ($p<0.005$). The only exception was sample 45S5-B who showed the same tendency but due to high standard deviation, it was not statistically significant.

3.1.10. Real time PCR

Results of relative expression of genes for alkaline phosphatase (ALP), type I collagen (COL1), osteocalcin (OC), osteoprotegerin (OPG), osteonectin (ON), osteopontin (OPN) were shown in Figure 21. GAPDH was used as a reference gene. Gene expression was determined on days 3 and 14 (Fig. 21 A-F).

C)

D)
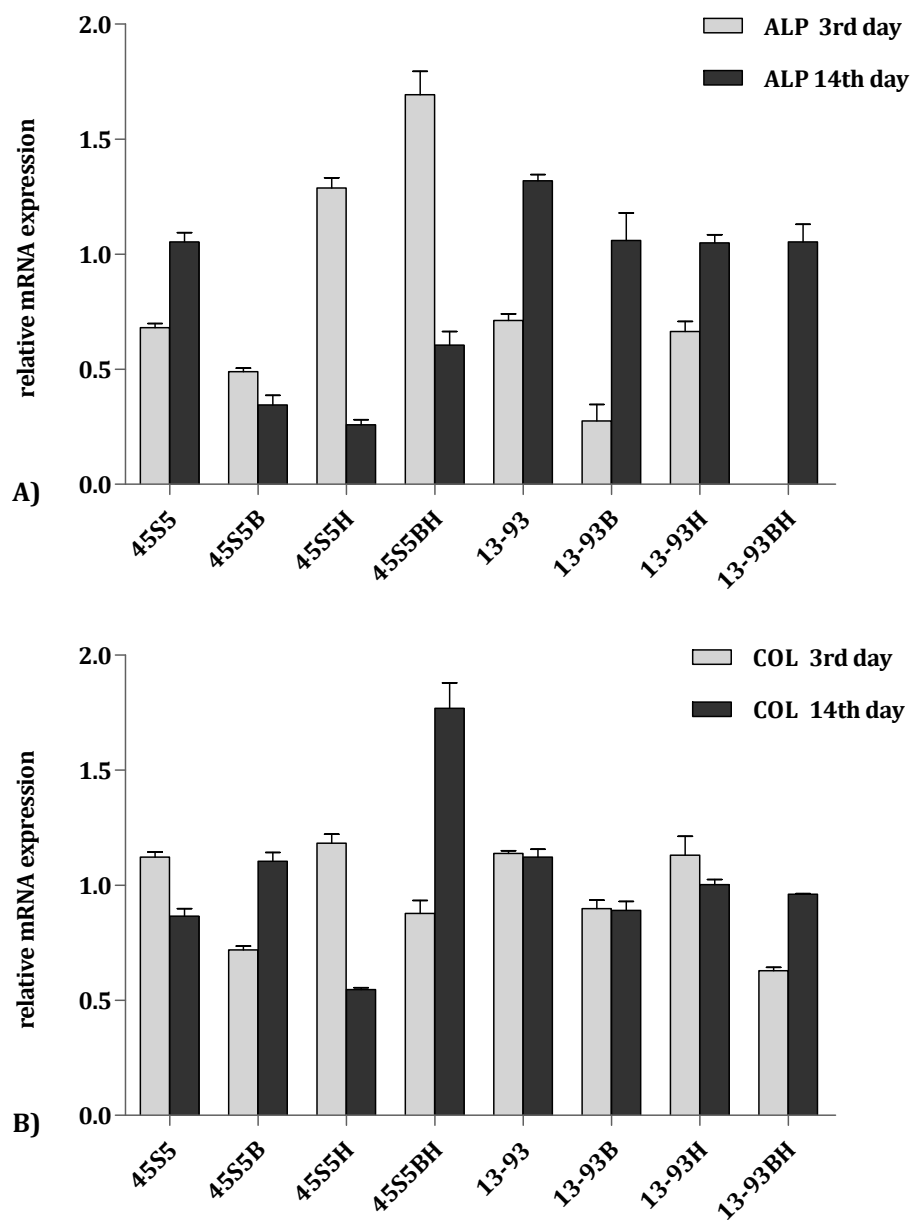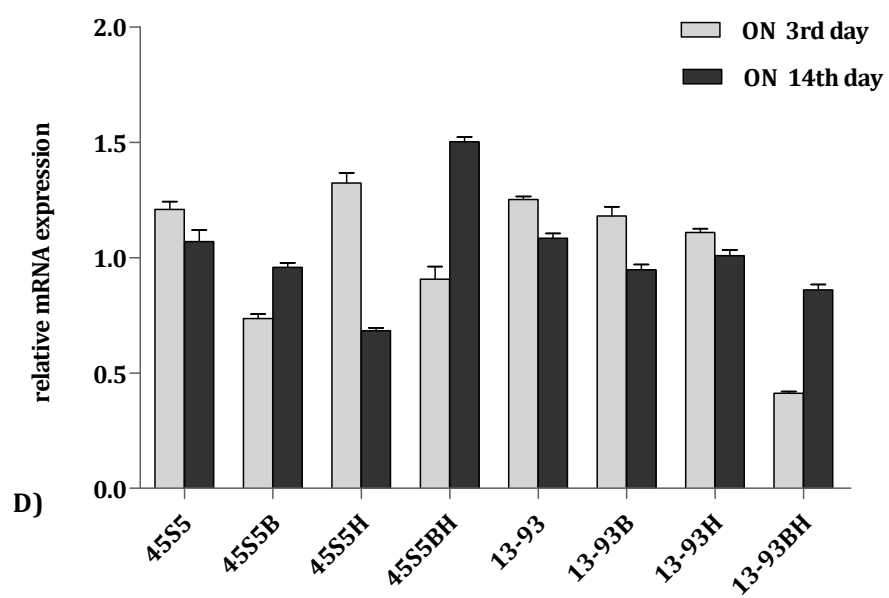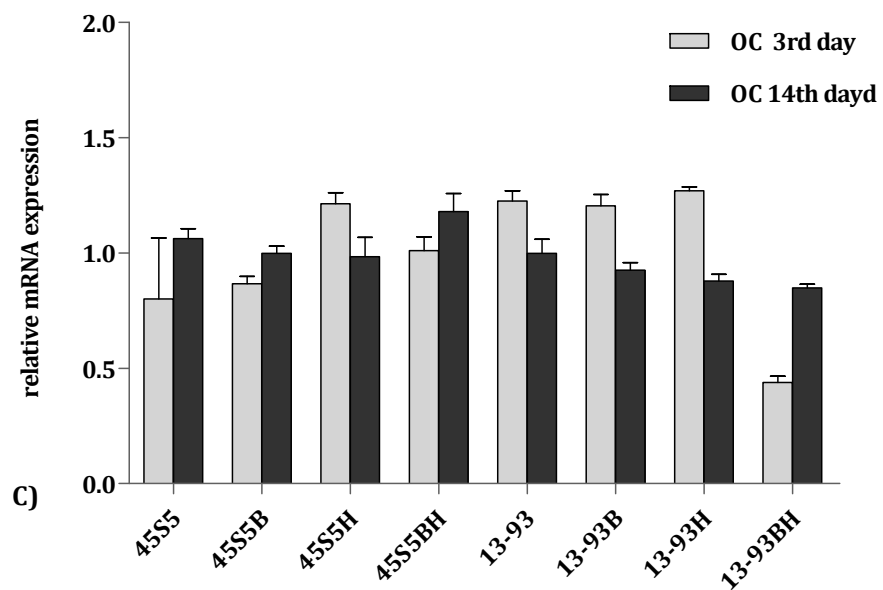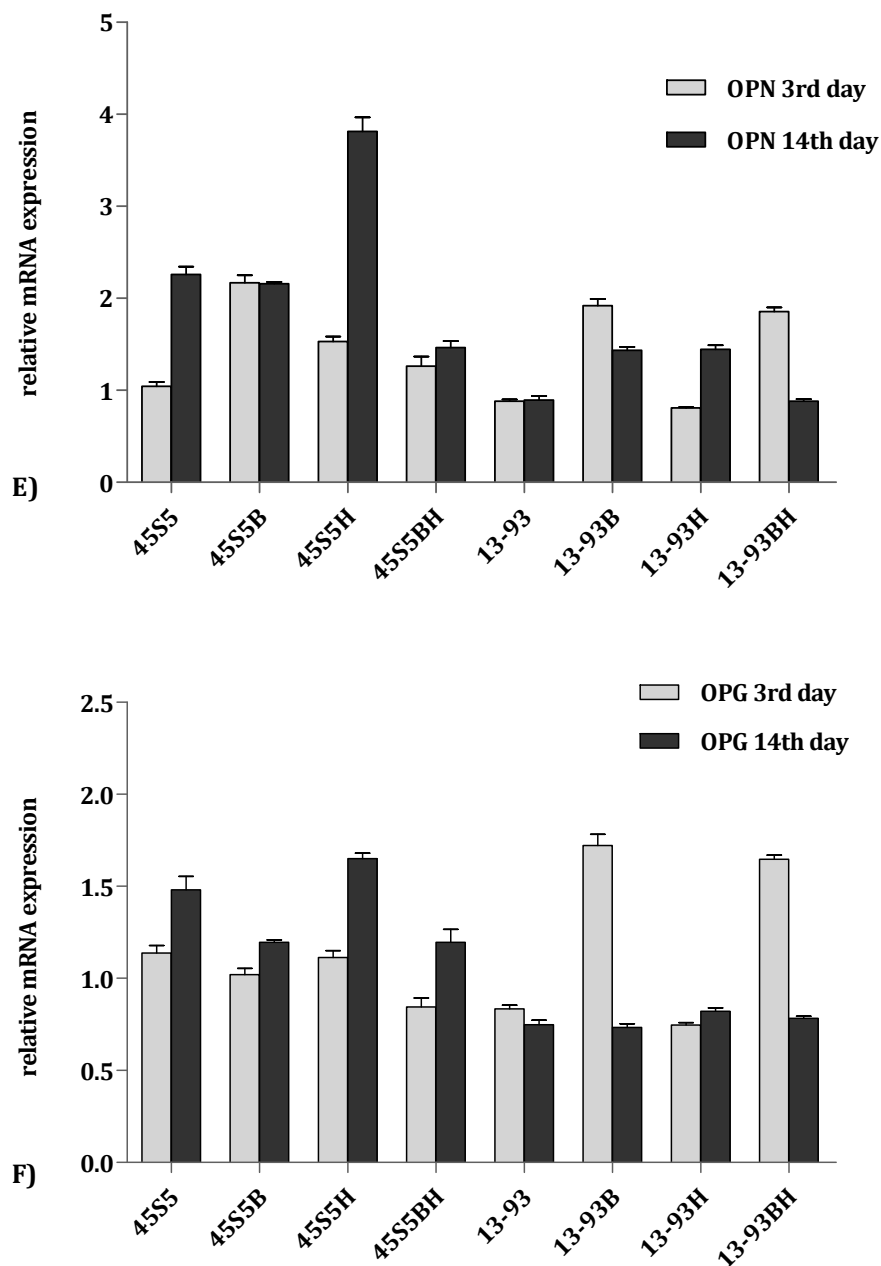
Figure 21. Real time PCR analyses of: A) ALP; B) COL1; C) OC; D) ON; E) OPN; and F) OPG

Statistical comparisons were done using two-way analysis of variance (ANOVA) and Bonferroni's post- test. Differences were considered statistically significant at p<0.05.

Results indicate that different coating treatment affects osteogenic markers differently in different time points. ALP, in the BG 45S5 was up regulated in the beginning (day 3) of cell culture for samples treated with HNE and BSA+HNE while in the BG 13-93, ALP was more expressed on day 14. COL1 expression was the highest in sample 45S5-BH on day 14. OC levels did not so significantly differ between the treatments and the days in culture. ON was found to be expressed in samples 45S5-H (day 3) and 45S5-BH (day 14). The highest fold-change in gene expression was observed for OPN in sample 45S5-H (day 14) with a 4-fold change observed in comparison to the reference gene. This gene was the most expressed in comparison to the other genes tested. According to the results obtained with this gene coating treatments seems to stimulate the osteogenic potential of the cell what is more pronounced for the BG type 45S5 even though it was also observed for the BG type 13-93. Moreover, expression of OPN was up-regulated in the reference sample 45S5 on day 14, in comparison to day 3, while in reference sample 13-93 there was no change. Higher expression of OPG, in comparison to different time points, was observed on day 14 in most samples of BG type 45S5, especially the one coated with HNE and the reference sample, while, in case of the BG type 13-93, higher expression was observed on day 3 in samples coated with BSA or BSA+HNE.

3.1.11. Western-blot analyses

Results of the western blot analyses have shown that p44/42 (ERK 1/2) signalling pathway is activated during cell growth on the surfaces of BGs while p38 signalling pathway remained inactive, no phosphorilated p38 proteins were detected (data not shown).

Analysis of SAPK/JNK was also carried out but no bands were detected with both, phosphorilated or unphosphorilated antibodies (data not shown).

A)
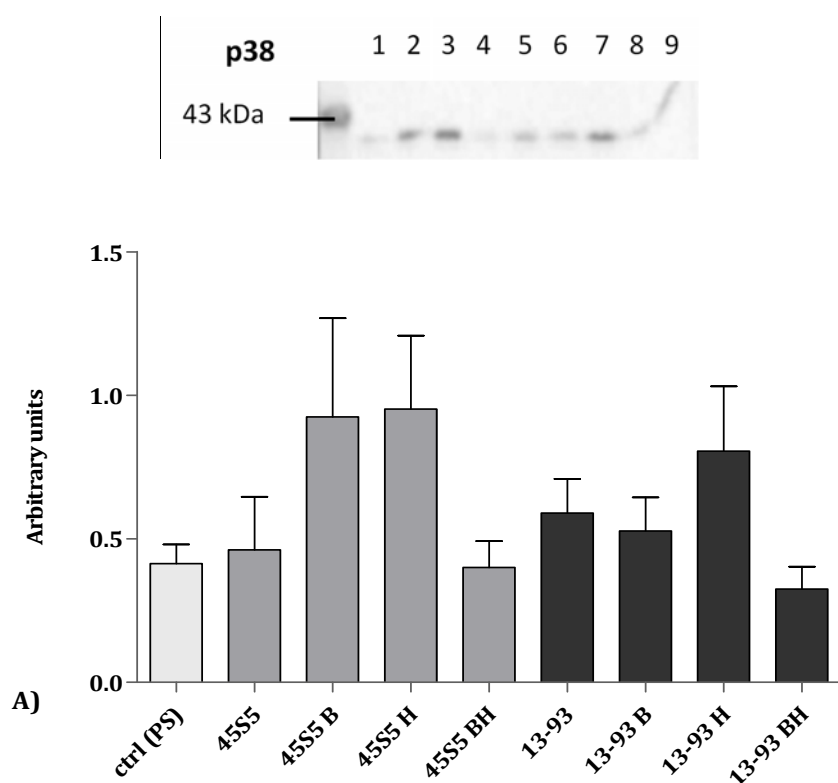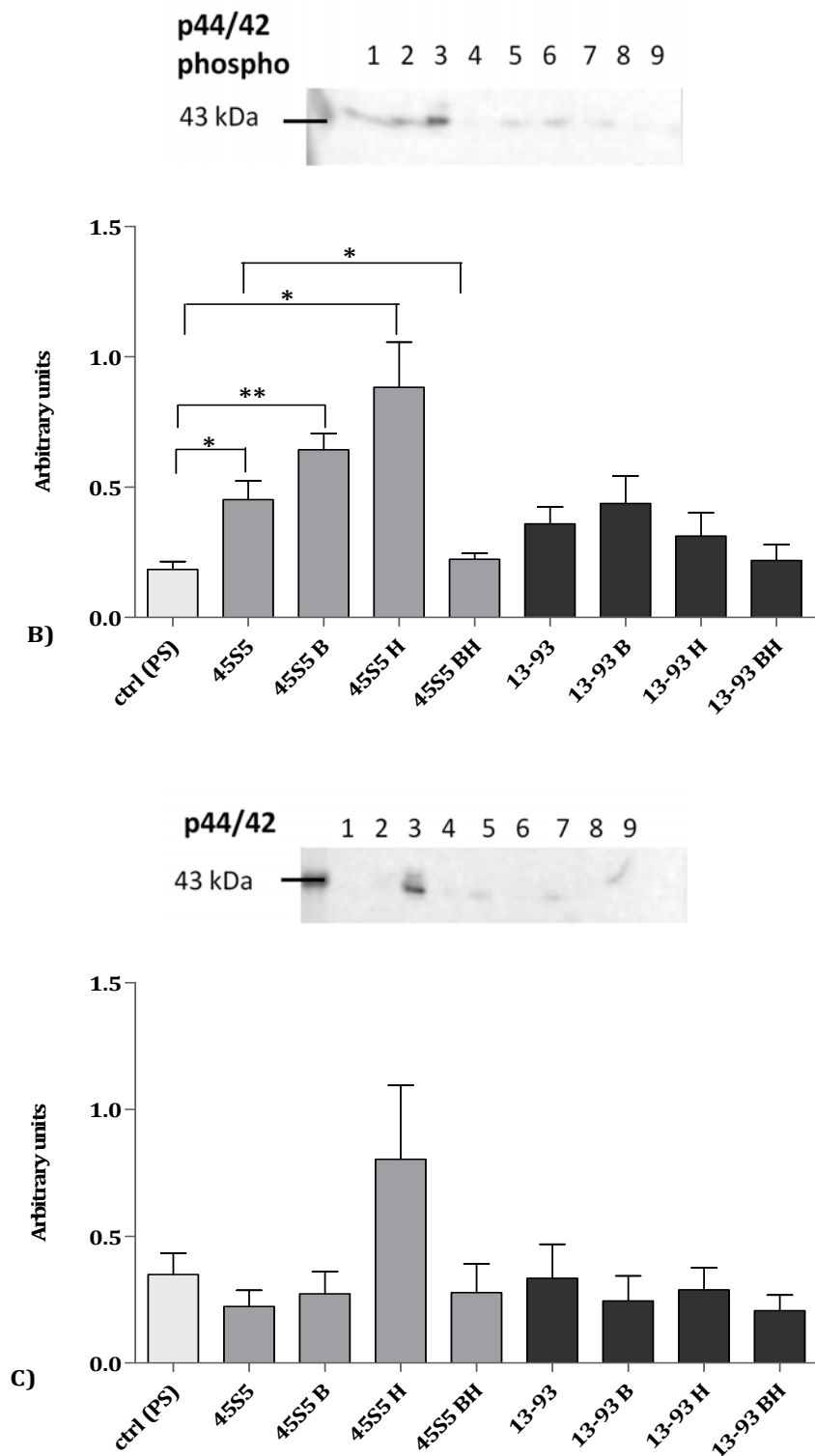
Figure 22. Western-blot analysis of p38 (A), phosphorilated p44/42 (B), and p44/42 (C) MAPK signalling pathway

Sample marks: 1-45S5;   2-45S5-B;   3-45S5-H;   4-45S5-BH;   5-13-93;

                6- 13-93-B;   7-13-93-H;   8-13-93-BH;   9-ctrl (cells grown on plastic)

Treatment marks: B- 0.5 mg/ml BSA; H-2.5 µM HNE; BH – 0.5 mg/ml BSA + 2.5 µM HNE

      * $p < 0.05$; ** $p < 0.01$

In comparison to the control sample (cells grown on plastic in 48-well plate), significant increase in phosphorilated p44/42 were observed in samples: 45S5 ($p < 0.05$), 45S5-B ($p < 0.01$) and especially 45S5-H ($p < 0.05$). This results suggest that 45S5 BG itself activate the p44/42 MAPK pathway more than 13-93 BG and that coatings, with BSA or with HNE, activate this pathway even more. The coating made with combination of BSA and HNE, in both BGs, did not increase the activation of p44/42 pathway but rather it stayed in the levels of control sample, grown on the plastic, which was even lower than the control sample of 45S5 BG (without the coating).

3.2. Results obtained with BG, type 45S5, with or without copper

3.2.1. Cell viability

A cytotoxic effect of the 45S5-1Cu and 45S5-2.5Cu samples was observed as a decrease in cell viability at all time points. On day 3, cell viability of the 45S5-1Cu sample was approximately 50%, when compared to the 45S5-Ref (p<0.005), and it decreased to ~26% on days 7 and 14 (p<0.001). Cell viability observed on 45S5-2.5Cu samples was lower than 20% at all 3 time points (p<0.001). In contrast, a trend of growth enhancement with a significant increase in viability (p<0.05) was observed after 14 days for 45S5-0.1Cu (Fig 23). Results are expressed as percentage to the respective control (45S5-Ref).
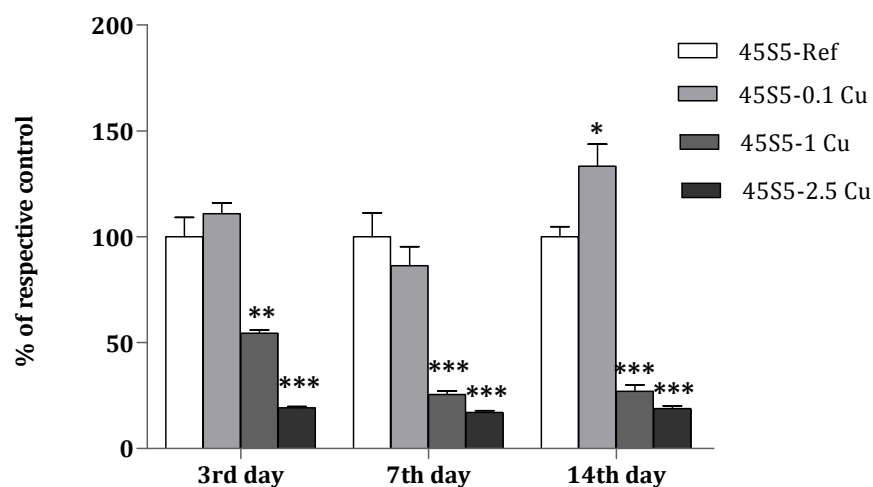
Figure 23. Cell viability of the HOS cells grown on the bioactive glass samples measured by MTT assay at days: 3, 7 and 14. The results are given as a percentage of the respective control (45S5-Ref). Cell viability was increased for the 45S5-0.1Cu at day 14 (* p<0.05) while it was decreased for the 45S5-1Cu and 45S5-2.5Cu sample at all time points:

45S5-1Cu – 50% decrease at day 3 (** p<0.005) followed by the ~75% at days 7 and 14 (*** p<0.001).

45S5-2.5Cu – >80% decrease at all time points (*** p<0.001).

3.2.2. Cell growth and material characterization

3.2.2.1. DAPI staining

DAPI stained images correlated with the cell viability results observed in Section 3.1. Specifically, after 14 days, confluent cells were observed on the 45S5-Ref and 45S5-0.1Cu BG surfaces. However, few cells were present on 45S5-1Cu and 45S5-2.5Cu BG surfaces (Fig 24).
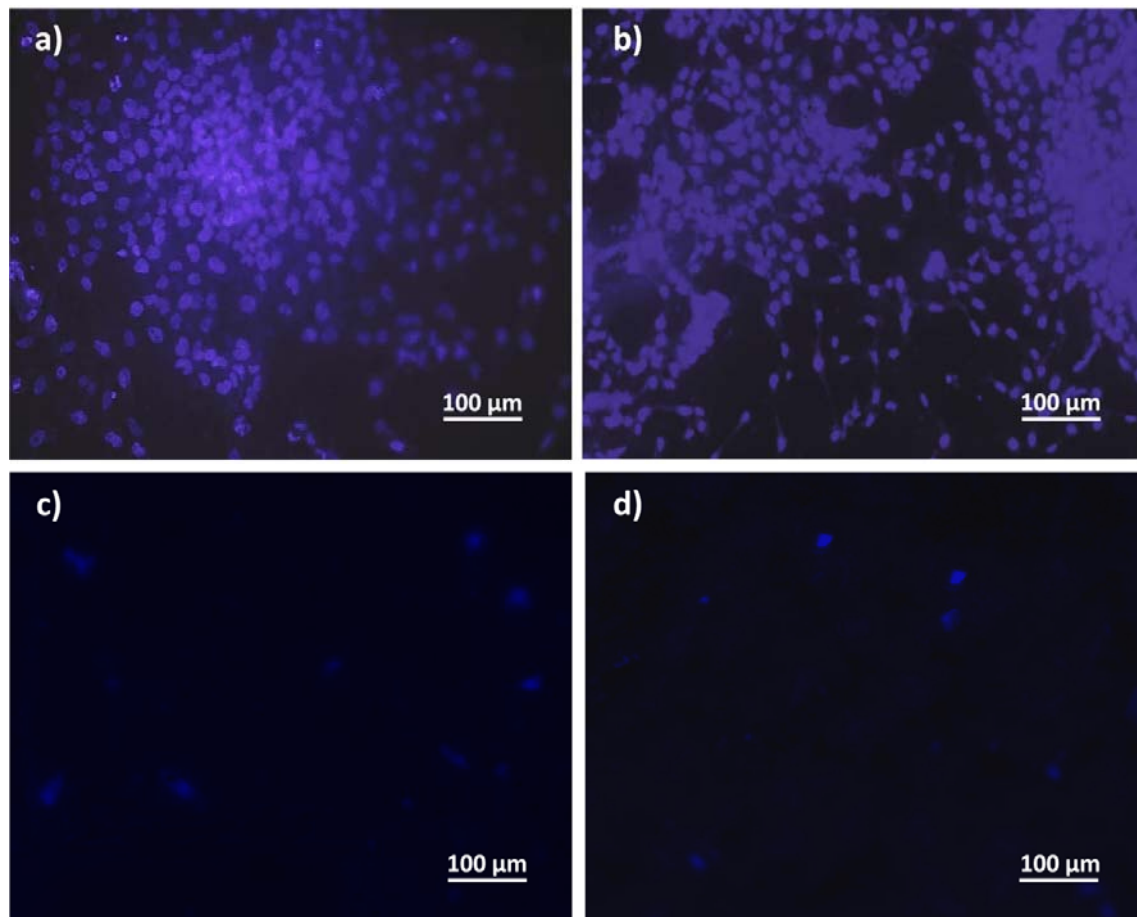
Figure 24. DAPI staining images obtained at the day 14: a) 45S5-Ref, b) 45S5-0.1Cu, c) 45S5-1Cu and d) 45S5-2.5Cu.

3.2.2.2. SEM and EDX analysis

SEM images on day 7 of culture showed a nicely spread cell on the surface of the 45S5-Ref while on the 45S5-1Cu surface a lot of precipitates could be seen which seemed to interfere with the cell growth (Fig 25 a & b).
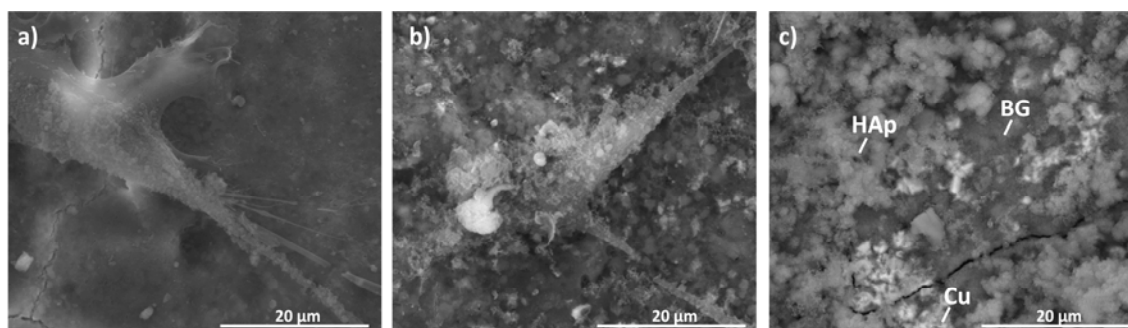
Figure 25. SEM figures of a) 45S5-Ref; b) 45S5-1Cu and c) 45S5-2.5Cu samples after 7 days in cell culture medium.

The SEM image of the BG 45S5-2.5Cu sample surface (Fig 25 c) indicated three different phases, i.e., (i) glass matrix ("BG"), (ii) calcium phosphate precipitates ("HAp") and (iii) copper-rich precipitations ("Cu"). The corresponding elemental concentrations derived from EDX measurements of the precipitates are shown in Table 4. For the calcium rich area, the determined Ca/P ratio of ~1.61 confirmed the formation of hydroxyapatite on the glass surface. However, the Cu-rich areas seemed to contain up to ~13 At.-% Cu.

Table 4. EDX analysis of the 45S5-2.5Cu (atomic %). Areas of measurement correspond to Fig. 25c.

Sample	Si	P	Ca	Cu
45S5-2.5Cu				
Region "BG"	15.53	4.09	6.66	0.36
Region "HAp"	1.03	5.79	9.36	0.26
Region "Cu"	3.06	6.12	6.33	13.00

3.2.3. Immunoblot analysis

The growth of the control cells (45S5-Ref) from day 3 to days 7 and 14 was associated with a gradual increase of the HNE-protein adducts (Fig 26). All cell samples that were grown on Cu-doped 45S5 BG showed enhanced formation of the HNE-protein adducts. The enhancement was particularly pronounced on days 3 ($p<0.001$) and 14 ($p<0.01$), for the cells grown on 45S5-2.5Cu samples.
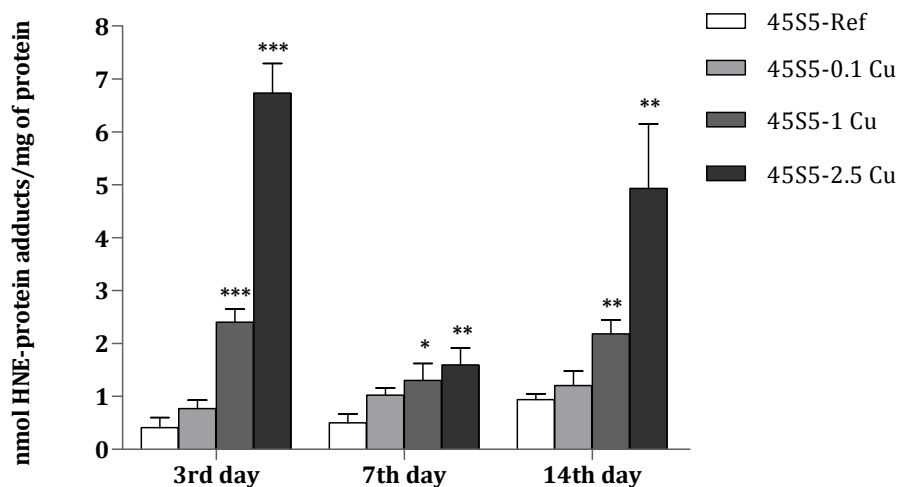
Figure 26. Immunoblotting (dot-blot) analyses of the HNE-protein adducts formation at days 3, 7 and 14. Results are expressed as nmol of HNE-protein adducts/mg of protein.

Enhancement of the lipid peroxidation was in particular pronounced on days 3 (***, $p<0.001$) and 14 (**, $p<0.01$), for the cells grown on 45S5-2.5Cu samples. * denotes $p<0.05$.

4. DISCUSSION

Immunochemical analysis of the reference BGs types 45S5 and 13-93 revealed that during incubation of human bone cells *in vitro* on their surface, HNE is generated within the cells, unlike while growing on the normal histological glass (Figure 11.). This suggests possible physiological role of HNE in bone regeneration process which was not associated with cytotoxicity because human osteoblast-like cells were proliferating (increasing their number) during cultivation period. Moreover, since HNE is considered as "second messenger of free radicals", this evidence gives additional support that oxidative stress and lipid peroxidation should not only be considered as generators of biomolecular damage, and thus important contributors to aging as well as causative factors of diseases, but should also be recognized as significant mediators of normal physiological functions [57]. That allowed consideration of oxidative stress also as physiological process introducing new term "oxidative homeostasis", which implies involvements of reactive oxygen species (ROS) and lipid peroxidation in various physiological processes [80]. In favour of this possibility is also difference of the growth pattern observed when HOS cells were culture on BGs. Namely, the cells grown on standard histological glass were growing as typical monolayer cultures and did not produce endogenous HNE-protein adducts, while those grown on BGs were growing overlapping in a tissue-like form producing abundant HNE (Figure 11).

Since no HNE-histidine adducts were detected in the cells cultured on normal histological glass, but only if the cells were grown on BGs, conclusion arises that enhanced growth of the HOS cells in tissue-like pattern on BGs was associated with production of HNE, known to act as growth regulating factor and signalling molecule considered also as a second messenger of free radicals [67].

To further reveal if the HOS cells grown on BGs undergo physiological oxidative stress manifested by ROS and HNE production, endogenous ROS production was determined to be present during cell growth on the BGs by specific fluorescence method (DCF, Figure 13). ROS may trigger lipid peroxidation and generation of HNE, which is on the other hand able to induce ROS production [101], which usually lead to the self-catalysed process of lipid peroxidation that could destroy the cells. However, in this study it appeared to enhance the growth of HOS cells on BGs.

There is growing evidence about the physiological generation of ROS that can occur as a byproduct of other biological reactions. NADPH oxidase is known to be the major source of ROS,

but ROS generation also occurs with mitochondria, peroxisomes, cytochrome P-450, and other cellular elements [102]. Several growth factors and cytokines binding to different types of cell membrane receptors can elicit a rise in intracellular ROS. It was found that generation of ROS is induced with TGF-β in mouse osteoblastic cells and in human lung fibroblasts [103] and with PDGF in human lens epithelial cells [104]. Furthermore, it has been reported that ROS activate MAPK pathways in several systems, including extracellular signal regulated kinase (ERK)1/2, Jun-NH2-terminal kinase and p38 MAPK cascades [105].

In the second step, coating of BGs with HNE, BSA or their combination have shown that the coating of the BG samples was efficient and that results obtained are due to the coating treatment and joined activity of the BG itself. Immunochemical detection of HNE present in cells was in compliance with the first observations, that HNE-protein adducts were present in all BG samples, even in control samples and samples coated with BSA. Results of the ROS production were conforming immunocytochemical results since in all BG samples, coated or the reference ones, the increase in endogenous ROS, in comparison to the cells grown in a culture plate plastic, was observed. This finding indicates the relevance of oxidative stress and lipid peroxidation in the process of enhanced growth of human osteoblast-like cells on the surface of the BGs [29,106]. Moreover, when compared to their reference samples, both BGs coated with BSA or with BSA+HNE for BG type 13-93, showed increased ROS production. Recent finding of albumin-induced upregulation of matrix metalloproteinase-9 (MMP-9) via increase of ROS production and activation of p38 MAPK signalling pathway [107], could potentially link observed increase of ROS levels in BG samples coated with BSA with the coating itself.

Analysis of the levels of HNE-protein adducts in cell lysates grown on BG samples showed gradual increase in endogenous concentration of HNE-protein adducts with time in culture for all samples with the exception to the ones treated with BSA+HNE for the 45S5 BG. In this sample the highest level of HNE-protein adducts was observed on day 7 and decreasing on day 14. This could be due to the boosting of the antioxidative capacity of the cells exposed to higher concentration of HNE-protein adducts on day 7. Moreover, results obtained with the BG type 13-93, are showing the same trend, gradual increase of HNE-protein adduct in all samples with the exception for the BSA+HNE sample. In this sample the lowest level was observed on day 7 and the highest on day 14. Since levels of HNE-protein adducts on day 3 were higher in this sample than in all others, there is a possibility of earlier activation of antioxidative mechanisms. Although, it was already reported that HNE is enhancing gene expression of antioxidant and detoxifying enzymes through Nrf2 and that Nrf2-ARE signalling mechanism in the detoxification

of HNE is very important [108] in order to confirm these claims additional experiments are needed.

When present in cells, HNE forms stabile covalent-bonded HNE-protein adducts by protein and peptide modifications mostly through reaction with cysteine, lysine and histidine amino acid residues [65,67]. These protein-adduct were found in normal skeletal development during embryogenesis [109] and in various tissues of animal and human origin [80]. The impact of HNE on the fate of the cell is dose-dependent; at low levels, HNE promotes cell proliferation, whereas at higher concentrations, it induces cell cycle arrest, differentiation, and finally apoptosis [110]. Exposure to HNE induces vascular smooth muscle growth, accompanied by the activation of MAPKs (ERK, c-Jun NH2-terminal kinase, and p38), the induction of c-fos and c-jun gene expression, and activator protein 1 (AP-1) DNA binding activity [70]. Other reported that conjugates of, the most important antioxidant in cells involved in HNE detoxification, GSH with HNE activate PKC and stimulate NF-κB and AP-1-dependent gene transcription leading to an increase in cell growth [84]. Furthermore, recent observations show that stimulation with HNE at sublethal concentrations induces adaptive response and enhances cell tolerance, thereby protecting cells against the forthcoming oxidative stress [58].

In addition, for the coating treatment with HNE or its combination with BSA, 2.5 μM HNE was used, the concentration already shown to have stimulatory effect on the growth of the human osteoblast-like cells [62]. Furthermore, evaluation of apoptosis, micronucleus formation, necrosis and mitotic index carried out by the DAPI staining method, has shown that the coating treatments were not cytotoxic and genotoxic to the cells. There were no differences between the samples and therefore the treatments were not negatively affecting cell growth.

On the contrary, coating treatment with HNE seems to further stimulate cell growth on the surface of both BG while it is more pronounced in the BG type 45S5. This was observed by both cell proliferation, analysed by the trypan blue exclusion test, and cell viability, analysed by the MTT test that is, in fact, a measure of cellular metabolic activity.

Samples treatments with HNE and BSA+HNE on the 45S5 BG enhanced cell differentiation and matrix mineralization what was observed by the gene expression analysis of specific osteogenic markers, and also stainings for ALP and with Alizarin Red. Results of the gene expression of the osteogenic markers indicate that different coating treatment affects them differently in different time points. In the BG type 45S5, ALP, as an early osteogenic marker, was up regulated in the beginning (day 3) of cell culture for samples treated with HNE and BSA+HNE while in the BG 13-93, ALP was more expressed in all samples on day 14. The highest fold-

change in gene expression was observed for OPN in sample 45S5-H (day 14) with a 4-fold change observed in comparison to the reference gene. This gene was the most expressed in comparison to the other genes tested. According to the results obtained with this gene, coating treatments seems to stimulate the osteogenic potential [111] of the cell what is more pronounced for the BG type 45S5 even though it was also observed for the BG type 13-93.

Results of ALP staining and quantification have shown the same trend, increase in ALP between days 3 and 14 in both BGs, which was statistically significant when BGs were coated with HNE or BSA+HNE for BG type 13-93. While HNE coating notably increased ALP on day 14 in 45S5 BG, the same treatment decreased ALP in 13-93 type BG. The same effect was observed for 13-93 type BG coated with BSA+HNE. On the other hand, in both BG samples coated with BSA, detected levels of alkaline phosphatase were somewhere in the range of the results obtained for the reference samples (without coatings) for both time points.

Moreover, a significant increase in mineralisation of extracellular matrix was observed in all BG samples when compared to the control sample, cells grown in 48-well plate on polystyrene plastic ($p<0.005$). The only exception was sample 45S5-B where the same tendency was shown, but due to high standard deviation, it was not statistically significant. Therefore, above mentioned results give evidence of the stimulatory effects of the treatments (especially with HNE) upon cell differentiation and mineralization, and thus support of bone growth.

The complexity of biological response that is involved in bone regeneration process should be also mentioned. There are several possible mechanism reported like Indian hedgehog (Ihh) pathway, bone morphogenetic protein (BMP) pathway, canonical Wnt-β-catenin pathway and for our point of view the most interesting MAPK pathway. MAPK pathway was found to be obligatory transducer and a crucial for post-fracture bone healing because it transduces signals from several growth factors (FGF, IGF, EGF) [112].

BGs in contact with the body fluid, or in this case culture medium, behave specifically, that is, start to initiate a sequence of reactions in order to create carbonated hydroxyapatite layer, similar to the mineral in bone, which is considered as indication of their bioactivity. Consequently, ionic dissolution products of BG are released into the medium and stimulate gene expression of human osteoblasts and thus enhance osteogenesis as well as angiogenesis [113]. Furthermore, BG ionic dissolution products were found to stimulate few growth factors including IGF-II, a key regulator of osteoblast homeostasis, and VEGF, a member of the fibroblast growth factor family with osteogenic potential and also important in angiogenesis [25].

In addition, several intracellular signalling molecules are involved in osteoblast activation due to IGF- II and VEGF, including ERK and MAPK pathways. Four kinases were shown to be induced by the treatment, MAPKAP kinase-2, MAPK-2, MAPK p38, and ERK1 [29].

The western blot analyses have revealed that p44/p42 (ERK 1/2) MAPK signalling pathway is activated while p38 is not. In comparison to the control sample (cells grown on plastic), significant increase in phosphorylated p44/42 was observed in samples: 45S5, 45S5-B and especially 45S5-H ($p < 0.05$). This results suggest that 45S5 BG itself activate the p44/42 MAPK pathway more than 13-93 BG and that coatings, with BSA or with HNE, activate this pathway even more. The coating made with combination of BSA and HNE, in both BGs, did not increase the activation of p44/42 pathway but rather it stayed in the levels of control sample, grown on the plastic, which was even lower than the control sample of 45S5 BG (without the coating).

Hence, taking all mentioned in consideration, the proposed mechanism of bone regeneration during fracture healing supported by BGs, includes effect of BG dissolution products that, on one hand, initiate oxidative stress and ROS formation, which triggers lipid peroxidation and generation of HNE. On the other hand, these dissolution products, together with HNE, acting as a signalling molecule, enhance bone formation through MAPK pathway, more precisely ERK 1/2 MAPK signalling pathway (Fig. 27).

Therefore, the primary assumption that BG functionalized with physiological concentration of HNE, prior to its implantation in damaged bone tissue, could trigger signalling reactions and together with positive effects of BG might reflect in enhanced osteogenesis, was shown to be true. These observations are supported by the report of successful use of functionally activated carbon nanotubes with HNE for stimulation of *in vitro* neuronal growth [114].
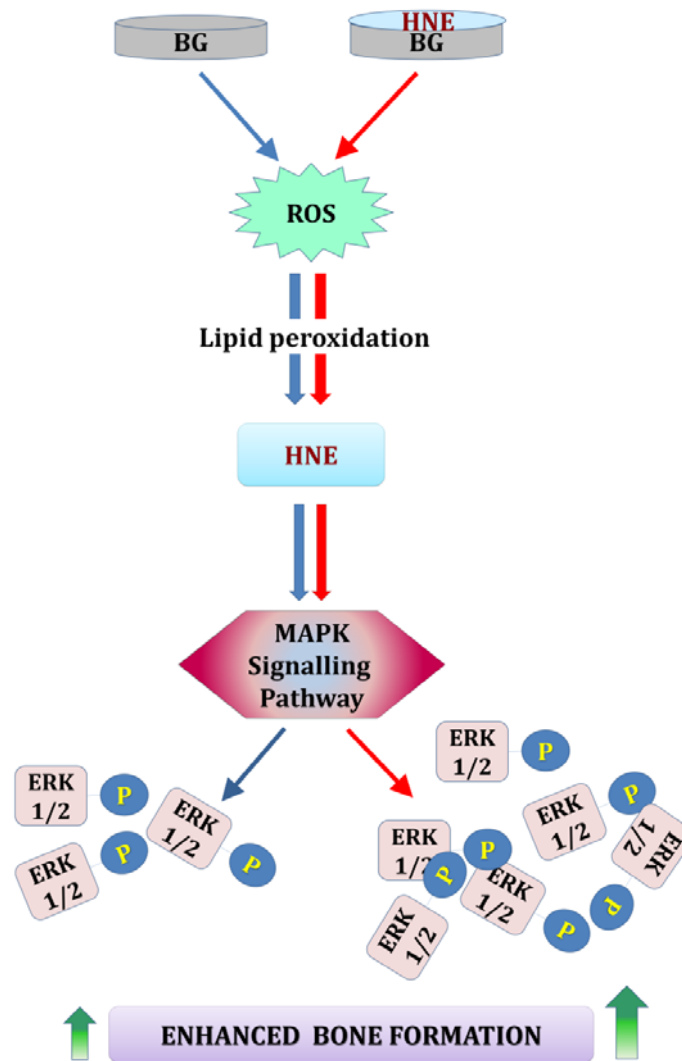
Fig. 27. Proposed mechanism of BG dissolution products without or with HNE that through production of ROS, induction of lipid peroxidation enhance bone formation during fracture healing, which is mediated through ERK 1/2 MAPK pathway.

In the other part of experiment with the BG type 45S5 prepared with certain amount of cooper, results have revealed following.

EDX analysis showed that the Cu-rich area seems to contain up to ~13 At.-% Cu even though the initial composition of the 45S5-2.5 Cu sample was only 2.5% (w/w) Cu. It is likely that such a pronounced and rapid release of Cu in the initial stage of the cell culture incubation results in focal saturation that might lead to precipitation of Cu-containing mineral phases. While more detailed surface specific analysis would be necessary for determination of the exact origin of the three phases distinguished on the 45S5-2.5 Cu sample, the finding of a Cu-rich area explains the cell viability decrease observed for both, 45S5-2.5Cu and 45S5-1Cu. In contrast, the 45S5-0.1Cu sample showed did not show decrease in viability but an enhanced cell growth.

The observed results could be explained by the fact that an excess of Cu, an essential trace element vital for to the health of living organisms under physiological conditions, induces cellular toxicity through the production of oxygen free radicals and direct oxidation of lipids, proteins and DNA [42,44]. Thus, a delicate mechanism that balances the concentration of Cu is needed not only at the cellular level, but also at the tissue and organ levels [44]. One of the most accepted explanations for Cu-induced cytotoxicity presumes that Cu ions are prone to participate in the formation of reactive oxygen species (ROS) via Fenton reaction [115], while the major consequence of Cu excess is peroxidative damage to membrane lipids [116].

In this respect, lipid peroxidation results in a formation of reactive aldehydes among which HNE is one of the most intensively studied since it is a highly electrophilic molecule that easily reacts with macromolecules (proteins, peptides, DNA and phospholipids) [59,60]. As already mentioned, HNE is an important signalling molecule involved in various cellular processes, from cell proliferation to differentiation as well as cell death in a concentration-dependent manner [64,66,71,117]. Moreover, HNE forms stable covalent HNE-protein adducts by reaction with cysteine, lysine and histidine residues, within the cell [65,69].

Results showed a gradual increase in the amount of HNE-protein adducts from day 3 to day 14 for the BG 45S5 samples without Cu (45S5-Ref). The same trend was observed for 45S5-0.1 Cu samples. Moreover, when compared to the control sample, 45S5-Ref, all samples of Cu-doped 45S5 BG showed an enhanced formation of the HNE-protein adducts, especially 45S5-2.5Cu samples on days 3 and 14. However, lower HNE values were observed on the 7th day for 45S5-1 Cu and 45S5-2.5 Cu samples which is most likely due to the cell adaptation upon the initial Cu-induced generation of ROS and, consequently, HNE. This is inferred since the well-

known mechanism that stimulate cells to adaptation is through an increase of their intracellular antioxidant mechanisms [42,68], although at this point we have not experimentally confirmed it.

The present results are in agreement with previous findings, which showed that growth of human bone cells on BG is associated with lipid peroxidation, i.e. formation of HNE-protein adducts [63]. This process is enhanced if the BG contains Cu, with a slight difference in that, on the one hand, enhanced lipid peroxidation induces a cytotoxic effect, as shown for 1% and 2.5%, respectively, while at 0.1% of Cu enhanced lipid peroxidation was associated with enhanced cell growth and not cytotoxycity. These results are in compliance with the concentration-dependent role of HNE in regulation of cell growth and cell death [64,66,71,89]. Hence, it should be mentioned that cells exposed to levels of lipid peroxidation above physiological are still able to adjust to them[63,66], as observed for the 45S5-0.1 Cu sample. The mechanisms of such cellular hormesis, an adaptive response of cells and organisms to a moderate (usually intermittent) stress [118], are not yet understood. It is certain that initially HNE acts through regulation of the c-fos expression, which is cytokine dependent and leads to the cascade of multiple intracellular and intercellular events affecting proliferation, differentiation and apoptosis of the cells exposed to the different levels of HNE[74]. Furthermore, it was also reported that HNE activates nuclear factor erythroid 2-related factor 2 (Nrf2) and antioxidant gene expression in vascular cells [119] as well as other adaptive stress response pathways that promote the survival of cells [120,121].

While principles of the bone growth enhancement remain to be elucidated, it is clear that HOS cells growing on BGs produce HNE, which makes stable protein adducts, indicating the fundamental role of HNE in the bone cell growth enhancement by BG. The findings of concentration dependent Cu-induced, effects on HOS cell growth relative to cellular production levels of HNE are relevant towards a better understanding of the mechanisms involved in the bone regeneration process as well as the regeneration enhancement by BG. The complexity of the bone regeneration process is also clear, with several signalling and metabolic pathways possibly linked to HNE in potential cytotoxic or growth-regulatory capacities. Thus, Cu-containing BG could offer a possible system to control the level of lipid peroxidation resulting in increased osteogenesis and may prove valuable in tissue engineering applications.

5. CONCLUSIONS

Coating of BGs with HNE, BSA or the combination was efficient and results obtained are due to combined effect of coating treatment and BG dissolution products.

Coating treatments are not genotoxic nor induce apoptosis or necrosis and therefore do not negatively affect cell growth.

Immunochemical detection of HNE present in cells has revealed its presence in all BG samples, even the reference ones, implicating its possible role in osteogenesis.

Increase in endogenous ROS was observed in all BG samples in comparison to cells grown in a culture , which is in compliance with immunocytochemistry results.

Coating treatment with HNE seems to further stimulate cell growth on the surface of BGs, more pronounced for BG type 45S5.

Levels of HNE-protein adducts in cell lysates show gradual increase in endogenous concentration of HNE-protein adducts with time in culture for all samples except ones coated with BSA+HNE. Antioxidative capacity should be investigated.

Samples treatments with HNE and BSA+HNE on the 45S5 BG enhanced cell differentiation and matrix mineralization what was observed as a gene expression and also stainings for ALP and with Alizarin Red.

The western blot analyses have revealed that p44/p42 (ERK 1/2) MAPK signalling pathway is activated while p38 is not.

For the experiments with the 45S5 type BGs with different Cu contents (0, 0.1, 1 and 2.5% (w/w)) results have shown that HOS cell growth on all 45S5 BG samples was associated with lipid peroxidation, as measured through the formation of HNE-protein adducts. This process was enhanced on the Cu containing BG in concentration-dependent manner.

Cu content was cytotoxic when present at 1% and higher concentrations.

On the contrary, in the case of 0.1% Cu an enhanced lipid peroxidation was not associated with cytotoxicity but with growth enhancement.

Therefore, Cu containing 45S5 type BG might represent a novel, attractive bioactive material for studies of the role of lipid peroxidation involved in the bone regeneration process.

Overall conclusion is that lipid peroxidation is involved in a process of enhanced osteogenesis of the cells grown on the BGs and therefore the obtained results are opening new perspectives in tissue engineering and in the field of regenerative medicine.

6. REFERENCES

6. REFERENCES

[1]   Gray H. Anatomy of the Human Body. 20th ed. Philadelphia: Lea & Febiger, 1918; Bartleby.com, 2000.; 2000.

[2]   Marieb EN, Hoehn K. Human Anatomy & Physiology. 7th editio. Pearson Prentice Hall; 2007.

[3]   Kini U, Nandeesh BN. Physiology of Bone Formation, Remodeling, and Metabolism. In: Fogelman I, Gnanasegaran G, Wall H, editors. Radionucl. Hybrid Bone Imaging, Berlin, Heidelberg: Springer Berlin Heidelberg; 2012, p. 1046.

[4]   Eriksen EF, Axelrod DW, Melsen F. Bone histomorphometry. New York: Raven Press; 1994.

[5]   Buckwalter JA, Glimcher MJ, Cooper RR, Recker R. Bone Biology. J Bone Jt Surgery 1995;77:1276–89.

[6]   Clarke B. Normal bone anatomy and physiology. Clin J Am Soc Nephrol 2008;3 Suppl 3:S131–9.

[7]   Brodsky B, Persikov A V. Molecular structure of the collagen triple helix. Adv Protein Chem 2005;70:301–39.

[8]   Sroga GE, Karim L, Colón W, Vashishth D. Biochemical characterization of major bone-matrix proteins using nanoscale-size bone samples and proteomics methodology. Mol Cell Proteomics 2011;10:M110.006718.

[9]   Delany A, Amling M, Priemel M, Howe C, Baron R, Canalis E. Osteopenia and decreased bone formation in osteonectin-deficient mice. J Clin Invest 2000;105:1325.

[10]   McKee MD, Nanci A. Osteopontin at mineralized tissue interfaces in bone, teeth, and osseointegrated implants: ultrastructural distribution and implications for mineralized tissue formation, turnover, and repair. Microsc Res Tech 1996;33:141–64.

[11]   Golub EE, Harrison G, Taylor a G, Camper S, Shapiro IM. The role of alkaline phosphatase in cartilage mineralization. Bone Miner 1992;17:273–8.

[12]   Zaidi M. Skeletal remodeling in health and disease. Nat Med 2007;13:791–801.

[13]   Teitelbaum SL. Bone Resorption by Osteoclasts. Science (80-) 2000;289:1504–8.

[14]   Hadjidakis DJ, Androulakis II. Bone remodeling. Ann N Y Acad Sci 2006;1092:385–96.

[15]   Buckwalter JA, Glimcher MJ, Cooper RR, Recker R. Bone biology. I: Structure, blood supply, cells, matrix, and mineralization. Instr Course Lect 1996;45:371–86.

[16]   Tsiridis E, Upadhyay N, Giannoudis P. Molecular aspects of fracture healing: which are the important molecules? Injury 2007;38 Suppl 1:S11–25.

[17] Dimitriou R, Tsiridis E, Giannoudis P V. Current concepts of molecular aspects of bone healing. Injury 2005;36:1392–404.

[18] Giannoudis P V, Einhorn T a, Marsh D. Fracture healing: the diamond concept. Injury 2007;38 Suppl 4:S3–6.

[19] Kalfas IH. Principles of bone healing. Neurosurg Focus 2001;10:E1.

[20] Salgado AJ, Coutinho OP, Reis RL. Bone tissue engineering: state of the art and future trends. Macromol Biosci 2004;4:743–65.

[21] Hench LL, Splinter RJ, Allen WC, Greenlee TK. Bonding mechanisms at the interface of ceramic prosthetic materials. J Biomed Mater Res 1971;5:117–41.

[22] Kitsugi T, Nakamura T, Yamamura T, Kokubu T, Shibuya T, Takagi M. SEM-EPMA observation of three types of apatite-containing glass-ceramics implanted in bone: the variance of a Ca-P-rich layer. J Biomed Mater Res 1987;21:1255–71.

[23] Ohgushi H, Dohi Y, Yoshikawa T, Tamai S, Tabata S, Okunaga K, et al. Osteogenic differentiation of cultured marrow stromal stem cells on the surface of bioactive glass ceramics. J Biomed Mater Res 1996;32:341–8.

[24] Rahaman MN, Day DE, Bal BS, Fu Q, Jung SB, Bonewald LF, et al. Bioactive glass in tissue engineering. Acta Biomater 2011;7:2355–73.

[25] Hench LL, Thompson I. Twenty-first century challenges for biomaterials. J R Soc Interface 2010;7 Suppl 4:S379–91.

[26] Chen QZ, Thompson ID, Boccaccini AR. 45S5 Bioglass-derived glass-ceramic scaffolds for bone tissue engineering. Biomaterials 2006;27:2414–25.

[27] Peitl Filho O, LaTorre GP, Hench LL. Effect of crystallization on apatite-layer formation of bioactive glass 45S5. J Biomed Mater Res 1996;30:509–14.

[28] Huang W, Day DE, Kittiratanapiboon K, Rahaman MN. Kinetics and mechanisms of the conversion of silicate (45S5), borate, and borosilicate glasses to hydroxyapatite in dilute phosphate solutions. J Mater Sci Mater Med 2006;17:583–96.

[29] Xynos ID, Hukkanen MVJ, Batten JJ, Buttery LD, Hench LL, Polak JM. Bioglass 45S5 Stimulates Osteoblast Turnover and Enhances Bone Formation In Vitro : Implications and Applications for Bone Tissue Engineering 2000:321–9.

[30] Tsigkou O, Jones JR, Polak JM, Stevens MM. Differentiation of fetal osteoblasts and formation of mineralized bone nodules by 45S5 Bioglass conditioned medium in the absence of osteogenic supplements. Biomaterials 2009;30:3542–50.

[31] Day RM, Boccaccini AR, Shurey S, Roether JA, Forbes A, Hench LL, et al. Assessment of polyglycolic acid mesh and bioactive glass for soft-tissue engineering scaffolds. Biomaterials 2004;25:5857–66.

[32] Fu Q, Rahaman MN, Bal BS, Brown RF, Day DE. Mechanical and in vitro performance of 13-93 bioactive glass scaffolds prepared by a polymer foam replication technique. Acta Biomater 2008;4:1854–64.

[33] Brown RF, Day DE, Day TE, Jung S, Rahaman MN, Fu Q. Growth and differentiation of osteoblastic cells on 13-93 bioactive glass fibers and scaffolds. Acta Biomater 2008;4:387–96.

[34] Sies H. Oxidative stress: Introductory remarks. In: Sies H, editor. Oxidative Stress, London: Academic Press; 1985, p. 1–7.

[35] Valko M, Rhodes CJ, Moncol J, Izakovic M, Mazur M. Free radicals, metals and antioxidants in oxidative stress-induced cancer. Chem Biol Interact 2006;160:1–40.

[36] Li X, Fang P, Mai J, Choi ET, Wang H, Yang X. Targeting mitochondrial reactive oxygen species as novel therapy for inflammatory diseases and cancers. J Hematol Oncol 2013;6:19.

[37] Klaunig JE, Kamendulis LM, Hocevar B a. Oxidative stress and oxidative damage in carcinogenesis. Toxicol Pathol 2010;38:96–109.

[38] Veskoukis AS, Tsatsakis AM, Kouretas D. Dietary oxidative stress and antioxidant defense with an emphasis on plant extract administration. Cell Stress Chaperones 2012;17:11–21.

[39] Nordberg J, Arnér ES. Reactive oxygen species, antioxidants, and the mammalian thioredoxin system. Free Radic Biol Med 2001;31:1287–312.

[40] Sosa V, Moliné T, Somoza R, Paciucci R, Kondoh H, LLeonart ME. Oxidative stress and cancer: an overview. Ageing Res Rev 2013;12:376–90.

[41] Fridovich I. Biological effects of the superoxide radical. Arch Biochem Biophys 1986;247:1–11.

[42] Valko M, Leibfritz D, Moncol J, Cronin MTD, Mazur M, Telser J. Free radicals and antioxidants in normal physiological functions and human disease. Int J Biochem Cell Biol 2007;39:44–84.

[43] Gough DR, Cotter TG. Hydrogen peroxide: a Jekyll and Hyde signalling molecule. Cell Death Dis 2011;2:e213.

[44] Valko M, Morris H, Cronin MTD. Metals, toxicity and oxidative stress. Curr Med Chem 2005;12:1161–208.

[45] Lloyd R V, Hanna PM, Mason RP. The origin of the hydroxyl radical oxygen in the Fenton reaction. Free Radic Biol Med 1997;22:885–8.

[46] Trachootham D, Lu W, Ogasawara M a, Nilsa R-DV, Huang P. Redox regulation of cell survival. Antioxid Redox Signal 2008;10:1343–74.

[47] Ray PD, Huang B-W, Tsuji Y. Reactive oxygen species (ROS) homeostasis and redox regulation in cellular signaling. Cell Signal 2012;24:981–90.

[48]   Eaton P. Protein thiol oxidation in health and disease: techniques for measuring disulfides and related modifications in complex protein mixtures. Free Radic Biol Med 2006;40:1889–99.

[49]   Collins Y, Chouchani ET, James AM, Menger KE, Cochemé HM, Murphy MP. Mitochondrial redox signalling at a glance. J Cell Sci 2012;125:801–6.

[50]   D'Autréaux B, Toledano MB. ROS as signalling molecules: mechanisms that generate specificity in ROS homeostasis. Nat Rev Mol Cell Biol 2007;8:813–24.

[51]   Matsuzawa A, Ichijo H. Redox control of cell fate by MAP kinase: physiological roles of ASK1-MAP kinase pathway in stress signaling. Biochim Biophys Acta 2008;1780:1325–36.

[52]   Nguyen T, Nioi P, Pickett CB. The Nrf2-antioxidant response element signaling pathway and its activation by oxidative stress. J Biol Chem 2009;284:13291–5.

[53]   Baraibar M a, Liu L, Ahmed EK, Friguet B. Protein oxidative damage at the crossroads of cellular senescence, aging, and age-related diseases. Oxid Med Cell Longev 2012;2012:919832.

[54]   Poppek D, Grune T. Proteasomal defense of oxidative protein modifications. Antioxid Redox Signal n.d.;8:173–84.

[55]   Cooke MS, Evans MD, Dizdaroglu M, Lunec J. Oxidative DNA damage: mechanisms, mutation, and disease. FASEB J 2003;17:1195–214.

[56]   Gago-Dominguez M, Jiang X, Castelao JE. Lipid peroxidation, oxidative stress genes and dietary factors in breast cancer protection: a hypothesis. Breast Cancer Res 2007;9:201.

[57]   Wildburger R, Mrakovcic L, Stroser M, Andrisic L, Borovic Sunjic S, Zarkovic K, et al. Lipid Peroxidation and Age-Associated Diseases-Cause or Consequence?: Review. Turkiye Klin J Med Sci 2009;29:189–93.

[58]   Niki E. Lipid peroxidation: physiological levels and dual biological effects. Free Radic Biol Med 2009;47:469–84.

[59]   Guéraud F, Atalay M, Bresgen N, Cipak a, Eckl PM, Huc L, et al. Chemistry and biochemistry of lipid peroxidation products. Free Radic Res 2010;44:1098–124.

[60]   Esterbauer H, Schaur RJ, Zollner H. Chemistry and biochemistry of 4-hydroxynonenal, malonaldehyde and related aldehydes. Free Radic Biol Med 1991;11:81–128.

[61]   Negre-Salvayre A, Auge N, Ayala V, Basaga H, Boada J, Brenke R, et al. Pathological aspects of lipid peroxidation. Free Radic Res 2010;44:1125–71.

[62]   Borovic S, Cipak A, Meinitzer A, Kejla Z, Perovic D, Waeg G, et al. Differential sensitivity to 4-hydroxynonenal for normal and malignant mesenchymal cells. Redox Rep 2007;12:50–4.

[63]   Mrakovcic L, Wildburger R, Jaganjac M, Cindric M, Cipak A, Borovic-Sunjic S, et al. Lipid peroxidation product 4-hydroxynonenal as factor of oxidative homeostasis supporting bone regeneration with bioactive glasses. Acta Biochim Pol 2010;57:173–8.

[64]   Rudić M, Milković L, Zarković K, Borović-Šunjić S, Sterkers O, Waeg G, et al. The effects of angiotensin II and the oxidative stress mediator 4-hydroxynonenal on human osteoblast-like cell growth: possible relevance to otosclerosis. Free Radic Biol Med 2012;57C:22–8.

[65]   Uchida K. 4-Hydroxy-2-nonenal: a product and mediator of oxidative stress. Prog Lipid Res 2003;42:318–43.

[66]   Zarkovic N, Ilic Z, Jurin M, Schaur RJ, Puhl H, Esterbauer H. Stimulation of HeLa cell growth by physiological concentrations of 4-hydroxynonenal. Cell Biochem Funct 1993;11:279–86.

[67]   Zarkovic N. 4-hydroxynonenal as a bioactive marker of pathophysiological processes. Mol Aspects Med 2003;24:281–91.

[68]   Siems W, Grune T. Intracellular metabolism of 4-hydroxynonenal. Mol Aspects Med 2003;24:167–75.

[69]   Zarkovic N, Cipak A, Jaganjac M, Borovic S, Zarkovic K. Pathophysiological relevance of aldehydic protein modifications. J Proteomics 2013.

[70]   Kakishita H, Hattori Y. Vascular smooth muscle cell activation and growth by 4-hydroxynonenal. Life Sci 2001;69:689–97.

[71]   Borovic S, Sunjic I, Wildburger R, Mittelbach M, Waeg G, Zarkovic N. Lipid peroxidation end product as a modulator of cell growth. In: Hayashi T, editor. Prog. Cell Growth Process Res., New York: Nova Science Publishers, Inc. F. Columbus, New York, Inc.; 2008, p. 237.

[72]   Allevi P, Anastasia M, Cajone F, Ciuffreda P, Sanvito AM. Structural requirements of aldehydes produced in LPO for the activation of the heat-shock genes in HeLa cells. Free Radic Biol Med 1995;18:107–16.

[73]   Barrera G, Pizzimenti S, Laurora S, Briatore F, Toaldo C, Dianzani MU. 4-hydroxynonenal and cell cycle. Biofactors 2005;24:151–7.

[74]   Kreuzer T, Grube R, Wutte A, Zarkovic N, Schaur RJ. 4-Hydroxynonenal modifies the effects of serum growth factors on the expression of the c-fos proto-oncogene and the proliferation of HeLa carcinoma cells. Free Radic Biol Med 1998;25:42–9.

[75]   Ruef J, Rao GN, Li F, Bode C, Patterson C, Bhatnagar A, et al. Induction of rat aortic smooth muscle cell growth by the lipid peroxidation product 4-hydroxy-2-nonenal. Circulation 1998;97:1071–8.

[76]   Barrera G, Pizzimenti S, Serra A, Ferretti C, Fazio VM, Saglio G, et al. 4-hydroxynonenal specifically inhibits c-myb but does not affect c-fos expressions in HL-60 cells. Biochem Biophys Res Commun 1996;227:589–93.

[77]   Laurora S, Tamagno E, Briatore F, Bardini P, Pizzimenti S, Toaldo C, et al. 4-Hydroxynonenal modulation of p53 family gene expression in the SK-N-BE neuroblastoma cell line. Free Radic Biol Med 2005;38:215–25.

[78]   Zamara E, Novo E, Marra F, Gentilini A, Romanelli RG, Caligiuri A, et al. 4-Hydroxynonenal as a selective pro-fibrogenic stimulus for activated human hepatic stellate cells. J Hepatol 2004;40:60–8.

[79]   Zanetti D, Poli G, Vizio B, Zingaro B, Chiarpotto E, Biasi F. 4-Hydroxynonenal and transforming growth factor-β1 expression in colon cancer. Mol Aspects Med 2003;24:273–80.

[80]   Zarkovic N, Cipak A, Cindric M, Waeg G, Borovic Sunjic S, Mrakovcic L, et al. 4-Hydroxynonenal-protein adducts as biomarkers of oxidative stress, lipid peroxidation and oxidative homeostasis. Free Radicals, Heal Lifestyle 2009:37–45.

[81]   Kreuzer T, Grube R, Wutte A, Zarkovic N, Schaur RJ. 4-Hydroxynonenal modifies the effects of serum growth factors on the expression of the c-fos proto-oncogene and the proliferation of HeLa carcinoma cells. Free Radic Biol Med 1998;25:42–9.

[82]   Lushchak VI. Glutathione homeostasis and functions: potential targets for medical interventions. J Amino Acids 2012;2012:736837.

[83]   Awasthi S, Singhal SS, Awasthi YC, Martin B, Woo J-H, Cunningham CC, et al. RLIP76 and Cancer. Clin Cancer Res 2008;14:4372–7.

[84]   Ramana K V, Bhatnagar A, Srivastava S, Yadav UC, Awasthi S, Awasthi YC, et al. Mitogenic responses of vascular smooth muscle cells to lipid peroxidation-derived aldehyde 4-hydroxy-trans-2-nonenal (HNE): role of aldose reductase-catalyzed reduction of the HNE-glutathione conjugates in regulating cell growth. J Biol Chem 2006;281:17652–60.

[85]   Leonarduzzi G, Robbesyn F, Poli G. Signaling kinases modulated by 4-hydroxynonenal. Free Radic Biol Med 2004;37:1694–702.

[86]   Wildburger R, Zarković N, Egger G, Petek W, Meinitzer a, Borović S, et al. Comparison of the values of basic fibroblast growth factor determined by an immunoassay in the sera of patients with traumatic brain injury and enhanced osteogenesis and the effects of the same sera on the fibroblast growth in vitro. Eur J Clin Chem Clin Biochem 1995;33:693–8.

[87]   Wildburger R, Zarkovic N, Leb G, Borovic S, Zarkovic K, Tatzber F. Post-traumatic changes in insulin-like growth factor type 1 and growth hormone in patients with bone fractures and traumatic brain injury. Wien Klin Wochenschr 2001;113:119–26.

[88]   Wildburger R, Borović S, Zarković N, Tatzber F. Post-traumatic dynamic changes in the antibody titer against oxidized low density lipoproteins. Wien Klin Wochenschr 2000;112:798–803.

[89]   Sunjic SB, Cipak A, Rabuzin F, Wildburger R, Zarkovic N. The influence of 4-hydroxy-2-nonenal on proliferation, differentiation and apoptosis of human osteosarcoma cells. Biofactors 2005;24:141–8.

[90]   Gerhardt L-C, Boccaccini AR. Bioactive Glass and Glass-Ceramic Scaffolds for Bone Tissue Engineering. Materials (Basel) 2010;3:3867–910.

[91]   Hayashi T, Shishido N, Nakayama K, Nunomura A, Smith M a, Perry G, et al. Lipid peroxidation and 4-hydroxy-2-nonenal formation by copper ion bound to amyloid-beta peptide. Free Radic Biol Med 2007;43:1552–9.

[92]   Waeg G, Dimsity G, Esterbauer H. Monoclonal antibodies for detection of 4-hydroxynonenal modified proteins. Free Radic Res 1996;25:149–59.

[93]   Zarkovic K, Zarkovic N, Schlag G, Redl H. Histological Aspects of Sepsis Induced Brain Changes in a Baboon Model. In: Schlag G, Redl H, Traber D, editors. Shock. Sepsis Organ Fail. Brain Damage Second. to Hemorrhagic-Traumatic Shock. Sepsis Trauma. Brain Inj., Heilderberg: Springer-Verlag; 1997, p. 146–68.

[94]   Milkovic L, Hoppe A, Detsch R, Boccaccini AR, Zarkovic N. Effects of Cu-doped 45S5 bioactive glass on the lipid peroxidation-associated growth of human osteoblast-like cells in vitro. J Biomed Mater Res A 2013.

[95]   Bradford MM. A rapid and sensitive method for the quantitation of microgram quantities of protein utilizing the principle of protein-dye binding. Anal Biochem 1976;72:248–54.

[96]   Jørgensen P, Milkovic L, Zarkovic N, Waeg G, Rattan SIS. Lipid peroxidation-derived 4-hydroxynonenal-modified proteins accumulate in human facial skin fibroblasts during ageing in vitro. Biogerontology 2014;15:105–10.

[97]   Gartland A, Buckley KA, Dillon JP, Curran JM, Hunt JA, Gallagher JA. Isolation and Culture of Human Osteoblasts. In: Picot J, editor. Hum. Cell Cult. Protoc. (from Methods Mol. Med. Ser., Humana Press; 2005, p. 29–54.

[98]   Cicione C, Muiños-López E, Hermida-Gómez T, Fuentes-Boquete I, Díaz-Prado S, Blanco FJ. Effects of severe hypoxia on bone marrow mesenchymal stem cells differentiation potential. Stem Cells Int 2013;2013:232896.

[99]   Schneider S, Yochim J, Brabender J, Uchida K, Danenberg KD, Metzger R, et al. Osteopontin but not osteonectin messenger RNA expression is a prognostic marker in curatively resected non-small cell lung cancer. Clin Cancer Res 2004;10:1588–96.

[100]   Zhang Y, Ba Y, Liu C, Sun G, Ding L, Gao S, et al. PGC-1alpha induces apoptosis in human epithelial ovarian cancer cells through a PPARgamma-dependent pathway. Cell Res 2007;17:363–73.

[101]   Pillon NJ, Soulage CO. Lipid Peroxidation by-Products and the Metabolic Syndrome. In: Catala A, editor. Biochem. Genet. Mol. Biol.» "Lipid Peroxidation," InTech; 2012, p. 409–36.

[102]   Bedard K, Krause K-H. The NOX family of ROS-generating NADPH oxidases: physiology and pathophysiology. Physiol Rev 2007;87:245–313.

[103]   Kamata H, Hirata H. Redox regulation of cellular signalling. Cell Signal 1999;11:1–14.

[104] Chen KC-W, Zhou Y, Zhang W, Lou MF. Control of PDGF-induced reactive oxygen species (ROS) generation and signal transduction in human lens epithelial cells. Mol Vis 2007;13:374–87.

[105] Henrotin Y. The role of reactive oxygen species in homeostasis and degradation of cartilage. Osteoarthr Cartil 2003;11:747–55.

[106] Hench LL. The story of Bioglass. J Mater Sci Mater Med 2006;17:967–78.

[107] Ralay Ranaivo H, Hodge JN, Choi N, Wainwright MS. Albumin induces upregulation of matrix metalloproteinase-9 in astrocytes via MAPK and reactive oxygen species-dependent pathways. J Neuroinflammation 2012;9:68.

[108] Allen R., Tresini M. Oxidative stress and gene regulation. Free Radic Biol Med 2000;28:463–99.

[109] Yan J, Hales BF. Depletion of Glutathione Induces 4-Hydroxynonenal Protein Adducts and Hydroxyurea Teratogenicity in the Organogenesis Stage Mouse Embryo 2006;319:613–21.

[110] Awasthi YC, Ansari GAS, Awasthi S. Regulation of 4-hydroxynonenal mediated signaling by glutathione S-transferases. Methods Enzymol 2005;401:379–407.

[111] Uemura T, Nemoto A, Liu Y, Kojima H, Dong J, Yabe T, et al. Osteopontin involvement in bone remodeling and its effects on in vivo osteogenic potential of bone marrow-derived osteoblasts/porous hydroxyapatite constructs. Mater Sci Eng C 2001;17:33–6.

[112] Deschaseaux F, Sensébé L, Heymann D. Mechanisms of bone repair and regeneration. Trends Mol Med 2009;15:417–29.

[113] Hoppe A, Güldal NS, Boccaccini AR. A review of the biological response to ionic dissolution products from bioactive glasses and glass-ceramics. Biomaterials 2011;32:2757–74.

[114] Mattson MP, Meffert MK. Roles for NF-kappaB in nerve cell survival, plasticity, and disease. Cell Death Differ 2006;13:852–60.

[115] Lynch SM, Frei B. Mechanisms of copper- and iron-dependent oxidative modification of human low density lipoprotein. J Lipid Res 1993;34:1745–53.

[116] Gaetke L. Copper toxicity, oxidative stress, and antioxidant nutrients. Toxicology 2003;189:147–63.

[117] Awasthi YC, Yang Y, Tiwari NK, Patrick B, Sharma A, Li J, et al. Regulation of 4-hydroxynonenal-mediated signaling by glutathione S-transferases. Free Radic Biol Med 2004;37:607–19.

[118] Mattson MP. Hormesis defined. Ageing Res Rev 2008;7:1–7.

[119] Siow RCM, Ishii T, Mann GE. Modulation of antioxidant gene expression by 4-hydroxynonenal: atheroprotective role of the Nrf2/ARE transcription pathway. Redox Rep 2007;12:11–5.

[120] Parola M, Bellomo G, Robino G, Barrera G, Dianzani MU. 4-Hydroxynonenal as a biological signal: molecular basis and pathophysiological implications. Antioxid Redox Signal 1999;1:255–84.

[121] Calabrese V, Cornelius C, Dinkova-Kostova AT, Calabrese EJ, Mattson MP. Cellular stress responses, the hormesis paradigm, and vitagenes: novel targets for therapeutic intervention in neurodegenerative disorders. Antioxid Redox Signal 2010;13:1763–811.

7. SUMMARY

Complex bone fractures require surgical intervention and use of bone grafts in order to aid proper healing. The bioactive glasses (BGs) are synthetic bone grafts with osteoinductive and osteoconductive properties, which stimulate the bone healing process. While the principles of BG actions are yet not completely understood, nor are the complex processes of fracture repair, continuous research is attempting to improve the BG properties with addition of bioactive molecules, or by incorporation of specific therapeutic ions.

Our previous research has shown that lipid peroxidation (LPO), and especially its product and mediator 4-hydroxynonenal (HNE), known as signalling molecule in the proliferation, differentiation and apoptosis of cells, can control the growth of bone cells. The aim of this study was to investigate the role of LPO in the growth of bone cells on the BGs.

The obtained findings of an involvement of lipid peroxidation in the process of enhanced osteogenesis assisted with the BGs will lead to improved understanding of the principles governing the bone repair, which may result in creation of new, improved biomaterials and applications for the enhanced regeneration of the bone tissue.

8. SAŽETAK

Frakture kostiju, osobito one dugih kostiju, velikih zglobova te višestruke frakture, predstavljaju značajan medicinski, ali i socijalni problem zbog dugotrajnog oporavka i mogućnosti invaliditeta, koje je posebice naglašeno kod starijih ljudi. Veliki dio tih fraktura zahtjeva kiruršku intervenciju te korištenje nekih od koštanih usadaka koji omogućuju potporu, ispunjavaju nastalu prazninu i potiču biološko cijeljenje nastalog defekta. Zbog toga je današnja regenerativna medicina usmjerena k razvoju inženjerstva tkiva kosti, pri čemu je veliki naglasak pridan biomaterijalima. Kao jedni od atraktivnih predstavnika biomaterijala, pojavila su se bioaktivna stakla koja imaju pogodnu površinu koja potiče rast stanica i stvaranje nove kosti, odnosno posjeduju osteokonduktivna i osteoinduktivna svojstva. Obzirom da tijekom procesa cijeljenja frakture bitnu ulogu igraju i molekularni mehanizmi potaknuti određenim signalnim molekulama, citokinima i faktorima rasta, današnja istraživanja u tkivnom inženjerstvu usmjerena su k poboljšanju svojstava postojećih bioaktivnih stakala tako da ih kombiniraju s bioaktivnim molekulama ili im se dodaju metalni ioni, kao na primjer bakar (Cu), koji će se postepeno otpuštati u okolini defekta i tako dodatno stvarati terapeutski učinak.

Prijašnja istraživanja otkrila su vezu između sistemskog odgovora pacijenata s traumatskom ozljedom glave i fenomena ubrzane osteogeneze fraktura kostiju gdje je kao bitan parametar definirana lipidna peroksidacija (LPO). Jedan od produkata LPO, 4-hidroksinonenal (HNE) prvotno smatran kao toksična i nepoželjna molekula vezana uz različita patološka stanja, danas je poznat i po svojoj fiziološkoj ulozi djelujući kao signalna molekula. HNE, ovisno o koncentraciji, usmjerava stanice k proliferaciji, diferencijaciji ili u smrt apoptozom. Stoga je cilj ovog rada bio razjasniti koju ulogu imaju LPO i lipidna peroksidacija kod poboljšane osteogeneze pri rastu stanica na BS.

Kako bi se to ispitalo napravljena je imunocitokemijska analiza koja je ukazala na jednu jako zanimljivu činjenicu, a to je da stanice stvaraju endogeni HNE kad rastu na BS. Uzevši u obzir novo saznanje, a i činjenicu da je danas veliki dio istraživanja usmjeren ka pronalasku novih načina i molekula koje će poboljšati postojeća svojstva BS, u radu se krenulo ka funkcionalizaciji BS, 45S5 i 13-93 s albuminom (o,5 mg/ml), fiziološkom koncentracijom HNEa (2,5 μM) odnosno njihovom kombinacijom.

Dobiveni rezultati su ukazali da korišteni tretmani nisu toksični te da je lipidna peroksidacija uključena u rast stanica na BS. Nadalje pokazano je poticajno djelovanje HNEa na rast i

diferencijaciju stanica te razjašnjeno da je p44/p42 (ERK1/2) MAPK signalni put aktiviran, a put p38 nije.

Drugi dio ispitivanja je napravljen na biostaklu 45S5 s dodatkom bakra (Cu; 0.1, 1 i 2.5%)) te je potvrđena uloga lipidne peroksidacije u procesu rasta stanica na bioaktivnom staklu s time da je kod stakala s 1 i 2.5% Cu ona bila negativna tj. te koncentracije su se pokazale toksičnima dok je kod BS s 0.1% Cu ona stimulirala stanice na rast.

Stoga možemo zaključiti da lipidna peroksidacija igra bitnu ulogu u rastu stanica na BS te bi dobiveni rezultati mogli poslužiti u stvaranju novih, poboljšanih biomaterijala i postupaka za poticanje regeneracije tkiva kosti.

9. CURRICULUM VITAE

Personal information

Name and surname:	Lidija Milković
Academic title:	Dipl. ing. of biotechnology; Scientific novice (PhD student)
Address:	Rudjer Boskovic Institute, Laboratory for Oxidative Stress
	Bijenicka cesta 54, 10000 Zagreb
Phone:	+38514571212
E-mail:	lidija.milkovic@irb.hr
Citizenship:	Croatian
Date and place of birth:	27.11.1977. Zagreb, Croatia

Work experience

Since 1st of June, 2008. -	Scientific novice, PhD student in the Laboratory for oxidative stress at the Rudjer Boskovic Institute
2004. – 2008.	R&D associate in Kvasac Ltd.
1996.-1997.	Laboratory technician in the laboratory for microbiology at the Clinical Hospital "Dr. Fran Mihaljevic"

Education

2008.-2014.	Specialist graduate professional study Project management, joined study of Rudjer Boskovic Institute and Graduate school for business and management ''Baltazar Adam Krcelic''
2007. -	University Postgraduate Interdisciplinary Doctoral Study of Molecular Biosciences; Josip Juraj Strossmayer University of Osijek, University of Dubrovnik and Rudjer Boskovic Institute in Zagreb
1997. – 2003.	University of Zagreb, Faculty of Food Technology and Biotechnology; Study: Biotechnology-Biochemical engineering

Research and other projects

2013. – 2014.	Researcher on the Croatian-German bilateral project: "The role of lipid peroxidation products in growth regulation of the bone cells stimulated by the novel types of Cu-doped 45S5 bioactive glass"
2012. – 2013.	Researcher on the Croatian-Austrian bilateral project: "Effects of oxidatively modified collagen on breast cancer stem cell growth and differentiation"
2012.	Researcher on the Croatian-German bilateral project: "Effect of novel Cu-bioglass and lipid peroxidation products on bone regeneration"
2010. – 2011.	Researcher on the Croatian-Slovenian bilateral project: "Improvement of adhesive properties of biomedical materials by plasma treatment"
2007.-2008.	Researcher on the Croatian-French bilateral project: "The use of novel, genuine assays for lipid peroxidation evaluation in experimental carcinogenesis"
2006.-2008.	Researcher on a project „Novel method to support bone growth by bioactive glass coated with protein/lipid peroxidation products" supported by Austrian bank Jubiläumsfonds der Oesterreichischen Nationalbank.

Membership in science organizations and bodies

Croatian Society for Cancer Research (HDIR),
The European Association for Cancer Research (EACR)
The International HNE-Club
COST CM1106 Stemchem Action

Publications

1. **Milkovic, Lidija**; Hoppe, Alexander; Detsch, Rainer; Boccaccini, Aldo R.; Zarkovic, Neven. Effects of Cu-doped 45S5 bioactive glass on the lipid peroxidation-associated growth of human osteoblast-like cells in vitro. Journal of biomedical materials research. Part A. (2013) in press.

2. Jaganjac, M; Vesel, A; **Milkovic, L**; Recek, N; Kolar, M; Zarkovic, N; Latiff, A; Kleinschek, K.-S; Mozetic, M. Oxygen-rich coating promotes binding of proteins and endothelialization of polyethylene terephthalate polymers. Journal of biomedical materials research. Part A. (2013) in press.

3. Jørgensen, Peter; **Milkovic, Lidija**; Zarkovic, Neven; Waeg, Georg; Rattan, Suresh I.S. Lipid peroxidation-derived 4-hydroxynonenal-modified proteins accumulate in human facial skin fibroblasts during ageing in vitro. Biogerontology (Dordrecht). (2013) in press.

4. Weber, D*; **Milkovic, L***; Bennett, S.J; Griffiths, H.R; Zarkovic, N; Grune, T. Measurement of HNE-protein adducts in human plasma and serum by ELISA-Comparison of two primary antibodies. Redox Biology. 1 (2013); 226-233.

5. Cindrić, Marina; Čipak, Ana; Zapletal, Emilija; Jaganjac, Morana; **Milković, Lidija**; Waeg, G.; Stolc, S.; Žarković, Neven; Borović Šunjić, Suzana. Stobadine attenuates impairment of an intestinal barrier model caused by 4-hydroxynonenal. Toxicology in vitro. 27 (2013), 1; 426-432.

6. Recek, Nina; Jaganjac, Morana; Kolar, Metod; **Milkovic, Lidija**; Mozetič, Miran; Stana-Kleinschek, Karin; Vesel, Alenka. Protein Adsorption on Various Plasma-Treated Polyethylene Terephthalate Substrates. Molecules. 18 (2013), 10; 12441-12463.

7. Recek, N; Mozetič, M; Jaganjac, M; **Milković, L**; Žarković, N; Vesel, A. Improved proliferation of human osteosarcoma cells on oxygen plasma treated polystyrene. Vacuum. 98 (2013); 116-121.

8. Rudić, M; **Milković, L**; Žarković, K; Borović-Šunjić, S; Sterkers, O; Waeg, G; Ferrary, E; Bozorg Grayeli, A; Žarković, N. The effects of angiotensin II and the oxidative stress mediator 4-hydroxynonenal on human osteoblast-like cell growth: Possible relevance to otosclerosis. Free radical biology & medicine. 57 (2013); 22-28.

9. Jaganjac, Morana; Prah, Iva Ozana; Čipak, Ana; Cindrić, Marina; **Mrakovčić, Lidija**; Tatzber, Franz; Ilinčić, Petar; Rukavina, Vinko; Spehar, Branka; Parlov Vuković, Jelena; Telen, Sanda; Uchida, Koji; Lulić, Zoran; Žarković, Neven. Effects of Bioreactive Acrolein from Automotive Exhaust Gases on Human Cells In Vitro. Environmental toxicology. 27 (2012), 11; 644-652.

10. Rudić, Milan; Nguyen, C.; Nguyen, Y.; **Milković, Lidija**; Žarković, Neven; Sterkers, O.; Ferrary, E.; Grayeli, A.B. Effect of Angiotensin II on Inflammation Pathways in Human Primary Bone Cell Cultures in Otosclerosis. Audiology and neuro-otology. 17 (2012), 3; 169-178.

11. Jaganjac, Morana; **Milković, Lidija**; Čipak Gašparović, Ana; Mozetič, Miran; Recek, Nina; Žarković, Neven; Vesel, Alenka. Cell adhesion on hydrophobic polymer surfaces. Materiali in Tehnologije. 46 (2012); 53-56.

12. Lovaković, Tomislava; Poljak-Blaži, Marija; Duburs, Gunars; Čipak, Ana; Cindrić, Marina; Vigante, Brigita; Bisenieks, Egils; Jaganjac, Morana; **Mrakovčić, Lidija**; Dedić, Azra; Žarković, Neven. Growth modulation of human cells in vitro by mild oxidative stress and 1, 4-dihydropyridine derivative antioxidants. Collegium antropologicum. 35 (2011), 1; 137-141.

13. Vesel, Alenka; Mozetič, Miran; Jaganjac, Morana; **Milković, Lidija**; Čipak Gašparović, Ana; Žarković, Neven. Biocompatibility of oxygen-plasma-treated polystyrene substrates. European physical journal-applied physics. 56 (2011), 2; 24024-1-24024-4.

14. Breusing, Nicolle; Grune, Tilman; Andrišić, Luka; Atalay, Mustafa; Bartosz, Grzegorz; Biasi, Fiorella; Borović, Suzana; Bravo, Laura; Casals, Isidre; Casillas, Rosario; Dinischiotu, Anca; Drzewinska, Joanna; Faber, Heidemarie; Mohd Fauzi, Norsyahida; Gajewska, Agnieszka; Gambini, Juan; Gradinaru, Daniela; Kokkola, Tarja; Lojek, Antonin; Luczaj, Wojciech; Margina, Denisa; Mascia, Cinzia; Mateos, Raquel; Meinitzer, Andreas; Mitjavila, María Teresa; **Mrakovčić, Lidija**; Munteanu, Maria Cristina; Podborska, Martina; Poli, Giuseppe; Sicinska, Paulina; Skrzydlewska, Elzbieta; Vina, Jose; Wiswedel, Ingrid; Žarković, Neven; Zelzer, Sieglinde; Spickett, Corinne M. An inter-laboratory validation of methods of lipid peroxidation measurement in UVA-treated human plasma samples. Free radical research. 44 (2010), 10; 1203-1215

15. Cindrić, Marina; Čipak, Ana; Serly, Julianna; Plotniece, Aiva; Jaganjac, Morana; **Mrakovčić, Lidija**; Lovaković, Tomislava; Dedić, Azra; Soldo, Ivo; Duburs, Gunars; Žarković, Neven; Molnár, József. Reversal of Multidrug Resistance in Murine Lymphoma Cells by Amphiphilic Dihydropyridine Antioxidant Derivative. Anticancer research. 30 (2010), 10; 4063-4070.

16. **Mrakovčić, Lidija**; Wildburger, Renate; Jaganjac, Morana; Cindrić, Marina; Čipak, Ana; Borović Šunjić, Suzana; Waeg, Georg; Mogus Milanković, Andrea; Žarković, Neven. Lipid peroxidation product 4-hydroxynonenal as factor of oxidative homeostasis supporting bone regeneration with bioactive glasses. Acta biochimica Polonica. 57 (2010), 2; 173-178.

17. Čipak, Ana; **Mrakovčić, Lidija**; Ciz, Milan; Lojek, Antonin; Mihaylova, Boryana; Goshev, Ivan; Jaganjac, Morana; Cindrić, Marina; Sitić, Sanda; Margaritoni, Marko; Waeg, Georg; Balić, Marija; Žarković, Neven. Growth suppression of human breast carcinoma stem

cells by lipid peroxidation product 4-hydroxy-2-nonenal and hydroxyl radical-modified collagen. Acta biochimica Polonica. 57 (2010), 2; 165-171.

18. Jaganjac, Morana; Matijević, Tanja; Cindrić, Marina; Čipak, Ana; **Mrakovčić, Lidija**; Gubisch, Wolfgang; Žarković, Neven. Induction of CMV-1 promoter by 4-Hydroxy-2-nonenal in human embryonic kidney cells in vitro. Acta biochimica Polonica. 57 (2010), 2; 179-183.

19. **Mrakovčić, Lidija**; Cindrić, Marina; Žarković, Neven; Borović Šunjic, Suzana; Moguš Milanković, Andrea; Wildburger, Renate. In vitro model of bone regeneration with bioactive glass and lipid peroxidation. Clinical and Experimental Medical Journal. 4 (2010); 73-78.

20. Čipak, Ana; Borović, Suzana; Jaganjac, Morana; Bresgen, Nikolaus; Kirac, Iva; Grbeša, Ivana; **Mrakovčić, Lidija**; Cindrić, Marina; Šćukanec-Špoljar, Mira; Gall-Trošelj, Koraljka; Ćorić, Marijana; Eckl, Peter; Žarković, Neven. Influence of 4-hydroxynonenal and spleen cells on primary hepatocyte culture and a novel liver-derived cell line resembling hepatocyte stem cells. Acta biochimica Polonica. 57 (2010), 2; 185-191.

21. Cindrić, Marina; Čipak, Ana; **Mrakovčić, Lidija**; Žarković, Kamelija; Borović, Suzana; Wilburger, Renate; Žarković, Neven. Homeostasis, Stress & Aging. Türkiye Klinikleri = Journal of Medical Sciences. 29 (2009), 5-S1; S3-S5.

22. Wildburger, Renate; **Mrakovčić, Lidija**; Štroser, Marina; Andrišić, Luka; Borović Šunjić, Suzana; Žarković, Kamelija; Žarković, Neven. Peroxidation and Age-Associated Diseases-Cause or Consequence?. Türkiye Klinikleri = Journal of Medical Sciences. 29 (2009) 189-193.